

FROM STRUCTURE TO FUNCTION: A CHARACTERIZATION OF THE UPPER-
THORACIC ERECTOR SPINAE

BRIAN CARL NAIRN

A DISSERTATION SUBMITTED TO
THE FACULTY OF GRADUATE STUDIES
IN PARTIAL FULFILMENT OF THE REQUIREMENTS
FOR THE DEGREE OF
DOCTOR OF PHILOSOPHY

GRADUATE PROGRAM IN KINESIOLOGY AND HEALTH SCIENCE
YORK UNIVERSITY
TORONTO, ONTARIO

AUGUST 2017

© Brian Carl Nairn, 2017

Abstract

The upper back, centred about the 4th vertebrae of thoracic spine, is between the shoulder and low back where the scapular and spine muscles interface. In order to improve our understanding of the shoulder-low back relationship it is important to establish quantitative techniques and document general structure-function changes in this transition region. Therefore, the purpose was to assess ultrasound imaging (USI), maximum voluntary contractions (MVCs), and kinematic collection methods from the upper back, and to apply these methods to assess T4 erector spinae muscle (T4ES) structure and function.

Five studies were produced that included a total of 86 university-aged participants. Study#1 assessed the reliability and accuracy of muscle thickness and pennation angle measured from USI compared to magnetic resonance imaging (MRI). Electromyography (EMG) MVC techniques (e.g. Active postures) targeting T4ES were tested in Study#2; while Study#3 analyzed the reliability and accuracy of measuring sagittal plane spine angles in Passive postures (Upright, Flex, Slump) from a flexible ruler (Flexi) compared to an optoelectronic motion capture (MoCap). Study#4 looked at the relationship between EMG and changes in T4ES thickness and pennation angles from USI during the same Active and Postures as Studies #2 and #3. Finally, Study#5 was an application pilot study into the function of T4ES during breathing tasks.

Overall, USI and Flexi were reliable and comparable to the gold standards of MRI and MoCap, respectively, and the thoracic extension technique was recommended to normalize T4ES activation, though caution should be used when assessing overhead work due to possible crosstalk. The T4ES region showed complex changes in morphometry during the MVC (Active) techniques and Passive postures. However, distinguishable changes in morphometry were

exhibited within the Passive postures, particularly Flex and Slump compared to Upright.

Therefore, it was suggested that Flexi and USI could replace MoCap and EMG, if the intent were to analyze different components of static postures. This could be especially useful where access to/use of typical kinematic and EMG equipment may be lacking/inappropriate, but access to USI and Flexi are more readily available and feasible. Thus, allowing for much needed upper back quantification in clinical and industrial settings.

Dedication

This one is for Mom. For all of the support (of varying types) and believing in me throughout this process, I cannot thank you enough. I know I wasn't always the most pleasant to talk to, but you never stopped caring to ask how everything was going. Thank you for everything, now and always.

Acknowledgements

First off, a big thank you to my supervisor Dr. Janessa Drake. You let me take it and run with it and really let me find my own way. You were always supportive of my teaching interests and encouraged the additional activities I partook in.

To all of my lab mates past and present, you guys were awesome. Special thanks to the following people:

- Alison: Yup. You got me through the first half of this thing. Thanks for being a great friend then and now. Good times travelling around to all of our conferences, now looking forward to kicking back with some cold ones up north.
- Aaron and Susari: You guys rock. Aaron my desk buddy, thanks for letting me leak over into you. Susari, finally someone else who appreciates a good pun! Had lots of fun and looking forward to see what happens next for all of us.
- Jeev and Dmitry: We were in this together from the start, and happy we got to finish together too. I will always appreciate the late nights, cold beers, and good talks.
- Brendan and Graham: You left me. But I still love you. Always there when I needed a good sports talk and I know we'll be good friends for a long time.

On a personal level, all of my friends and family who were there from the start. Special shout out to my love Cheryl...you've put up with the good, the bad, and the worse. You were my rock for the last few years and I appreciate everything more than you know.

I would also like to thank my committee members, Dr. Gage and Dr. Kuk for your support and insights into my projects. To Joy Williams for running the MRI for us, and to my co-authors Dr. Jack Callaghan, Graham Mayberry, and Colin McKinnon.

Thank you everyone. I could not have done this without you!

Table of Contents

Abstract	ii
Dedication	iv
Acknowledgements	v
Tables of Contents	vi
List of Tables	x
List of Figures	xii
List of Abbreviations	xvi
1. General Introduction	1
1.1 Introduction	1
1.2 Specific Research Questions	7
1.3 Specific Hypotheses	8
2. Review of Literature	10
2.1 Shoulder-Low Back Trade-off	10
2.2 Functional Anatomy of the Thoracic Spine	13
2.3 Ultrasound and Magnetic Resonance Imaging.....	17
2.3.1 Ultrasound Imaging	17
2.3.2 Magnetic Resonance Imaging	17
2.3.3 Ultrasound Reliability and Validity	19
2.4 Collection Techniques of the Thoracic Spine	20
2.4.1 Kinematic Data.....	21
2.4.2 Electromyography	22
2.5 Passive and Active Postures in the Thoracic Spine.....	24
2.6 Trunk Muscles and Challenged Breathing	25
2.7 Summary of Key Points	26
3. Common Methods.....	28
3.1 Participants	28
3.2 Ultrasound Imaging.....	29

3.3 Electromyography	30
3.3.1 Collection Specifications.....	30
3.3.2 Maximum Voluntary Contractions.....	31
3.3.3 Linear Envelope.....	32
3.4 Active Postures.....	32
3.5 Statistical Analyses	32
4. Study #1: USI-MRI.....	34
4.1 USI-MRI Introduction.....	34
4.2 USI-MRI Methods.....	37
4.2.1 Participants	37
4.2.2 Instrumentation.....	38
4.2.3 Data Collection.....	38
4.2.4 MRI Protocol	40
4.2.5 Data Processing	41
4.2.6 Statistical Analyses.....	43
4.3 USI-MRI Results.....	45
4.3.1 Thickness Measures.....	45
4.3.1.1 Analysis of Variance.....	45
4.3.1.2 Reliability Analyses	47
4.3.1.3 Bland-Altman.....	47
4.3.2 Pennation Angle Measures	48
4.3.2.1 Analysis of Variance.....	48
4.3.2.2 Reliability Analyses	48
4.3.2.3 Bland-Altman.....	49
4.4 USI-MRI Discussion.....	50
5. Study #2: T4ES-MVC.....	56
5.1 T4ES-MVC Introduction.....	56
5.2 T4ES-MVC Methods	59
5.2.1 Participants	59
5.2.2 Instrumentation.....	59

5.2.3 Data Collection.....	61
5.2.4 Data Processing	62
5.2.5 Statistical Analyses.....	64
5.3 T4ES-MVC Results.....	64
5.4 T4ES-MVC Discussion.....	66
6. Study #3: Flexi-MoCap.....	71
6.1 Flexi-MoCap Introduction.....	71
6.2 Flexi-MoCap Methods	74
6.2.1 Participants	74
6.2.2 Data Collection.....	75
6.2.3 Data Processing	77
6.2.3.1 Flexible Ruler.....	77
6.2.3.2 Motion Capture	77
6.2.4 Data Analysis.....	79
6.2.4.1 Bland-Altman.....	79
6.2.4.2 Statistics	80
6.2.4.3 Overall Acceptability Criteria.....	81
6.3 Flexi-MoCap Results.....	81
6.4 Flexi-MoCap Discussion.....	85
7. Study #4: USI-EMG	90
7.1 USI-EMG Introduction	90
7.2 USI-EMG Methods	93
7.2.1 Participants	93
7.2.2 Instrumentation.....	93
7.2.3 Data Collection.....	94
7.2.4 Data Processing	95
7.2.5 Statistical Analyses.....	97
7.3 USI-EMG Results	98
7.3.1 Correlation.....	98

7.3.2 Analysis of Variance	103
7.4 USI-EMG Discussion.....	107
8. General Discussion	115
8.1 General Contributions	115
8.2 Specific Contributions	116
8.3 General Limitations.....	118
8.4 Hypotheses Revisited	120
8.5 Future Directions.....	122
8.6 General Conclusions	123
References.....	124
Appendix A: Study #5: Application-Pilot.....	145
Appendix B: Flexi-MoCap Additional Results.....	149
Appendix C: USI-EMG Additional Results	163

List of Tables

Table 3.1. Full description of the Active Postures used in Study #2: T4ES-MVC and Study #4: USI-EMG.....	33
Table 4.1. Mean (<i>SD</i>) characteristics of participants by Male (n=10) and Female (n=10).....	38
Table 4.2. Summary of ANOVA results for both thickness and angle measures. $\alpha = 0.05$	46
Table 4.3. Summary of mean (<i>SD</i>), reliability, and Bland-Altman results from T4ES thickness measures from both ultrasound imaging (USI) and magnetic resonance imaging (MRI). Included are: intraclass correlation coefficients (ICC), the standard error of measurement (SEM), the minimum detectable change (MDC), the mean difference between the measures (Mean Diff), and the upper and lower limits of agreement (Upper LoA and Lower LoA, respectively).....	47
Table 4.4. Summary of mean (<i>SD</i>), reliability, and Bland-Altman results from T4ES angle measures from both ultrasound imaging (USI) and magnetic resonance imaging (MRI). Included are: intraclass correlation coefficients (ICC), the standard error of measurement (SEM), the minimum detectable change (MDC), the mean difference between the measures (Mean Diff), and the upper and lower limits of agreement (Upper LoA and Lower LoA, respectively).....	50
Table 6.1. Summary of the angles and postures from the main analysis that were deemed acceptable (n=20). The shaded cell indicates where the Limit of Agreement was violated, yet the maximum difference was under 10°.	82
Table 6.2. Summary of the angles and postures from the subset analysis that were deemed acceptable (n=10). Where the Limit of Agreement was violated, the maximum value obtained is presented.....	83
Table 7.1. Summary of correlation analyses for each of the Active postures. Significant correlations are designated by shaded cells with bold font.....	103
Table 7.2. Summary of correlation analyses for each of the Passive postures. Significant correlations are designated by shaded cells with bold font.....	104
Table B.1. Mean (<i>SD</i>) Flexi angles recorded from each region and posture. (n=20).	149
Table B.2. Mean (<i>SD</i>) MoCap angles recorded from each region and posture. (n=20).	149
Table B.3. Mean (<i>SD</i>) bias analyses from Bland-Altman of the Upright-Stand trial. Proportional bias is based on regression slope significantly different from 0, and systematic bias is based on mean difference being significantly different from 0.	160

Table B.4. Mean (*SD*) bias analyses from Bland-Altman of the Flex-Stand trial. Proportional bias is based on regression slope significantly different from 0, and systematic bias is based on mean difference being significantly different from 0.160

Table B.5. Mean (*SD*) bias analyses from Bland-Altman of the Slump-Stand trial. Proportional bias is based on regression slope significantly different from 0, and systematic bias is based on mean difference being significantly different from 0.161

Table B.6. Mean (*SD*) bias analyses from Bland-Altman of the Upright-Sit trial. Proportional bias is based on regression slope significantly different from 0, and systematic bias is based on mean difference being significantly different from 0.161

Table B.7. Mean (*SD*) bias analyses from Bland-Altman of the Flex-Sit trial. Proportional bias is based on regression slope significantly different from 0, and systematic bias is based on mean difference being significantly different from 0.162

Table B.8. Mean (*SD*) bias analyses from Bland-Altman of the Slump-Sit trial. Proportional bias is based on regression slope significantly different from 0, and systematic bias is based on mean difference being significantly different from 0.162

Table C.1. Mean (*SD*) pennation angle and thickness for T4ES, rhomboids, and trapezius for each posture.163

List of Figures

Figure 4.1. The spinous process at T4 was palpated and marked, as indicated by the black arrow (A). A transfer board with a hole cut out was used (B), which allowed the marked area to be exposed while supine (C). The transfer board was placed on a custom-built gurney (D).39

Figure 4.2. The ultrasound image calibration procedure. Known on-screen caliper length of 2.01 cm (A). A measured line was drawn between the crosshairs to indicate a length of 156 pixels, and the known value (2.01 cm) was entered as the length of the drawn line (B). The result was a calibrated length to use for each of the images.42

Figure 4.3. Location and measurement process from both ultrasound imaging (USI) and magnetic resonance imaging (MRI). The MRI localizer scan was used to identify the anatomical region of interest, and confirmed with an externally placed vitamin E capsule (A). A representation of the USI highlighting the transverse process (arrow), erector spine (yellow), rhomboid major (blue), trapezius (red), and the layers of skin and subcutaneous fat (grey) (B). The same USI as (B) is shown with the on-screen measurements made of thickness and pennation angle (C). The same participant with the measurements made from the reconstructed MRI slice (D).43

Figure 4.4. Mean (*SD*) thickness measures from ultrasound imaging (USI) and magnetic resonance imaging (MRI), $p = 0.719$46

Figure 4.5. Bland-Altman plot comparing thickness measured by ultrasound imaging (USI) and magnetic resonance imaging (MRI). The solid blue line is the mean difference between the methods, and the dashed green lines are the upper and lower limits of agreement. The regression line and equation are included as the slope of the line was used to determine the presence of proportional bias.48

Figure 4.6. Mean (*SD*) angle measures from ultrasound imaging (USI) and magnetic resonance imaging (MRI), $p = 0.146$49

Figure 4.7. Bland-Altman plot comparing fibre angles measured by ultrasound imaging (USI) and magnetic resonance imaging (MRI). The solid blue line is the mean difference between the methods, and the dashed green lines are the upper and lower limits of agreement. The regression line and equation are included as the slope of the line was used to determine the presence of proportional bias.50

Figure 5.1. Electrode placement for the upper-thoracic erector spinae at the T4 level (T4ES) and the middle trapezius (MidTrap)60

Figure 5.2 Representation of each MVC technique: ThorExt (A), LumbExt (B), Raise-Stand (C), Raise-Sit (D), Row-Stand (E), Row-Sit (F), LatPull-Stand (G), LatPull-Sit (H). Note: Care was taken to ensure no pressure was applied directly to the electrodes.63

Figure 5.3. Results of the ANOVA highlighting the effect of posture on T4ES (%ThorExt) ($p < 0.01$). Levels not connected by the same letter were considered significant at $p < 0.05$65

Figure 5.4. Results of the ANOVA highlighting the effect of MVC technique on MidTrap (%Raise-Stand) ($p < 0.01$). Levels not connected by the same letter were considered significant at $p < 0.05$66

Figure 6.1. Photo showing the flexible ruler (A) and optoelectronic motion capture marker clusters (B). The locations of the palpated vertebrae are labelled with the arrows76

Figure 6.2. Representation of a flexible ruler tracing (solid black line) with the angles drawn. The grey circles are the specific spinous processes. The segmental method (A) is represented by the blue lines that connect the spinous process points, and the angles between these lines are MidSeg and LowSeg. The tangential method (B) is represented by the red angles between the tangent lines, shown as UpTTan, LowTTan, and LumbTan angles.78

Figure 6.3. Bland-Altman plot of the MidSeg angle in Stand-Upright. This flexicurve angle was considered ‘acceptable’.83

Figure 6.4. Interaction effect of Sex (Males and Females) and Method (Flexi and MoCap) on LumbTan lordosis angle. Asterisks (*) represent a difference between Sex for each Method ($p < 0.024$). Unmatched lettering between females represent a difference in Method ($p = 0.001$). .84

Figure 6.5. Bland-Altman plot of the UpTTan angle in Stand-Upright ($n = 20$). This Flexi angle was considered ‘not acceptable’ because of the large Limits of Agreement.85

Figure 7.1. (A-H). Representation of transducer and the visible layers (A), including: skin and subcutaneous fat (SSF), trapezius (TR), rhomboid major (RM), erector spinae (ES), and the transverse process and acoustic shadow it creates (TPAS). Postures include: Prone (B), Upright-Stand (C), Upright-Sit (D), Flex-Stand (E), Flex-Sit (F), Slump-Stand (G), and Slump-Sit (H).99

Figure 7.1. [cont’d] (I-P). Images showing: skin and subcutaneous fat (SSF), trapezius (TR), rhomboid major (RM), erector spinae (ES), and the transverse process and acoustic shadow it creates (TPAS). Postures include: ThorExt (I), LumbExt (J), Raise-Stand (K), Raise-Sit (L), Row-Stand (M), Row-Sit (N), Lat-Stand (O), and Lat-Sit (P).100

Figure 7.2. Correlation of EMG to %ThickChange for all postures and all participants combined ($n = 354$). $r = 0.297$, $p < 0.01$101

Figure 7.3. Correlation of EMG to %AngleChange for all postures and all participants combined ($n = 354$). $r = 0.265$, $p < 0.01$102

Figure 7.4. Correlation of %AngleChange to %ThickChange for all postures and all participants combined ($n = 416$). $r = 0.378$, $p < 0.001$102

Figure 7.5. Summary of EMG ANOVA results for all postures. Levels not connected by the same letter are statistically different ($p < 0.045$).	105
Figure 7.6. Summary of ultrasound thickness (%change) results for all postures. Levels not connected by the same letter are statistically different ($p < 0.046$).	105
Figure 7.7. Summary of ultrasound thickness (%change) results for all postures. Levels not connected by the same letter are statistically different ($p < 0.045$).	106
Figure A.1. Mean (<i>SD</i>) rating of perceived exertion after the treadmill task and maximum voluntary ventilation (MVV) task.....	147
Figure A.2. Mean (<i>SD</i>) peak heart rate (BPM) after the treadmill task and maximum voluntary ventilation (MVV) task.	148
Figure A.3. Mean (<i>SD</i>) of T4ES activation (%MVC) before and after the treadmill task, and before, during, and after the maximum voluntary ventilation (MVV) task.....	148
Figure B.1. Bland-Altman plot for the UpTTan angle in Upright-Stand.....	150
Figure B.2. Bland-Altman plot for the MidSeg angle in Upright-Stand.....	150
Figure B.3. Bland-Altman plot for the LowTTan angle in Upright-Stand.	150
Figure B.4. Bland-Altman plot for the LowSeg angle in Upright-Stand.	151
Figure B.5. Bland-Altman plot for the Lumbar angle in Upright-Stand.....	151
Figure B.6. Bland-Altman plot for the UpTTan angle in Flex-Stand.....	151
Figure B.7. Bland-Altman plot for the MidSeg angle in Flex-Stand.	152
Figure B.8. Bland-Altman plot for the LowTTan angle in Flex-Stand.....	152
Figure B.9. Bland-Altman plot for the LowSeg angle in Flex-Stand.	152
Figure B.10. Bland-Altman plot for the Lumbar angle in Flex-Stand.....	153
Figure B.11. Bland-Altman plot for the UpTTan angle in Slump-Stand.....	153
Figure B.12. Bland-Altman plot for the MidSeg angle in Slump-Stand.....	153
Figure B.13. Bland-Altman plot for the LowTTan angle in Slump-Stand.	154
Figure B.14. Bland-Altman plot for the LowSeg angle in Slump-Stand.....	154

Figure B.15. Bland-Altman plot for the Lumbar angle in Slump-Stand.....	154
Figure B.16. Bland-Altman plot for the UpTTan angle in Upright-Sit.	155
Figure B.17. Bland-Altman plot for the MidSeg angle in Upright-Sit.	155
Figure B.18. Bland-Altman plot for the LowTTan angle in Upright-Sit.....	155
Figure B.19. Bland-Altman plot for the LowSeg angle in Upright-Sit.....	156
Figure B.20. Bland-Altman plot for the Lumbar angle in Upright-Sit.	156
Figure B.21. Bland-Altman plot for the UpTTan angle in Flex-Sit.....	156
Figure B.22. Bland-Altman plot for the MidSeg angle in Flex-Sit.....	157
Figure B.23. Bland-Altman plot for the LowTTan angle in Flex-Sit.	157
Figure B.24. Bland-Altman plot for the LowSeg angle in Flex-Sit.	157
Figure B.25. Bland-Altman plot for the Lumbar angle in Flex-Sit.....	158
Figure B.26. Bland-Altman plot for the UpTTan angle in Slump-Sit.	158
Figure B.27. Bland-Altman plot for the MidSeg angle in Slump-Sit.	158
Figure B.28. Bland-Altman plot for the LowTTan angle in Slump-Sit.....	159
Figure B.29. Bland-Altman plot for the LowSeg angle in Slump-Sit.....	159
Figure B.30. Bland-Altman plot for the Lumbar angle in Slump-Sit.	159

List of Abbreviations

Active Postures: The static postures that required volitional muscle contraction. For this dissertation, these were the eight maximum voluntary contraction postures

b-mode: “Brightness” mode, referring to the type of ultrasound imaged acquired

C7: The 7th cervical vertebra

COPD: Chronic Obstruction Pulmonary Disease

CSA: Cross-sectional Area

EMG: Electromyography

EO: External Oblique

ES: Erector Spinae

Flexi: A flexible ruler (e.g. flexicurve). A strip of malleable metal coated in plastic that will retain its shape in one plane when contoured.

HR: Heart Rate

ICC: Intraclass Correlation Coefficient

IO: Internal Oblique

T1-T12: Representing the specific thoracic levels according to vertebrae

T4ES: Erector spinae muscle group at the T4 level

L1-L5: Representing the specific lumbar levels according to vertebrae

L5/S1: Lumbo-sacral joint

LatPull-Sit: Seated lateral pulldown MVC technique

LatPull-Stand: Standing lateral pulldown MVC technique

LCS: Local Coordinate System

LES: Lumbar Erector Spinae

LBP: Low Back Pain

LumbExt: Lumbar extension MVC technique

MDC: Minimum Detectable Change

MeanDiff: Mean Difference

MidTrap: Middle-trapezius muscle at the T3 level

MoCap: Optoelectronic Motion Capture

MRI: Magnetic Resonance Imaging

MVC: Maximum Voluntary Contraction

MVV: Maximum Voluntary Ventilation

Passive Postures: The static postures that involved minimal muscle activation to adopt and maintain. These included Upright, Flex, and Slump

Raise-Sit: Seated arm raise MVC technique

Raise-Stand: Standing arm raise MVC technique

Row-Sit: Seated MVC technique involving pulling

Row-Stand: Standing MVC technique involving pulling

RPE: Rating of Perceived Exertion

SEM: Standard Error of Measurement

TE: Echo Time

ThorExt: Thoracic extension MVC technique

TR: Repetition Time

TransAb: Transverse abdominis muscle

USI: Ultrasound Imaging

Chapter 1: General Introduction

1.1 Introduction

A major injury concern from both an occupational and subsequent clinical perspective is the trade-off between shoulder and low back loading; specifically, how the loads are transferred through the thoracic spine. Changes in muscle morphometry, such as thickness and pennation angle can be influenced by body position and muscle contraction and can impact the load transfer. For example, as the pennation angle changes, the force line of action also changes (Potvin et al., 1991), and changes in thickness and pennation angle can indicate changes in the lengthening/shortening of the muscle (Dieterich et al., 2014). As the force-length characteristics differ along with the direction of the muscle loading, the transmission of the forces down the thoracic spine from the shoulder could be altered. In the lumbar spine, it is well established that passive flexion increases the shear forces generated by the muscles due to the change in fascicle orientation (Macintosh et al., 1993), which is a result of a reduction in the cosine (compression) angle (McGill et al., 2000). Furthermore, active contraction of lumbar erector spinae (LES) is accompanied by both increases in pennation angle, as well as increases in muscle thickness (Cuesta-Vargas & Gonzalez-Sanchez, 2013). This functional trade-off between passive postures, active contraction, and the underlying structural changes is less clear in the thoracic spine. In the upper-thoracic spine at the T4 level is part of where the scapulothoracic and axial skeleton regions interface, as the muscles that attach to and support the scapula (trapezius and rhomboids) also attach to the thoracic vertebrae (Vasavada et al., 2011). Additionally, Macintosh and Bogduk (1987) documented the longissimus thoracis portion of the erector spinae to arise from every transverse process of the thoracic spine and attach down to the lumbar and pelvis, while

longissimus cervicis has attachments from T4 transverse processes up to the cervical vertebrae (Vasavada et al., 2011). The proximity of the deep erector spinae at the T4 level (T4ES) to the scapulothoracic region implies that changes in arm and body position could have an effect on how this muscle group changes in structure and function, which in turn could impact any loading on the low back. However, prior to fully understanding the shoulder-low back trade-off (e.g. different arm and trunk postures and their effects on the shoulder and low back), it is important to establish methodological techniques and to document basic structure-function changes in order to help characterize the thoracic region in a standard, generalized manner.

The ‘gold standard’ for musculoskeletal imaging is considered to be magnetic resonance imaging (MRI) (Whittaker et al., 2007), though ultrasound imaging (USI) has been identified as a relatively inexpensive, easily accessible, and safe imaging modality compared to computed tomography and MRI (Tan et al., 2003). Ultrasound images have shown high reliability for measuring thickness of trunk and posterior shoulder muscles such as: the abdominal wall (Teyhen et al., 2011), LES (Belavý et al., 2015), multifidus (Sions et al., 2015), upper-trapezius (Bentman et al., 2010), lower-trapezius (O’Sullivan et al., 2007), and rhomboid major (Jeong et al., 2016). Additionally, thickness measures from USI have been validated against MRI in LES (Belavý et al., 2015) and multifidus (Belavý et al., 2015; Hides et al., 1995). However, it remains unclear the reliability and accuracy of USI when measuring muscle morphology such as thickness and pennation angle at T4ES. Validating the use of USI to assess thickness and pennation angle of T4ES was addressed in Study #1: USI-MRI and the results were used to further describe morphological changes in Study #4: USI-EMG.

Two common collection measures in spine biomechanics are surface electromyography (EMG) and optoelectronic kinematics, which are used to describe the movements that arise from

the underlying neuromuscular control. The EMG signal provides a way to represent the physiological processes that cause movement (De Luca, 1997), and has many practical functions both from a biomechanical and clinical perspective (Colloca & Hinrichs, 2005). However, the EMG signal can be misinterpreted if proper normalization procedures are not accounted for, such as reference to task means or peaks, sub-maximal contractions, or maximum voluntary contractions (MVC) (Burden, 2010). The most common normalization method is the MVC (Lehman & McGill 1999), which has been endorsed by the *Journal of Electromyography and Kinesiology* (Merletti, 1999). Concerning different trunk muscles, MVC techniques have been previously tested for in the abdominals and LES (Ng et al., 2002; Vera-Garcia et al., 2010), latissimus dorsi (Beaudette et al., 2014; Park & Yoo, 2013), and trapezius (Ekstrom et al., 2005). For T4ES, a thoracic extension MVC has been briefly described (Burnett et al., 2009); however, no specific testing of different MVC techniques on T4ES has been evaluated. Furthermore, a recent study of trunk and arm motion on EMG has shown arm abduction to elicit high levels of EMG from the T4ES channel (Siu et al., 2016), which could suggest possible interference from surrounding muscles. Considering the proximity of T4ES to the scapulothoracic-axial skeleton interface as describe above, it is possible that different contractions targeting specific muscles of the trunk and posterior shoulder could impact the activation recording of T4ES. This issue of establishing a standardized MVC technique for T4ES and monitoring the surrounding musculature was addressed in Study #2: T4ES-MVC and the results used for normalizing the EMG data in Study #4: USI-EMG.

In addition to EMG normalization, recording of sagittal plane spine angles is also important to consider for the thoracic region. Sagittal plane angles of the thoracic and lumbar spine have been reported previously using the ‘gold standard’ optoelectronic motion capture

(MoCap) (Nairn & Drake, 2014; Preuss & Popovic, 2010; Schinkel-Ivy et al., 2014), yet MoCap equipment is expensive and cumbersome, limiting its uses in the clinic or for on-site data collections. A cheaper, low-tech option to measure sagittal plane lumbar angles has been described by Burton (1986), which involved a flexible ruler (Flexi) to trace the contour of the spine onto paper and to make manual recordings of the angles. Different angular measurements from Flexi have been compared to external devices such as inclinometers (Tillotson & Burton, 1991) and Debrunner kyphometers (Greendale et al., 2011), but not to the gold standard MoCap; which was addressed in Study #3: Flexi-MoCap.

In terms of application of T4ES, one possible area is the function during ventilation. For example, other trunk muscles such as transverse abdominis (TransAb) and LES have shown to increase activation during expiration and inspiration, respectively (Hodges et al., 2000; Wang & McGill, 2008). Additionally, there have been clinical implications for the lumbar region as those with low back pain (LBP) have shown increased stability during challenged breathing (Grenier & McGill, 2008), and individuals with chronic obstruction pulmonary disease (COPD) have shown impaired balance recovery with increased LES muscle activity after bouts of exercise (Smith et al., 2016). It is possible that T4ES could play a role during breathing due to its proximity to the ribcage; however, the functional application of T4ES during challenged breathing remains unknown. This application of T4ES during challenged breathing was addressed in a pilot study, Study #5: Application-Pilot.

Overall, establishing collection techniques to help standardize future EMG comparisons, along with validating the use of a tool that potentially increases the ease of use and accessibility to capture sagittal plane spine angles, are both important considerations for thoracic spine research moving forward. Within this thesis, the results from Study #2: T4ES-MVC were used

as the MVC techniques to normalize the EMG from Study #4: USI-EMG and Study #5: Application-Pilot. Furthermore, the postures used from both Study #2: T4ES-MVC and Study #3: Flexi-MoCap were also the same ones adopted for Study #4: USI-EMG.

For the purposes of this thesis, the postures from Study #2: T4ES-MVC and Study #3: Flexi-MoCap were considered to be “active” and “passive” in nature, respectively, based on the required amount of muscle activation to produce/maintain the posture. Both types of postures were performed from a static position, and did not refer to dynamic motion or passive stretch of the muscles. Active postures were defined here as postures that required, or were instructed to provide, volitional contraction of the muscles crossing a joint that was being resisted manually. Examples would be the maximum and sub-maximum versions of the MVC techniques described in Study #2:T4ES-MVC, which included back extensions, arm raises, rows, and lateral pull downs. Active contractions have been associated with increases in both thickness and pennation angle within LES, (Cuesta-Vargas & Gonzalez-Sanchez, 2013); however, no relationship between contraction thickness and EMG has been found in muscles that are surrounded by layers of other muscle such as external oblique (EO) (Hodges et al., 2003) and gluteus minimus (Dieterich et al., 2014). Passive postures were referred to as sitting or standing postures that required minimal muscle activation to achieve and sustain, such as those presented in Study #3: Flexi-MoCap (Upright, Flex, and Slump). Prolonged exposures to standing and sitting have resulted in instances of different neuromuscular activation between pain and non-pain developers in standing (Nelson-Wong & Callaghan, 2010; Nelson-Wong et al., 2008), and sitting (Nairn et al., 2013b; Schinkel-Ivy et al., 2013); whereas short-term exposures to slumped sitting have also highlighted differences between pain groups (Dankaerts et al., 2006). In the lumbar region, flexion has been shown to change the ES muscle line of action resulting in a reduced ability to

resist anterior shear, which could place an individual at an increased risk for injury (McGill et al., 2000). Furthermore, Watanabe et al. (2004) showed that seated flexion reduced the thickness of the LES muscle compared to upright. However, in each of the active and passive postures presented above and in the previously mentioned dissertation Studies, it remained unclear how the muscle morphology of T4ES was changing, and how these changes were related to the recorded EMG signal. This issue was addressed in Study #4: USI-EMG, which provided direct examples of how changes in posture and activation altered the underlying structure of the muscle which potentially affected the function of T4ES.

In summary, quite a few gaps still remain in the literature regarding general collection methods of thoracic spine data, and specific structural and functional changes within T4ES, as identified here and in the upcoming Chapter 2: Review of Literature. The thoracic spine could play an important role in transferring loads to and from the shoulder and low back through the scapulothoracic-axial skeleton interface at the T4 level due to changes in the force line of action of the scapular muscles during overhead motion. However, the basic structure of T4ES *in vivo* is currently not described, including the reliability and accuracy of using USI for morphometry, which would help shed light on how the ES muscle is potentially generating force and in which direction. In addition, surface EMG measures can help with understanding muscle function, though application of the EMG signal depends on proper interpretation of the signal. Proper interpretation of the EMG signal often comes from normalizing the signal to a maximum reference value (e.g. MVC); however, different normalization techniques have not been tested for in T4ES. Passive postures have an important role in injury mechanism even with minimal muscle activation; therefore it is important that clinicians and on-site researchers have access to reliable, accurate, and cost-effective ways to measure sagittal plane spine angles in order to be

able to assess potentially compromising postures. Additionally, how the morphology and EMG signal of T4ES are related throughout a variety of active and passive postures remains unclear. Knowing the underlying structural changes in T4ES and how these changes relate to muscle activation, along with improvements in data collection techniques, could ultimately help with knowledge of how loads are transferred between the shoulder and low back regions through the thoracic spine.

1.2 Specific Research Questions

Based on the information provided above, the following research questions were developed to specifically address these issues:

Study #1: USI-MRI

Research Question: Is USI a reliable and accurate way to measure thickness and pennation angle in T4ES?

Study #2: T4ES-MVC

Research Question: What MVC technique provides that maximum activation from T4ES?

Study #3: Flexi-MoCap

Research Question: Is a flexible ruler a reliable tool for measuring thoracic spine sagittal plane angles in passive postures, and how do these angles compare to those obtained from optoelectronic motion capture?

Study #4: USI-EMG

Research Questions: What is the relationship between changes in morphometry and muscle activation at T4ES? Are any of these changes different across active and passive postures?

Study #5: Application-Pilot

Research Question: What was the role of T4ES during breathing tasks?

1.3 Specific Hypotheses

The following experimental hypotheses were developed in order to answer the specific questions outlined above:

Study #1: USI-MRI

Hypothesis #1: Ultrasound imaging will be reliable and accurate for measuring morphometry of T4ES.

Study #2: T4ES-MVC

Hypothesis #2: Thoracic extension will show the highest activation value in T4ES.

Study #3: Flexi-MoCap

Hypothesis #3: The Flexi angles will show high reliability and good agreement to MoCap angles.

Study #4: USI-EMG

Hypothesis #4: The relationship between EMG and changes in morphometry will show a strong positive relationship.

Hypothesis #5: Changes in EMG and morphometry will be reflected across the different postures, specifically, Active postures will show greater increase in thickness pennation angle compared to Passive postures.

Study #5: Application-Pilot

This study was strictly exploratory in nature with only descriptive results reported, therefore no formal hypotheses were generated for this study.

Chapter 2: Review of Literature

2.1 Shoulder-Low Back Trade-off

The shoulder and low back are two body regions commonly reported on in epidemiological literature regarding work-related musculoskeletal disorders (Punnett & Wegman, 2004). From a biomechanical perspective, a review by Radwin et al. (2002) noted that external loading of both the upper limbs and low back were related to the biomechanical internal (tissue) loading and pain/discomfort in that region. One of the main conclusions from the review was that biomechanics forms the basis to reduce external loading, which could help prevent injury to the shoulder and low back regions (Radwin et al., 2002). There are a number of occupationally-relevant tasks in which a trade-off in loading would occur between the shoulder and low back, such as pushing and pulling, lifting and lowering, seated or standing postures, and standing working height. Understanding the trade-off between the shoulder and low back during a variety of functional tasks would be an important factor for determining injury risk.

Pushing and pulling loading trade-offs are often assessed as a function of the task and handle height. For example, de Looze et al. (2000) had eight males push and pull on a cart and stationary bar while walking on a treadmill with the handle height ranging from 50-80% of shoulder height. Pulling resulted in higher absolute lumbo-sacral joint (L5/S1) moments while pushing resulted in higher shoulder moments (de Looze et al., 2000). However, the handle height was found to have a minimal effect on shoulder loading, whereas the higher handle resulted in a reduction of L5/S1 moments (de Looze et al., 2000). Similarly, Hoozemans et al. (2004) also found increased low back loading during pulling, and decreased maximum compression force with push or pull at shoulder height. However, handle height was related to

the net moment at the shoulder, indicating an increased handle height increased the net moment at the shoulder (Hoozemans et al., 2004). A study by Lee et al. (2012) did not quantify shoulder outcomes, yet used shoulder/arm posture to quantify the effects on muscle activity and moments on the low back during pushing. Eleven male participants pushed a 200 kg cart from hip and shoulder height, and EMG was collected from five ES sites and averaged together as the representative “extensor” activity (Lee et al., 2012). Overall, an increase in handle height resulted a larger internal moment at L5/S1 with a corresponding decrease in extensor EMG activation, which indicated lower trunk stiffness at shoulder height (Lee et al., 2012). Other push/pull factors that influence low back and shoulder loading such as surface type have also been investigated. Laursen and Schibye (2002) estimated shoulder and low back compression loads during push and pull up to 50 kg across smooth, bumpy, and soft surfaces in professional waste collectors. Generally, low back loading was small during pushing, with peak compression force being less than 1200 N, and peak shear under 200 N, and surface did not affect the low back region. On the contrary, shoulder moments were largest during the onset of 1-handed pulling, and all shoulder moments were higher on the non-smooth surfaces (Laursen & Schibye, 2002). Recently, Cudlip et al. (2015) examined the effects of sitting and standing on shoulder and low back moments during static and dynamic manual materials handling tasks, including pushing. These authors found that while pushing, the low back had larger moments in standing compared to sitting, whereas the shoulder showed an opposite effect, with higher moments found in sitting (Cudlip et al., 2015). As a whole, pulling tends to increase the loading on the low back, whereas pushing increases the load on the shoulder. Additionally, pushing while seated or from shoulder-height decreases the low back moment while increasing the shoulder moment, which highlights the importance of arm and body posture in determining low back loading.

The effect of working height is also influential on low back and shoulder loading throughout a variety of tasks. For example, Faber et al. (2009) compared the effects of concrete block mass and working height on low back and shoulder loading in nine experienced masonry workers. Using a single link-segment model, net moments and reaction forces were estimated at the shoulder using a top-down approach, and at L5/S1 using a bottom-up approach. It was found that the low back and shoulder loading had opposite effects during working height changes, as working close to the ground resulted in largest low back loading with the smallest shoulder loads, whereas working above shoulder height showed the largest loading in the shoulder and smallest at L5/S1 (Faber et al., 2009). Similar L5/S1 loading patterns were found by Davis and Marras (2005) from an EMG-assisted model used to estimate the compression and shear forces at L5/S1 during changes in lift origin and destination. Lifting from combinations of shoulder, elbow, and knee height, it was found that knee height produced the greatest amount of compression, whereas anterior-posterior shear was largest when the shoulder height was the destination (Davis & Marras, 2005). Furthermore, a recent study of 25 experienced cashiers evaluated the influence of workstation height, packaging type, and workload intensity on neuromuscular demand of upper-extremity and trunk muscles in a mocked-up cashier checkout station (Maciukiewicz et al. (2017)). Overall, the muscular demand was found to be smallest when the workstation height was just below the elbow, and sensitivity to workstation height was higher in the shoulder musculature compared to the low back musculature (Maciukiewicz et al., 2017).

The overall trade-off between shoulder and low back loading is multifactorial in nature. In general, work performed closer to the ground tends to increase the loading demands on the low back, while decreasing those at the shoulder. On the contrary, upper-extremity positioning

above shoulder height tends to increase the demands at the shoulder while decreasing those at the low back. This loading trade-off is likely due to the changes in force transmission resulting from the changing arm position. For example, as the arms are raised overhead, the lines of action of the scapulothoracic muscles will change, however the ES will not, thus increasing the loading at the shoulder. As the arms are lowered and the spine is flexed towards ground-based work, the loading on the spine will be increased as the shoulder loading decreases due to the reduction in ES pennation angle, thereby requiring larger posterior-directed forces to resist the anterior shear forces. Furthermore, changes in body position such as sitting and standing also influence the loading in both the shoulder and low back. These results highlighted the importance of arm and body positioning for consideration of the loading trade-off between the shoulder and low back.

2.2 Functional Anatomy of the Thoracic Spine

The adult human vertebral column consists of 26 vertebrae: seven cervical, 12 thoracic, five lumbar, one sacrum (consisting of five fused sacral vertebrae), and one coccyx (consisting of three to four fused coccygeal vertebrae) (Tortora, 2004), with the thoracic region being the area of interest for the purpose of this dissertation. There are many unique anatomical features of the thoracic spine including the interaction with the rib cage, transitions between lumbar and cervical levels, and the interface with the scapulothoracic-axial skeleton.

The rib cage is one of the more notable features of the thoracic spine, with pairs of ribs attaching to each side of the thoracic vertebra, and the first seven ribs attaching directly to the sternum (Tortora, 2004). The rib cage provides a stabilizing feature which has been examined *in vitro* in human cadavers. For example, Oda et al. (2002) found an increase in range of motion in all three planes with unilateral removal of the rib joint, and Watkins et al. (2005) found that an

intact rib cage and sternum provided 42% of the stiffness during flexion/extension. In addition, mathematical modelling has suggested that articulation with the ribs provided more structural stability in the mid-thoracic region (Andriacchi et al., 1974), which suggested regional differences of the thoracic spine in terms of structure and function. Recently, Liebsch et al. (2017) tested six fresh frozen human thoracic spines (C7-L1) to assess the stabilizing effect of the rib cage on the thoracic spine during cardinal plane motions. When the rib cage was removed the range of motion in each direction was increased, highlighting the contribution of the rib cage to thoracic spine stability. It was concluded that the rib cage plays a large role in limiting the flexibility of the thoracic region and is the primary source of stability to that region, as opposed to the cervical and lumbar regions which are stabilized by surrounding musculature (Liebsch et al., 2017).

Differences in anatomical structure of the thoracic spine are found due to the natural curvature and the transitions between the cervical and lumbar regions. For example, rotation in the mid-thoracic region is thought to be greater than in the upper and lower regions because the axis of rotation lies inside the vertebral body of the mid-thoracic region, yet outside the vertebral body in the upper and lower region (Davis, 1959). Additionally, bony elements such as the spinous and transverse processes tend to decrease in length moving towards the lumbar regions (Panjabi et al., 1991), further highlighting difference within the thoracic region. Differences in functional anatomy between thoracic regions are important to note as there are implications for region-specific findings for different task demands, particularly in the upper-mid thoracic region at T4 where the scapulothoracic area of the shoulder connects to the axial skeleton (Peat, 1986).

The scapulothoracic area is located lateral to the midline and considered part of the shoulder complex where the scapula glides over the rib cage (Peat, 1986). An important

consideration here is the attachment of the scapula to the axial skeleton, as this region could play a role in shoulder-low back trade off through the thoracic spine. The muscles that connect from the medial border of the scapula to the spinous processes of the upper-mid thoracic spine (e.g. T4 level) include trapezius and rhomboids (Peat, 1986; Vasavada et al., 2011), which provide an adduction force to balance rotator cuff abduction (Peat, 1986). The trapezius and rhomboids also have different innervations, as trapezius is innervated by spinal accessory nerve (CN XI) and cranial nerves (C3-C4), whereas rhomboids are innervated by the dorsal scapular nerve (C5-C6) (Agur & Dalley, 2009). At the T4 level, the ES musculature is deep to both trapezius and rhomboids and the interaction that occurs between these superficial scapulothoracic muscles and the deep ES muscles remains unknown.

The ES at the T4 level appears to be a transition area between the origin of cervicis and insertion of thoracis muscles. For example, longissimus and semispinalis cervicis have origins at T4 transverse processes and insert onto the cervical vertebrae, whereas longissimus thoracis, spinalis thoracis, and semispinalis thoracis originate at the lumbar or lower thoracic vertebrae and have insertions at T4 (Tortora, 2004; Vasavada et al., 2011). However, each of these ES groupings are all innervated by the posterior rami of spinal nerves (Agur & Dalley, 2009). The multi-crossings of different ES muscles have implications for the T4 level to be a complex, multi-functioning region.

Complex anatomy and architecture are a characteristic of spinal muscles, though are often overlooked when assessing the function of these muscles (Vasavada et al., 2011). For the purpose of this dissertation, architectural characteristics (morphology) will refer specifically to the muscle thickness and pennation angle. It is generally well established that the obliquely oriented fibres of LES are capable of producing posterior shear forces (Potvin et al., 1991), with

changes in posture affecting the line of action of the LES (Macintosh et al., 1993). What is less clear however, are the changes in morphology of T4ES throughout a variety of postures.

Previous studies on human cadavers of longissimus thoracis showed little pennation angle, indicating forces are primarily acting in compression; however, during flexion large increases in shear production were found at the lumbar level, indicating shear forces were most sensitive to changes in orientation of the lumbar vertebrae (Macintosh & Bogduk, 1991). In an attempt to provide a dataset for modelling the lumbar, thoracic, and cervical spines, Bayoglu et al. (2017a & 2017b) measured pennation angles of ES from semispinalis thoracis at C7-T8, and longissimus thoracis starting from T4; however, these author's did not record pennation angles under 10°, thus did not provide an angle measurement for these muscles. However, Delp et al. (2001) recorded a mean (*SD*) pennation angle of 12.6° (5.8) from longissimus thoracis in five cadavers, which further supported a shallow pennation angle of the thoracis muscles. In terms of ES thickness, recent imaging findings have shown LES to range from 2.55 cm (Watanabe et al., 2004) to 3.88 cm (Belavý et al., 2015); however, the thickness of T4ES remains unknown.

Reviewing the functional anatomy of the thoracic spine revealed some key points in the literature. For example, the T4 region could be highly complex with its functioning due to its transition from cervical to thoracic, as well as the interface with the scapulothoracic musculature. As such, the interaction of the deep T4ES with the surrounding superficial muscles remains unclear; particularly in how the morphology of T4ES changes with varying postures, which could ultimately impact the function of this muscle in the region.

2.3 Ultrasound and Magnetic Resonance Imaging

2.3.1 Ultrasound Imaging

In terms of musculoskeletal imaging, USI is among the most widely used partly due to being cheap and fast to use (Bharath, 2009). The ultrasound image itself is accomplished with a pulse-echo technique of high frequency sound (> 20,000 Hz) generated by a transducer which produce echoes at anatomical boundaries (Kremkau, 2011). Briefly, the transducer houses crystals which are stimulated by an electrical current and generate ultrasound waves that penetrate into the tissues and are reflected back to the transducer (Whittaker & Stokes, 2011). The three parameters of the echo that determine the structure of the image (pixels) are: where along the transducer the sound wave arrives, how long it took, and the amplitude (strength) of the signal (Whittaker & Stokes, 2011). The horizontal and vertical placement of the pixel is dependent on where along the transducer the wave arrives and how long it took to go out and back, respectively, and the brightness is determined by the amplitude (Whittaker & Stokes, 2011). Tissues with more densely organized collagen fibres reflect sound better and appear bright white on the image, such as bone and the surrounding fascia within muscles (Whittaker & Stokes, 2011). These echogenic characteristics allow for evaluation of muscle morphology such as muscle thickness and pennation angle, and how these features change with contraction or tissue movement (Whittaker et al., 2007).

2.3.2 Magnetic Resonance Imaging

Conversely, MRI is widely considered the gold standard of musculoskeletal imaging (Whittaker et al., 2007), though it is more expensive and less accessible than USI (Tan et al.,

2003). Briefly, the basis of MRI comes from the spinning nucleus of a hydrogen (H^+) atom about its own axis, by which the nuclei tend to align their axis of rotation in an applied magnetic field, creating a dipole moment of the nuclei (Bharath, 2009). A radiofrequency pulse is then applied and 'tips' the dipole moment vector, which creates a longitudinal and transverse component (Buxton, 2002). The transverse component then precesses around the direction of the magnetic field which creates a detectable signal, and over time the nuclei return to their original states (Buxton, 2002). The timing of the return to the original state is known as the relaxation period, where the longitudinal component of the dipole moment vector recovers along the vertical (z-) axis (T1 relaxation) and the transverse component decays in the x-y plane (T2 relaxation) (Buxton, 2002). The radiofrequency pulse is then repeated at specific time intervals (repetition time: TR), which produces an echo of the original signal at the echo time (TE) as a result of the individual magnetization vectors coming back in-phase after the radiofrequency pulses (Buxton, 2002). The resulting image is a map of the local transverse magnetization of the hydrogen nuclei (Buxton, 2002), with different variations in contrast arising from the variations of T1 and T2 in the image tissues (Bharath, 2009).

The main tissues from where the hydrogen atoms come from within the human body are water and fat, with the oxygen-bound hydrogen from water and carbon-bound hydrogen from fat having different electrical properties (Nitz, 2006). It is the T1 and T2 weighting that separates these tissues by contrast, where an increase in T2 relaxation time indicates an increase in the mobility of the water molecules (Nitz, 2006). As such, a T2-weighted images means that tissues like muscle that have a short T2 relaxation time will show up darker, and tissues with longer T2 relaxation times such as fat and water will appear brighter (Nitz, 2006).

2.3.3 Ultrasound Reliability & Validity

The reliability and validity of USI is an important consideration for musculoskeletal imaging, particularly in paraspinal muscles. In the lumbar region, the multifidus is commonly examined with USI (Stokes et al., 2007), with high intra-rater reliability ($ICC(3,k) > 0.82$) typically being found in lumbar multifidus thickness measures (Djordjevic et al., 2014; Kiesel et al., 2007; Koppenhaver et al., 2009; Sions et al., 2015; Teyhen et al., 2011; Van et al., 2006; Wallwork et al., 2007). With LES, reliability of USI thickness has varied by spinal level and side ($ICC(1,1) = 0.57-0.87$; Belavý et al., 2015), and there are presently no studies that have looked at reliability of pennation angle measured by USI in the ES muscles.

In terms of comparing USI to MRI directly in paraspinal muscles, little research exists. For example, Hides et al. (1995) compared cross-sectional area (CSA) of lumbar multifidus from USI and MRI and found no differences between the measures. Additionally, Belavý et al. (2015) found that USI and MRI measures of LES thickness agreed with each other via Bland-Altman testing, though the correlation ranged from $r = 0.30-0.62$, which was likely a result of the lower reliability reported from USI. These results showed that USI was generally valid and reliable for paraspinal muscles; however, there remain relatively few comparisons between USI and MRI in the ES musculature. In particular, the T4ES morphology has not been documented *in vivo*, so a gap in the literature remains as to the reliability and validity of measures such as muscle thickness and pennation angle measured from both USI and MRI.

2.4 Collection Techniques of the Thoracic Spine

2.4.1 Kinematic Data

A number of methods have been identified over the years to allow the collection of kinematic data from different regions of thoracic spine, including bone pins, electromagnetic sensors, and electrogoniometers. Invasive techniques such as bone pins have been used in classical works to assess rotation at various thoracic levels (Gregersen & Lucas, 1967), whereas non-invasive techniques are more commonplace. Electromagnetic sensors have been employed during thoracic twist (Willems et al., 1996) and sagittal plane movement (Burnett et al., 2004; Claus et al., 2009); however, the accuracy of electromagnetic sensors is greatly dependent on the objects around the capture space, and distortion can also occur from non-ferrous aluminum and computer equipment (McGill et al., 1997). Utilization of electrogoniometers for angles of thoracic kyphosis has occurred in both a sport (Rajabi et al., 2008) and occupational setting (Nairn et al., 2013a); with high reliability and validity found in lower extremity motion (Bronner et al., 2010).

By far the most common method used to record thoracic spine angles is MoCap, which is considered the gold standard for motion recording. For example, Edmondston et al. (2007) looked at axial rotation of the mid-thoracic region using four passive-reflective markers, whereas Preuss and Popovic (2010) used 22 passive-reflective markers to partition the thoracic spine into four regions and found complex interactions amongst region in a variety of bend and twist trials. Partitioning the thoracic spine into different levels was also done using markers attached to semi-rigid plates (Cotter et al., 2014; Nairn et al., 2013b, 2013c; Nairn & Drake, 2014; Schinkel-Ivy et

al., 2013; Silvestri et al., 2013) and with three-dimensional protrusions of marker clusters (Schinkel-Ivy & Drake, 2015b; Schinkel-Ivy et al., 2014).

Another tool that is more clinical in nature is Flexi, which has been used to characterize sagittal plane spine angles. Briefly, Flexi is able to retain its shape when bent in one plane, so when contoured down the spine it can be removed and a tracing of the curvature can be made onto paper for further analysis. Originally developed for tracking kyphosis and lordosis by ratios of length and width in an ageing population (Milne & Lauder, 1974) there have been several applications to obtain an angular metric. For example, an angle of thoracic kyphosis calculated from trigonometric derivation of the length and width of the curvature has shown good correlation to radiographic measures (Hart & Rose, 1986). Additionally, a method has been described that involves drawing tangents to the curvature and measuring the angle between tangents (Burton, 1986); however, this has only been performed within the lumbar region (Taweetanalarp & Purepong, 2015; Tillotson & Burton, 1991; Youdas et al., 1996, 2006).

To summarize, optoelectronic motion capture is considered the gold standard, however other tools such as Flexi may be more readily available and require minimal technical expertise to utilize. To date, Flexi measures have been compared to other external measurement devices such as inclinometers (Thompson & Eales, 1994; Tillotson & Burton, 1991), and Debrunner kyphometers (Greendale et al., 2011; Tran et al., 2016); however, Flexi has not been compared to the gold standard MoCap, implying its true accuracy with respect to external measurements devices remains unknown.

2.4.2 Electromyography

The use of surface EMG is a common way to investigate muscle activity from the trunk. Before interpretation of EMG signal can occur, the signal is often normalized to a reference value, most frequently as percentage of a maximum voluntary contraction (%MVC) (Burden, 2010). Normalizing EMG to a %MVC allows for signal to show biological relevance and can be used to compare between individuals (Lehman & McGill, 1999). Testing different MVC postures on a muscle has been done previously in specific muscles such as latissimus dorsi (Beaudette et al., 2014; Park & Yoo, 2013) and trapezius (Ekstrom et al., 2005), as well as over a variety of trunk muscles (Ng et al., 2002, Vera-Garcia et al., 2010). Specific to the trunk, Ng et al., (2002) assessed the maximum activation of the abdominals, latissimus dorsi, and lumbar ES in the three different planes of motion. Large amounts of activity were found in non-sagittal planes in axial rotation (latissimus dorsi) and lateral bending, (LES) and it was concluded that non-traditional planes should also be examined with different MVC postures (Ng et al., 2002). Vera-Garcia et al. (2010) looked at 11 different MVC postures in the same muscles as Ng et al. (2002), but also included lower-thoracic ES at T9. Vera-Garcia et al. (2010) found sagittal plane extension produced the largest activation of ES; however, noted that an extension where the upper body was fixed and the lower-torso lifted was largest for T9ES. This extension posture was different than the traditional lumbar extension where the lower body was fixed and the upper-torso was lifted against resistance, which showed largest activation of LES (Vera-Garcia et al., 2010). This implied that the traditional lumbar extension where the upper-body is lifted from a fixed pelvis may not be best for all levels of ES.

A review of EMG normalization by Burden (2010) also noted other potential normalization techniques as an alternative to MVC. These other techniques include: the mean

EMG from the task being performed, the peak EMG from the task, and submaximal isometric and dynamic contractions (Burden, 2010). One of the key advantages to using techniques such as the peak or mean EMG from the task or a submaximal contraction is the reduction in inter-individual variation (Yang & Winter, 1984). However, these techniques do not provide information regarding the amount of muscle activation required to actually perform the task (Yang & Winter, 1984) and would show day-to-day variability thus limiting their use between different trials or individuals (Burden, 2010). In addition, if a standardized reference posture is to be used, it should reflect some of the required task demands to ensure a reasonable ratio of task demand to reference trial activation for interpretation purposes.

Recently, T4ES has garnered interest in the literature throughout a variety of tasks/functions, yet, there does not appear to be a standardized method for normalization. For example, T4ES has been analyzed as a cervico-thoracic extensor during sitting (Burnett et al., 2009; Caneiro et al., 2010; Edmondston et al., 2011), as well as a lumbar/trunk extensor during prolonged sitting (Schinkel-Ivy et al., 2013; Nairn et al., 2013b), short-duration sitting (Ang et al., 2016; Nairn et al., 2013c), and during functional tasks such as flexion/extension, lateral bend, and axial twist (Kienbacher et al., 2016; Nairn & Drake, 2014; Schinkel-Ivy & Drake, 2015a). Each of these analyses of T4ES have been reported as a %MVC and presumed to come from a traditional extension task, with the exception of Burnett et al., (2009), who briefly described a thoracic extension task where participants lifted their chest and shoulders off of a table from prone. However, this thoracic extension task, along with the traditional lumbar extension and any other out-of-plane movements designed to elicit a maximum contraction has not been tested in T4ES. This information would add to the literature of standardizing collection techniques for the T4ES muscle.

2.5 Passive and Active Postures in the Thoracic Spine

Passive postures are generally defined as relaxed in nature with minimal requirement for muscle activity (O’Sullivan et al., 2002). These include slump sitting (O’Sullivan et al., 2002) and standing (Dolan et al., 1988), and fully-flexed postures in sitting (Ang et al., 2016) and standing (Floyd & Silver, 1955), where end-range flexion has shown reduction in ES activity. For the purpose of this dissertation, upright sitting and standing were considered passive postures as no volitional contractions were required; however, it has been noted that upright sitting can increase thoracic ES activity when compared to slump sitting (Claus et al., 2009; Edmondston et al., 2011; Nairn et al., 2013c; O’Sullivan et al., 2002). It is also important to note that in the context of this dissertation, the term “passive” did not refer to the passive stretch that occurs in muscle, it was referring to the postures that have a lack of volitional contraction.

Each of upright, flexed, and slumped has important implications for injury risk. For example, Briggs et al. (2007) found that natural changes in upright kyphosis increased the shear and overall loading of the thoracic spine. End-range flexion has been shown to be a risk factor for workplace injury in combination with factors such as lift rate and lateral and twisting motions (Marras et al., 1993, 1995). Additionally, full flexion has been shown to decrease LES muscle thickness (Watanabe et al., 2004) and pennation angle (McGill et al., 2000), which could alter the loading pathways through the muscle. Slumped sitting has been characterized by posterior pelvic rotation, near full-range of flexion in the mid- and lower-thoracic regions, with near half-range in upper-thoracic and lumbar (Nairn et al., 2013c). It has been suggested that adopting passive postures is associated with motor dysfunction and tend to exacerbate low back pain (O’Sullivan, 2000). Considering that passive postures have resulted in changes to the underlying

muscle morphology, and the resulting muscle activation can have clinical implications, insight into these postures in T4ES would seem warranted.

Active postures were defined here as those which were sustained or produced by volitional muscle contraction. The term “active” was not synonymous with “dynamic”, as the contractions were still performed from a static posture. Concerning the T4ES muscle in particular, there were few studies which examined this muscle in active postures. For example, Nairn and Drake (2014) assessed the interaction between the thoracic and lumbar spines in a variety of planar and multi-planar movements. High activation of ipsilateral T4ES EMG during axial twist was reported (44 %MVC), indicating a possible functional role of this muscle other than a trunk extensor (Nairn & Drake, 2014). During flexion and extension tasks, the sequencing of T4ES in relation to other trunk muscles was assessed by cross-correlation (Schinkel-Ivy & Drake, 2015a), whereas Kienbacher et al. (2016) took the RMS of T4ES and LES to represent combined extension activity in a clinical low back pain population. Maximum voluntary contractions would also be considered active postures, as Burnett et al. (2009) briefly described their T4ES MVC extension protocol.

What is still unknown however, is how the underlying morphology of T4ES and the muscle activity that is recorded are related during both passive and active postures. This could provide insight into the complexity of movement patterns and muscle activation patterns currently viewed at the T4 level.

2.6 Trunk Muscles and Challenged Breathing

Trunk muscles play a large number of roles during activities of daily living, such as generating moments to produce movement, stabilizing the spine to prevent buckling, and even

during ventilation to assist with air flow (McGill et al., 1995). For example, Hodges and Gandevia (2000) used fine-wire EMG to record activation from the costal diaphragm at the 7th or 8th rib, fine-wire EMG from TransAb, and surface EMG from LES during quiet standing and rapid arm movements. Differences in breathing phase were found in TransAb, as activation was larger during expiration than inspiration, whereas LES did not show this phase difference (Hodges et al., 2000). Similarly, McGill et al., (1995) found that during normal and challenged breathing (10% CO₂ mixture), T9ES and L3ES activation did not change. On the contrary, in maximal voluntary ventilation (MVV) trials where participants breathed in and out as fast as possible with deep breaths, Wang and McGill (2008) found increased activation of L3ES during inspiration, which was attributed to the lifting of the rib cage. Clinical implications have also been discussed in relation to challenged breathing, as those with LBP have shown an increase in spinal stability while ventilating a 10% CO₂ mixture (Grenier & McGill, 2008). Additionally, individuals with breathing disorders such as COPD have shown impaired balance recovery and greater trunk muscle activity following exercise (Smith et al., 2016). The results of these studies highlighted the importance of the trunk musculature during a multitude of tasks. As such, it remains unclear what is the role, if any, of T4ES during ventilation. This information could be useful for future analyses such as spinal stability and the role of the thoracic musculature, as well as for potential clinical outcomes, such as those with LBP or COPD.

2.7 Summary of Key Points

Based on the above literature it was evident that there were gaps regarding the basic characterization of the upper-thoracic spine, even though its proximity to the scapulothoracic region indicated it could play a role in transferring loads from the shoulder to the low back. For

example, information on muscle morphometry *in vivo* was commonly assessed in lumbar multifidus, less so in LES, and virtually non-existent in T4ES. Additionally, standardized collection procedures, such as MVC protocols, were well established in the lower trunk and abdominal muscles, yet tests of different MVC postures have not been attempted on T4ES. Access to information was also an important consideration, which included the types of equipment available to collect spine kinematics. With a primarily clinical tool (Flexi) being used to provide estimates of sagittal plane spine angles, it was important to know how this tool compared to the gold standard MoCap. Furthermore, application of structural and functional changes in T4ES could be brought to light through analysis of passive and active posture, as well as during functional tasks such as breathing. By closing some of these gaps in the literature through this dissertation, there was a better understanding of how the upper-thoracic spine functioned, and how future work can continue to address the application of T4ES, such as the role during challenged breathing or load transfer.

Chapter 3: Common Methods

This section outlines all collection and processing methods that were shared by at least 2/5 of the studies. Specific methods were discussed in each Chapter, and readers were referred to this section where applicable. The following list briefly summarizes each of the studies:

- Study #1: USI-MRI – Testing the reliability and validity of USI to measure thickness and pennation angle of T4ES
- Study #2: T4ES-MVC – Analyzing MVC techniques in T4ES
- Study #3: Flexi-MoCap – Testing the reliability and validity of a pen-and-paper method for calculating sagittal plane spine angles
- Study #4: USI-EMG – Relating changes in T4ES thickness and pennation angle to muscle activation
- Study #5: Application-Pilot – An example of the application of T4ES during breathing

3.1 Participants

A total of 86 participants were recruited for the five studies, 44 males and 42 females. All participants were university-aged and free of neck, back, and shoulder pain for at least one year prior to collection. Recruitment took place by word-of-mouth convenience and through an online undergraduate research-participant system. All studies were approved by York University's Research Ethics Board, and informed consent was obtained for both collection and photography protocols. The same participants (n=30) were used for both Study #2: T4ES-MVC and Study #4: US-EMG, whereas Study #1: US-MRI, Study #3: Flexi-MoCap, and Study #5: Application-Pilot each had separate participant recruitment (n=20, 20 and 16, respectively).

3.2 Ultrasound Imaging

All ultrasound images were taken from a parasagittal view using “Brightness” mode (b-mode), which is the most common mode of USI acquisition that displays the ultrasound echo as a cross-sectional grey-scale image (Whittaker et al., 2007). Additionally, b-mode USI has been well established for measuring the static architecture (e.g. thickness and pennation angle) of a muscle, as well as changes to the architecture over time (Whittaker et al., 20017). The parasagittal view allows for both muscle thickness (cm) and pennation angle ($^{\circ}$) to be measured from a single image (Cuesta-Vargas & Gonzalez-Sanchez, 2013). Other USI views such as a transverse plane would allow for recording other metrics such as CSA (cm^2) and linear widths of the muscle. However, the variables of interest for this dissertation were muscle thickness and pennation angle, therefore a parasagittal b-mode USI was used.

Ultrasound imaging was used for Study #1: USI-MRI and Study #2: USI-EMG to analyze the thickness and fibre orientation angle of T4ES. Specific body position/trials were addressed in the appropriate chapters. Two different ultrasound systems were used: Study #1: USI-MRI used a SonoSite M-Turbo ultrasound system with linear transducer model HFL38x, 13-6 MHz (SonoSite Canada Inc., Toronto, Canada); whereas Study #2: USI-EMG used a Mindray DP-6900 ultrasound system with a linear transducer model 75L60EA, 7.5 MHz (Shenzhen Mindray Bio-medical Electronics Co., Ltd., Nanshan, P.R. China). Image processing for both Studies was done using Merge eFilm Workstation (v.4.2.0, Merge Healthcare, Chicago, USA).

3.3 Electromyography

Surface EMG electrodes were used to record muscle activation primarily from the T4 region. Surface electrodes are considered readily available and easy to apply compared to indwelling electrodes (Soderberg & Knutson, 2000). One of the drawbacks of surface EMG is that it can be limited when recording activity from a deep muscle (Kamen, 2004) and the recording is not selective to a given muscle (Soderberg & Knutson, 2000). However, the generalizability of surface EMG could provide insight into what the muscles of a certain region are doing. On the contrary, though indwelling EMG is considered ideal for deep muscle activation, its applications are limited as the recorded signal is from a specific muscle fibre (Soderberg & Knutson, 2000). Thus surface electrodes were used to provide an indication of the general muscle activity at the T4 level.

Electromyographical data were recorded for Study #2: T4ES-MVC, Study #4 USI-EMG, and Study #5: Fatigue-Pilot, but not for Study #1: USI-MRI or Study #3: Flexi-MoCap. The T4ES muscle was the region of interest specific to all three studies, and the middle-trapezius at T3 (MidTrap) was also analyzed in Study #2: T4ES-MVC. Though electrodes were also placed over the abdominals, LES, latissimus dorsi, and trapezius, these additional muscle sites were not the focus of the current research questions.

3.3.1 Collection Specifications

Prior to electrode placement, the skin was prepared by shave and alcohol swab over the area of interest in order to assist with adherence (Soderberg, (1992). Pairs of Ag-Ag/Cl surface EMG electrodes (Ambu® Blue Sensor N, Ambu A/S, Denmark) with a centre-to-centre spacing of 2.5 cm were placed approximately 2.0-2.5 cm from the midline at the T4 level, which was

located by palpating the spinous processes down from the 7th cervical vertebra (C7). For Study #2: T4ES-MVC and Study #4: USI-EMG, electrodes were placed unilaterally on the dominant side, while in Study #5: Fatigue-Pilot EMG data were recorded from T4ES bilaterally. The orientation of the electrodes was aligned with respect to the muscle fibres to ensure optimal recording of the amplitude of the signal (De Luca, 1997; Vigreux et al., 1979). All EMG signals were differentially amplified (frequency response 10-1000 Hz, common mode rejection 115 dB at 60 Hz, input impedance 10 G Ω ; model AMT-8, Bortec, Calgary, Canada) and converted from an analog to digital signal at a sample rate of 2048 Hz using an Optotrak system with NDI First Principles software (Northern Digital Inc., Waterloo, Canada).

3.3.2 Maximum Voluntary Contractions

Prior to interpreting the EMG signal in a biologically relevant manner between participants, it was important to normalize the signal to a standardized reference value (De Luca, 1997; Lehman & McGill, 1999). In a healthy population, the MVC is considered the most popular to use and the most powerful strategy for physiological interpretation of the EMG signal (Burden, 2010; Lehman & McGill, 1999).

As the MVC protocol for T4ES was the focus of Study #2: T4ES-MVC, details will be left for the specific study chapter. Briefly, the results of Study #2: T4ES-MVC recommended a thoracic back extension for eliciting a MVC. For this thoracic extension, participants were prone on a therapy table and positioned at the edge of the table at approximately the T6 level. Participants attempted to raise their upper-trunk while manual resistance was applied downward at the back of the shoulders. This protocol was then applied for the processing of Study #4: USI-EMG, and for the collection of Study #5: Application-Pilot.

3.3.3 Linear Envelope

All EMG data processing was done using Visual3D software (v. 5.02 & v.6.01.03, C-Motion Ltd., Germantown, USA). Briefly, EMG data were full-wave rectified, and low-pass filtered using a 4th order dual-pass Butterworth filter with a cut-off frequency of 2.5 Hz (Brereton & McGill, 1998) to produce the linear envelope of the signal. The linear envelope is essentially a moving average of the time-varying EMG signal, and was used due to it closely resembling the shape of the tension curve (Winter, 2009).

3.4 Active Postures

The term Active Posture is used to describe the static postures that require volitional muscle contraction. These are the MVC postures from Study #2: T4ES-MVC and the sub-max postures from Study #4: USI-EMG. Table 3.1 provides a description of these postures.

3.5 Statistical Analyses

All statistical analyses were performed using IBM SPSS Statistics (v.24, SPSS Inc., Chicago, IL). Common to each study was a mixed-model ANOVA, which included a within-factor repeated measures component, and a between-factor test for sex differences. Due to the repeated measures element, Sphericity was tested for using Mauchly's W test. Briefly, Sphericity is the assumption that the repeated measures demonstrated homogeneity of variance and homogeneity of covariance (Vincent, 2005). If any violations did not affect the results, the original degrees of freedom were reported, otherwise, a Greenhouse-Geisser correction was used (Vincent, 2005). For all statistical analyses alpha was set to 0.05.

Table 3.1. Full description of the Active Postures used in Study #2: T4ES-MVC and Study #4: USI-EMG.

Active Posture	Description
ThorExt	Thoracic extension MVC technique – prone position, extending over therapy table from ~T6 level with manual resistance applied downward
LumbExt	Lumbar extension MVC technique – prone position, extending over therapy table from the hips with manual resistance applied downward
Raise-Stand	Arm raise MVC technique while standing – shoulder abducted to 90°, elbow flexed to 90° so upper-arm and forearm are at right angles and both are parallel to the floor. Manual resistance was applied downward on upper arm while participants attempted arm abduction.
Raise-Sit	Same arm position as Raise-Stand – from a seated position
Row-Stand	Pulling MVC technique while standing – elbow flexed to 90° with 0° shoulder flexion/extension or ab/adduction. Manual resistance was applied behind the elbow and pulling towards researcher while the participant attempted to extend their upper arm while retracting their scapula.
Row-Sit	Same as Row-Stand – while seated at the end of a therapy table
LatPull-Stand	Lateral pulldown MVC technique while standing – shoulder abducted to 90°, elbow flexed to 90°, with the forearm rotated perpendicular to the floor, hand directed upwards. Manual resistance was applied upward at the elbow while participants were instructed to pull their arms down and “attempt to place their elbows into their back pockets”.
LatPull-Sit	Same as LatPull-Stand – while seated at the end of a therapy table

Chapter 4: Study #1: USI-MRI

4.1 USI-MRI Introduction

The thoracic spine is the anatomical region between the low back and shoulder, yet remains less understood compared to those surrounding regions. For example, two of the most common work-related musculoskeletal disorders issues reported in epidemiological literature are on the low back and shoulder (Punnett & Wegman, 2004). Additionally, a trade-off between working height and low back and shoulder loads has been reported (Faber et al., 2009); however, the mechanism of load transfer from the shoulder to the lumbar spine through the thoracic spine is not yet understood. Although motion in the thoracic spine is limited by anatomical features such as the ribcage (Watkins et al., 2005), it has been shown that analyzing the thoracic spine when partitioned into different segments reveals the complexity of the movement patterns within this region (Nairn & Drake, 2014; Preuss & Popovic, 2010). As such, analysis of sub-regions within the thoracic spine, particularly in the erector spinae at the T4 level (T4ES), is of interest given its proximity to the scapulothoracic interface. Changes in muscle morphometry such as thickness and pennation angle were shown to be related to changes in extremity and abdominal muscle activation (Hodges et al., 2003), highlighting the functional significance of underlying structural changes. In addition, changes in morphology such as increases in thickness and pennation angle have been associated with muscle activation in LES (Cuesta-Vargas & Gonzalez-Sanchez, 2013), with pennation angle changes dictating the direction of the forces (Macintosh et al., 1993). Less information about these characteristics are known in the thoracic spine, so understanding the structural morphometry of T4ES will begin to shed light on the

functional aspects of this region, which will further develop the interpretation of the shoulder-low back injury mechanism.

Ultrasound imaging has shown promise for musculoskeletal examination as it is safe and cost effective (Whittaker et al., 2009), and has demonstrated general reliability for paraspinal muscle measures (Stokes et al., 2007). Currently, lumbar multifidus is the most widely studied trunk muscle by USI, with recent interest in the trapezius muscle (Stokes et al., 2007). In the ES musculature, few studies have used USI to measure lumbar thickness (Belavý et al., 2015; Cuesta-Vargas & Gonzalez-Sanchez, 2013; Desmoulin & Milner, 2007; Watanabe et al., 2004) and lumbar pennation angle (Cuesta-Vargas & Gonzalez-Sanchez, 2013; Harriss & Brown, 2015; McGill et al., 2000; Singh et al., 2011), whereas there has not been any documented imaging of the T4ES morphometry measured by USI.

Reliability of USI muscle thickness has been reported in various levels of the trunk primarily using intraclass correlation coefficients (*ICC*), but also including measures such as the Standard Error of Measurement (*SEM*), and the Minimum Detectable Change (*MDC*). In the thoracic region, muscle thickness reliability has been reported as: lower-trapezius between T7-T9, *ICC* = 0.89-0.91 (O'Sullivan et al., 2007); middle-trapezius at T1, *ICC* = 0.67 (Bentman et al., 2010); and rhomboid major between T2-T5, *ICC* = 0.933-0.977, (Jeong et al., 2016). Lumbar ES thickness measures showed variable reliability from USI, as Belavý et al. (2015) reported *ICC* = 0.57-0.87, depending on the spinal level. Lumbar multifidus thickness measures tended to show high levels of reliability, with *ICC* ranges ranging from 0.85 – 0.98 (Djordjevic et al., 2014; Kiesel et al., 2007; Sions et al., 2015; Teyhen et al., 2011; Van et al., 2016; Wallwork et al., 2007). The *SEM* is an indication of the within-subject variability across repeated trials, and the *MDC* represents the amount of change needed to exceed the measurement

error (Wagner et al., 2008). Both of these measures have been recommended for complimenting USI reliability (Whittaker et al., 2007), and have been implemented in studying LES thickness reliability from USI. For example, Belavý et al., 2015 found *SEM* values of 0.20-0.40 cm and *MDC* values of 0.55-1.11 cm depending on side and level of LES with thickness ranges from 3.18-4.94 cm. Based on these findings, it is likely that the intra-rater reliability will be acceptable for the yet to be quantified T4ES USI measures, as shown through high *ICC* values and low *SEM* and *MDC* measures.

In terms of determining accuracy of USI, there have been relatively few studies that have directly compared USI to MRI in terms of paraspinous thickness, with no studies comparing ES pennation angle between modalities. For example, O'Sullivan et al. (2009) compared thickness measures of the upper-trapezius (C6), middle-trapezius (T1), and lower-trapezius (T5 and T8) between USI and MRI in 18 healthy participants. It was found that Pearson's *r* values ranged from -0.22 to 0.77, and mean differences between methods were up to 1.8 mm at the T5 level (O'Sullivan et al., 2009). Bilateral lumbar ES thickness in 23 healthy males at five spinal levels (L1-L5) was recently measured in USI and MRI by Belavý et al. (2015), with mean differences ranging from -0.06 -0.97 cm and an average thickness of 4.37 cm, and Pearson's *r* being described as 'typically moderate', ranging from $r = 0.30-0.62$. Lumbar multifidus CSAs from L2-S1 were compared in 10 female participants using inferential statistics, with no significant differences being found in multifidus CSA between right-left sides, or between USI and MRI methods (Hides et al., 1995). However, these authors did find significant differences in CSA by level, with L5 showing the largest CSA (7.13 cm²) and L2 the smallest (1.99 cm²) (Hides et al., 1995). Each of the preceding studies comparing USI to MRI has generally concluded that USI is a valid measurement tool compared to MRI for those specific muscles and measures. However,

a direct comparison of T4ES thickness and pennation angle measured by USI and MRI has not been completed.

It is important to consider that the thoracic spine is the intermediary between the shoulder and low back, with the T4 level being medial to the scapulothoracic interface. As changes in muscle structure can result in changes to the function, such as changes in the force line of action with changes in pennation angle, it is plausible that changes at the T4 level could impact the loading mechanism between the shoulder and the low back; however, there has not been any documented imaging of T4ES morphometry. Therefore, the purpose of this study was twofold: first, to assess the intra-rater reliability and level of agreement of thickness and pennation angles of T4ES between USI and MRI measures, and second, to quantify/document these thickness and pennation angle measures.

4.2 USI-MRI Methods

4.2.1 Participants

A total of 20 participants (10 male, 10 female) were recruited from the University population. The mean (*SD*) age, height, and weight characteristics are outlined in Table 4.1. All participants were free of neck, back, and shoulder pain at the time of, and at least one year prior to, data collection. Participants had not received any medical treatment nor lost any time from work or school as a result of any pain/injury to the neck, back, or shoulders within the one year prior to collection. Ethics approval was obtained from both York University's Research Ethics Board, and the University of Waterloo's Office of Research Ethics. Each participant gave

informed consent and filled out a MRI safety screening form with the MR technician prior to being scanned.

Table 4.1. Mean (*SD*) characteristics of participants by Male (n = 10) and Female (n = 10).

Participants	Age (y)	Height (m)	Weight (kg)
Males (n=10)	25 (2) y	1.77 (0.07) m	80.01 (8.51) kg
Females (n=10)	26 (4) y	1.67 (0.08) m	65.85 (8.88) kg
Total (N=20)	25 (3) y	1.72 (0.09) m	72.93 (11.15) kg

4.2.2 Instrumentation

Ultrasound images were taken as outlined in the **Common Methods 3.2: Ultrasound Imaging** section. Briefly, a SonoSite M-Turbo ultrasound system was used with a linear transducer (model HFL38x, 13-6 MHz; SonoSite Canada Inc., Toronto, Canada). The MRI scans were taken with a 3T Magnetom Trio system (Siemens Healthcare, Erlangen, Germany).

4.2.3 Data Collection

Prior to any imaging, the spinous process of T4 was palpated and marked laterally to the right with a marker as shown in Figure 4.1A. Participants were then positioned supine onto a transfer board (and secured with straps), which was placed on top of a custom-built MRI-safe wheeled gurney. The transfer board had a 6 cm wide by 22 cm long hole cut out on the right side to allow for USI and MRI to occur in same supine position (Figure 4.1B). Participants were instructed to lay flat with their arms resting at their sides for the duration of the protocol, and the T4 region was exposed through the cut out (Figure 4.1 C & D).

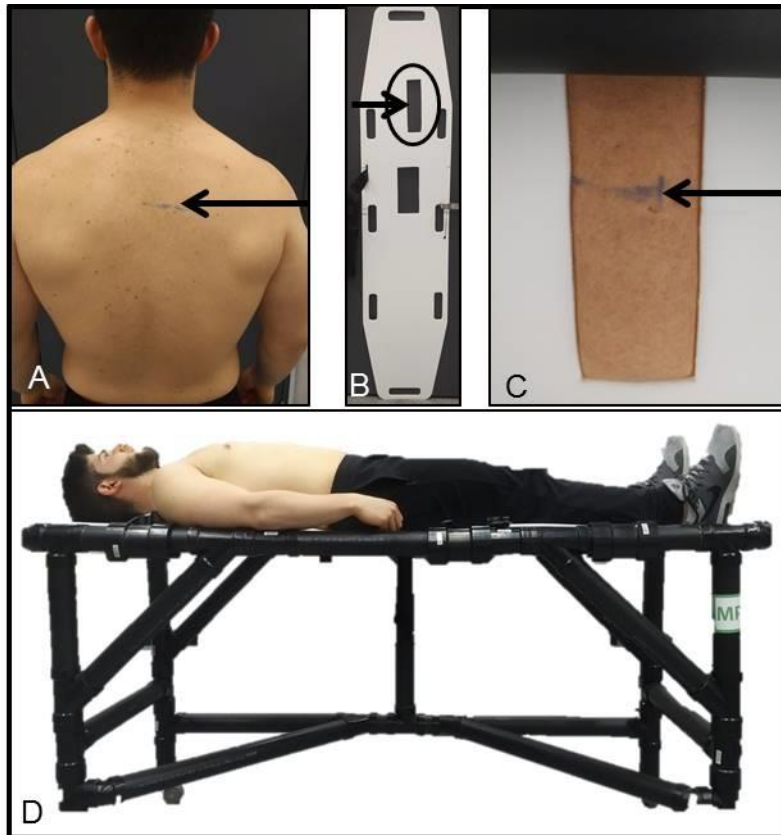


Figure 4.1. The spinous process at T4 was palpated and marked, as indicated by the black arrow (A). A transfer board with a hole cut out was used (B), which allowed the marked area to be exposed while supine (C). The transfer board was placed on a custom-built gurney (D).

The ultrasound transducer was then coated with a water-soluble conductive gel (Aquasonic Ultrasound Transmission Gel, Parker Laboratories, Inc., Fairfield, NJ, USA) and oriented along the long axis of the spine approximately 2.0-2.5 cm from the midline to produce a parasagittal USI. This parasagittal orientation allowed for both thickness and pennation angle to be measured from the same image. One image for each participant was recorded and saved as a .jpg format for offline processing. After the ultrasound imaging, a vitamin E capsule was adhered to the skin at the edge of the cut out at the level at which the image was taken. This capsule provided a measurable landmark without creating any interference during the MR scan.

Participants were then wheeled into the MR room and transferred to the MRI bore without actively moving, where they were then scanned in the same supine position.

Multiple participants were run in parallel due to logistical issues of collaboration with another institution from outside of the city, and having the MR room booked. For example, when Participant A was in the MR scanner, Participant B was getting prepared for USI. When Participant B was in the MR scanner, Participant A was wheeled back for a second round of lumbar USI as part of a larger study, followed by Participant C beginning the USI protocol. As a result, only one MRI and one USI were obtained for each participant.

4.2.4 MRI Protocol

All safety and facility precautions were adhered to as per the York MRI Facility guidelines. This included a pre-screen questionnaire administered by the MRI Technologist and signed informed consent acquired by the participants. Ear plugs were provided to prevent auditory damage, and an emergency squeeze bulb was given in case of immediate need to be removed from the bore. Additionally, foam pads were used on the arms to prevent direct contact with the magnetic bore, and the MRI Technologist maintained communication with the participant between scans to ensure general comfort and well-being.

The MR imaging took place at the York MRI Facility (Sherman Health Science Research Centre, York University) using a Siemens 3T Magnetom Tim Trio MR scanner with an integrated Spine Matrix Coil (Siemens Healthcare GmbH, Erlangen, Germany). Initially, a localizing scan was performed to ensure accuracy of the anatomical location, which was confirmed with visual identification of a vitamin E capsule placed externally on the skin. Two separate scans were then performed using a 3D SPACE sequence with T2 weighting, one in the

transverse plane and one in the frontal plane. Both scans had identical parameters that were set to the following values: Repetition Time = 1500 ms, Echo Time = 131 ms, Field of View = 220 mm, Slice Thickness = 1.0 mm, 80 slices with Voxel Size = 0.7 x 0.7 x 1.0 mm, parallel imaging mode GRAPPA with an acceleration factor of 2, and a total acquisition time of 3 min and 38 s.

4.2.5 Data Processing

Thickness and pennation angle measurements were taken offline one time per day for three consecutive days using Merge eFilm Workstation software (v.4.2.0, Merge Healthcare, Chicago, USA). Orthogonal MRI slices were generated using eFilm's Multi-Planar Reformatting (MPR) technique to match the orientation of the USI. The region of interest was located via the vitamin E capsule, and this slice location was recorded. The same MRI slice was used for each of the analyses, but both USIs and MRIs were presented in a different random order each day.

For the USI, a calibration image was used to convert the recorded images from pixels to cm. The calibration image was a previously-saved image from a phantom block with on-screen calipers (crosshairs) of known length (Figure 4.2A), by which a line was drawn from centre-to-centre of the caliper targets (between the crosshairs) (Figure 4.2B). The resulting line was then set as the calibration value in the software, with the following conversion: 156 pixels = 2.01 cm (Figure 4.2C). This calibration input allowed for automatic unit conversion on subsequent USIs. The calibration was only needed for the USIs because of the .jpg (picture) file format, whereas the information of the MRIs was stored as a Dicom file.

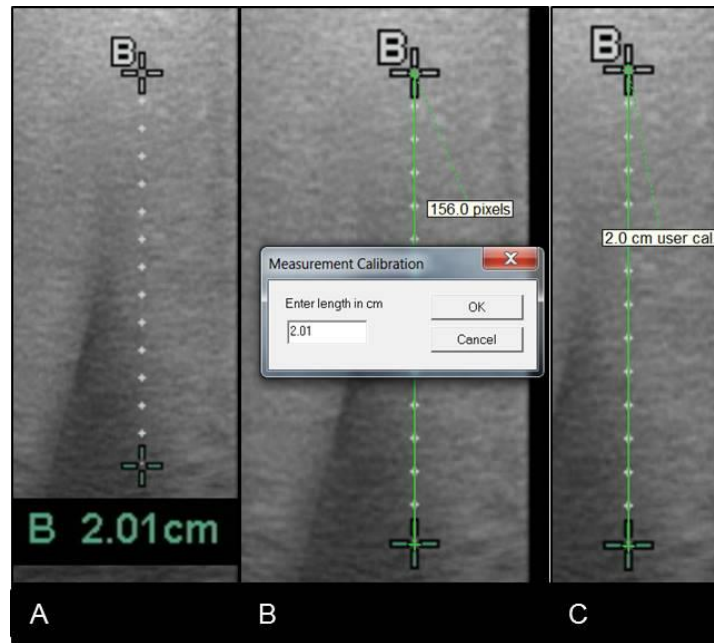


Figure 4.2. The ultrasound image calibration procedure. Known on-screen caliper length of 2.01 cm (A). A measured line was drawn between the crosshairs to indicate a length of 156 pixels, and the known value (2.01 cm) was entered as the length of the drawn line (B). The result was a calibrated length to use for each of the images.

Thickness measures were taken between the fascial border at the transverse process (Watanabe et al., 2004) and the echogenic fascial border (Bentman et al., 2010) of the muscle; and pennation angle measures were taken with respect to the skin (Harriss & Brown, 2015; McGill et al., 2000), as shown in Figure 4.3. Specifically, the transverse process was located (4.3B) and a line was drawn at 90° from the facial border of the transverse process to the border of the muscle (4.3C). A line was drawn along the skin and translated over to the muscle, and this line was used as the reference for the pennation angle of the muscle fibre (4.3C). This same process was used for the MRI slices (4.3D). A single rater measured the thickness and pennation angle of each image three times total, once per day for three consecutive days.

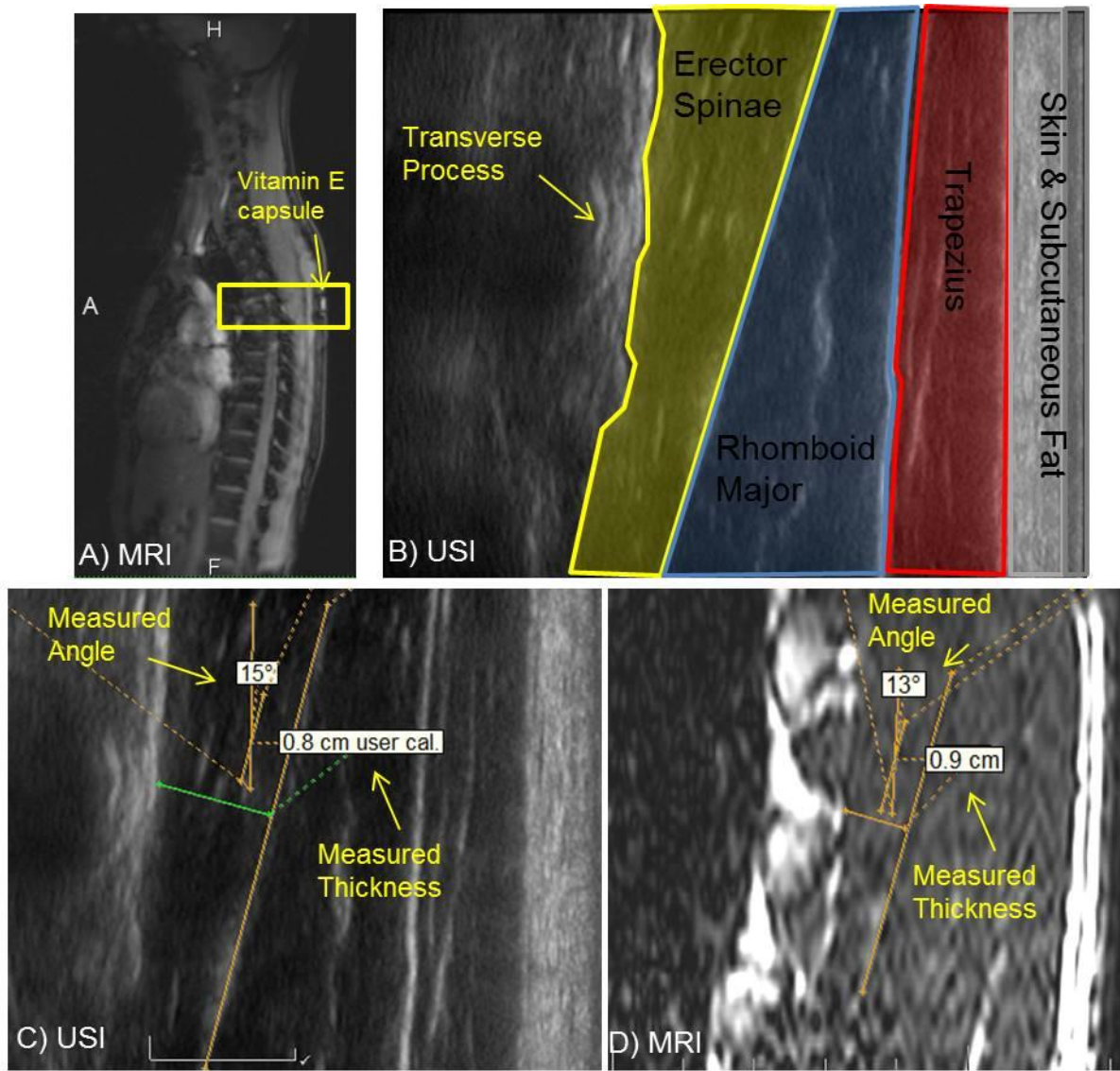


Figure 4.3. Location and measurement process from both ultrasound imaging (USI) and magnetic resonance imaging (MRI). The MRI localizer scan was used to identify the anatomical region of interest, and confirmed with an externally placed vitamin E capsule (A). A representation of the USI highlighting the transverse process (arrow), erector spine (yellow), rhomboid major (blue), trapezius (red), and the layers of skin and subcutaneous fat (grey) (B). The same USI as (B) is shown with the on-screen measurements made of thickness and pennation angle (C). The same participant with the measurements made from the reconstructed MRI slice (D).

4.2.6 Statistical Analyses

All statistical analyses were performed using SPSS v.24 software (IBM Corporation, Chicago, IL, USA). The two dependent measures (thickness and pennation angle) were analyzed

separately but identically. A 2×2 mixed-model ANOVA (Sex \times Method) was initially run to check for any Sex effects. Where no Sex effects were present, the subsequent reliability analyses used pooled male and female data.

The reliability analyses were chosen according to Whittaker et al., (2007), which recommended using each of *ICC*, *SEM*, *MDC*, and Bland-Altman plots for USI analyses. The between-day intra-rater reliability of the measure was calculated using a 2-way mixed-model intraclass correlation coefficient, *ICC* (3,3). The *ICC* ranges were designated as: poor (<0.400), moderate (0.400-0.599), good (0.600-0.749), or excellent (>0.750). These ranges were first noted by Fleiss (1981) and have been adopted in previous USI reliability studies of paraspinal muscle thickness (Djordjevic et al., 2014; Sions et al., 2015; Teyhen et al., 2011). The *SEM*, *MDC*, and Bland-Altman Limits of Agreement (LoA) were calculated as per Equations 4.1-4.4, respectively. Briefly, for Equation 4.1, *SD* is the pooled standard deviation from all observations (Wagner et al., 2008). For Equation 4.2, the *SEM* is the value from Equation 1, 1.96 is the 2-sided *z*-value for the 95% confidence interval (CI), and $\sqrt{3}$ was used to account for the variance of 3 measurements (Wagner et al., 2008). With Equations 4.3 and 4.4, the *MeanDiff* is the mean difference from USI-MRI, 1.96 is the 95% CI *z*-value, and *SD* is the standard deviation of the mean difference (Bland and Altman, 1986). The *ICC*, *SEM*, and *MDC* values were calculated for both USI and MRI, whereas the Bland-Altman plots were between the USI and MRI measures.

$$\text{Equation 4.1: } SEM = SD \times \sqrt{(1 - ICC)}$$

$$\text{Equation 4.2: } MDC = SEM \times 1.96 \times \sqrt{3}$$

$$\text{Equation 4.3: } \textit{Lower LoA} = \textit{MeanDiff} - 1.96 \times SD$$

$$\text{Equation 4.4: } \textit{Upper LoA} = \textit{MeanDiff} + 1.96 \times SD$$

In addition, the Bland-Altman information was used to assess the proportional and systematic biases from the slope of the regression line and the mean differences, respectively (Ludbrook, 2002). Specifically, proportional bias indicates that the two measures do not agree over the entire range, and is present if the slope of the regression of the differences on means is significantly different from zero (Ludbrook, 2002). The systematic bias between the measurements is determined if the mean difference significantly differs from zero (Ludbrook, 2002).

4.3 USI-MRI Results

Sex effects were not present for either thickness or pennation angle measures (ANOVA results, Table 4.2), thus the reliability analyses (*ICC*, *SEM*, *MDC*) were reported across both sexes. In general, both thickness and pennation angle measures of T4ES showed good to excellent reliability in both USI and MRI methods. Low mean differences and good agreement between the two methods were also present, showcasing the suitability of both methods to measure morphology of T4ES. Specific details of the findings are outlined below.

4.3.1 Thickness Measures

4.3.1.1 Analysis of Variance

No main or interaction effects were found on the T4ES thickness measure as shown by the ANOVA ($F(1,18) < 2.54$, $p > 0.129$) and detailed in Table 4.2. These results revealed that the mean (*SD*) thickness measured from USI (0.89 (0.34) cm) did not differ from that measured from MRI (0.88 (0.29) cm) (Figure 4.4).

Table 4.2. Summary of ANOVA results for both thickness and pennation angle measures. $\alpha = 0.05$.

Measure	Effect	$F(df)$ -value	p -value
Thickness	Method	$F(1,18) = 0.134$	$p = 0.719$
	Sex	$F(1,18) = 2.54$	$p = 0.129$
	Method \times Sex	$F(1,18) = 0.134$	$p = 0.719$
Angle	Method	$F(1,18) = 2.30$	$p = 0.146$
	Sex	$F(1,18) = 0.177$	$p = 0.679$
	Method \times Sex	$F(1,18) = 1.60$	$p = 0.222$

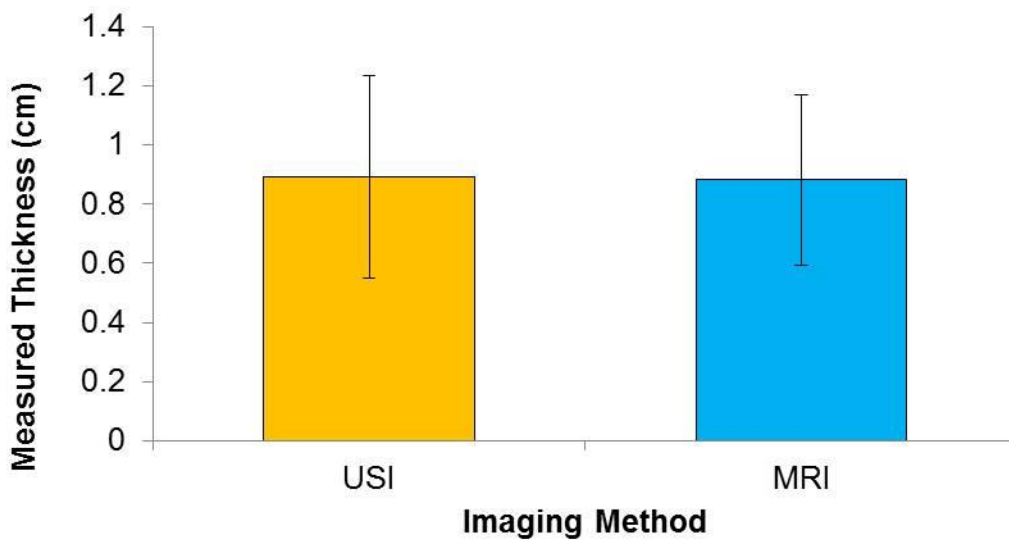


Figure 4.4. Mean (SD) thickness measures from ultrasound imaging (USI) and magnetic resonance imaging (MRI), $p = 0.719$.

4.3.1.2 Reliability Analyses

Generally the reliability of thickness measurement was excellent ($ICC > 0.979$) and the error measures low ($SEM < 0.04$ cm) for both USI and MRI methods, as detailed in Table 4.3. Overall, the USI thickness measurement showed greater reliability with more precision and a lower MDC compared to the MRI measurement (Table 4.3). This implied that USI was overall more effective for thickness measures; however, MRI was still reliable for this metric given the ICC and SEM results.

4.3.1.3 Bland-Altman

Ultrasound and MRI thickness measures showed good agreement between the methods as highlighted by the Bland-Altman plot in Figure 4.5. The mean difference (USI-MRI) was 0.01 cm, with the Upper and Lower LoA being 0.24 cm and -0.22 cm, respectively (Table 4.3). This indicated that 95% of the differences measured between the methods fell between the LoAs. The mean difference of 0.01 cm was not significantly different from 0 ($p = 0.712$) indicating no systematic bias between USI and MRI for thickness measures, however the slope of the regression line (0.18) was significantly different from 0 ($p = 0.04$) (Figure 4.5), indicating some proportional bias was present over the range of differences.

Table 4.3. Summary of mean (SD), reliability, and Bland-Altman results from T4ES thickness measures from both ultrasound imaging (USI) and magnetic resonance imaging (MRI). Included are: intraclass correlation coefficients (ICC), the standard error of measurement (SEM), the minimum detectable change (MDC), the mean difference between the measures (Mean Diff), and the upper and lower limits of agreement (Upper LoA and Lower LoA, respectively).

	Mean (SD) Thickness	ICC (3,3)	SEM	MDC	Mean Diff. (USI-MRI)	Upper LoA	Lower LoA
USI	0.89 (0.34) cm	0.995	0.02 cm	0.08 cm	0.01 cm	0.24 cm	-0.22 cm
MRI	0.88 (0.29) cm	0.979	0.04 cm	0.14 cm			

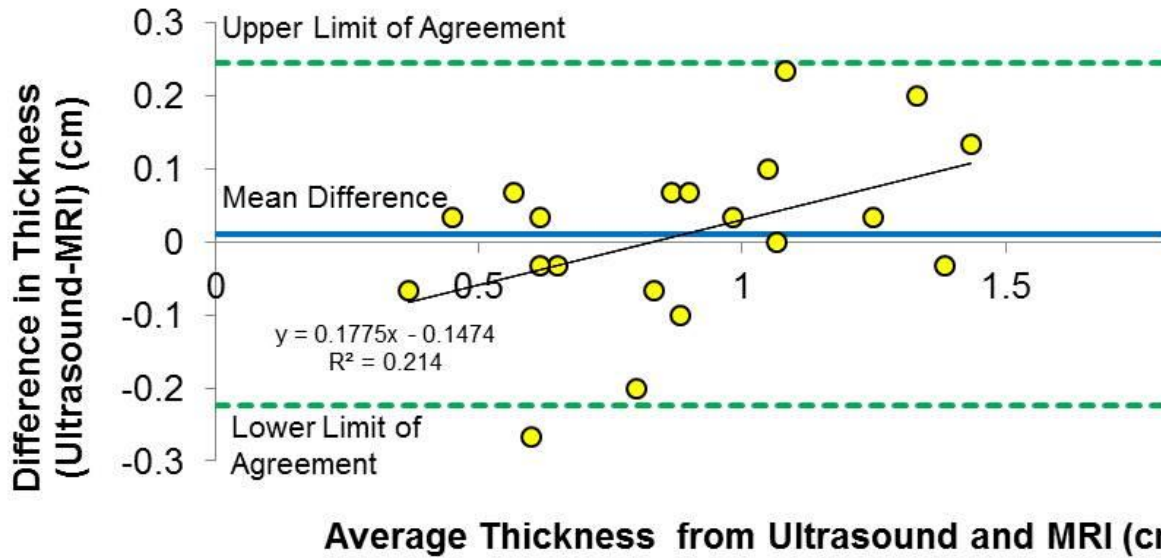


Figure 4.5. Bland-Altman plot comparing thickness measured by ultrasound imaging (USI) and magnetic resonance imaging (MRI). The solid blue line is the mean difference between the methods, and the dashed green lines are the upper and lower limits of agreement. The regression line and equation are included as the slope of the line was used to determine the presence of proportional bias.

4.3.2 Pennation Angle Measures

4.3.2.1 Analysis of Variance

The ANOVA results yielded no interaction effects or main effects for Sex or Method on T4ES pennation angle ($F(1,18) < 2.30, p > 0.146$; Table 4.1), showing that the mean (*SD*) pennation angle measured from USI ($13.8^\circ (4.0)$) did not differ from that measured from MRI ($14.4^\circ (3.4)$) (Figure 4.6).

4.3.2.2 Reliability Analyses

In general, the pennation angle measurements showed excellent intra-rater reliability ($ICC > 0.962$) and reasonably low error measures ($SEM < 0.68^\circ$), with full results shown in

Table 4.4. For the pennation angle, the USI had a higher *ICC* with similar *SEM* and *MDC* compared to the MRI measurement (Table 4.4), suggesting that USI provided very high-quality images of T4ES pennation angles.

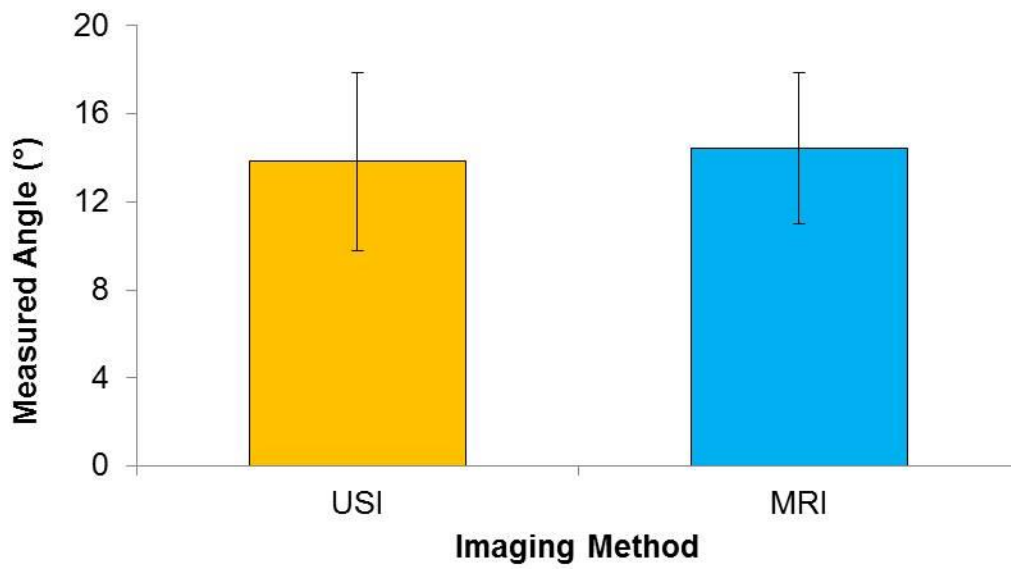


Figure 4.6. Mean (*SD*) angle measures from ultrasound imaging (USI) and magnetic resonance imaging (MRI), $p = 0.146$.

4.3.2.3 Bland-Altman

Ultrasound and MRI thickness measures showed reasonable agreement between the methods as highlighted by the Bland-Altman plot in Figure 4.7. The mean difference (USI-MRI) was -0.60° , with the Upper and Lower LoA being 2.92° and -4.12° , respectively (Table 4.4). The mean difference of -0.60° and the slope of the regression line (0.17) (Figure 4.7) were both not statistically different from 0 ($p > 0.142$) indicating no systematic or proportional bias was present between USI and MRI for pennation angle measures.

Table 4.4. Summary of mean (*SD*), reliability, and Bland-Altman results from T4ES angle measures from both ultrasound imaging (USI) and magnetic resonance imaging (MRI). Included are: intraclass correlation coefficients (ICC), the standard error of measurement (SEM), the minimum detectable change (MDC), the mean difference between the measures (Mean Diff), and the upper and lower limits of agreement (Upper LoA and Lower LoA, respectively).

	Mean (<i>SD</i>) Angle	ICC (3,3)	SEM	MDC	Mean Diff. (USI-MRI)	Upper LoA	Lower LoA
USI	13.8° (4.0)	0.972	0.68°	2.3°	-0.60°	2.92°	-4.12°
MRI	14.4° (3.4)	0.962	0.68°	2.3°			

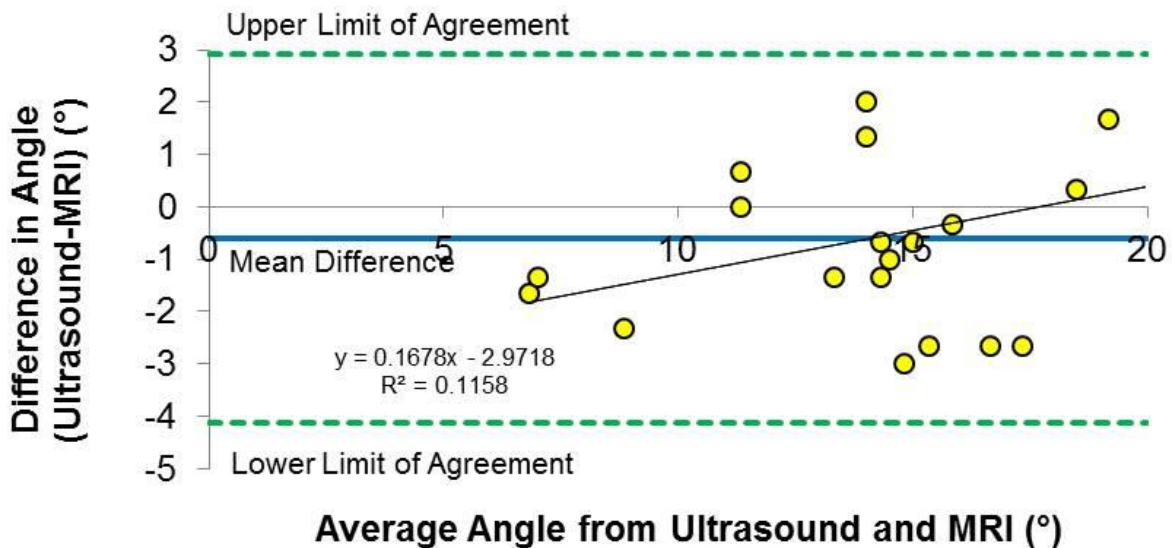


Figure 4.7. Bland-Altman plot comparing fibre angles measured by ultrasound imaging (USI) and magnetic resonance imaging (MRI). The solid blue line is the mean difference between the methods, and the dashed green lines are the upper and lower limits of agreement. The regression line and equation are included as the slope of the line was used to determine the presence of proportional bias

4.4 USI-MRI Discussion

This was the first study to document and compare thickness and pennation angle of T4ES *in vivo* using USI and MRI modalities. Both thickness and pennation angle results demonstrated

excellent reliability for both methods and a strong level of agreement between methods. Based on these results we conclude that USI is a reliable and valid method to record muscle thickness and fibre pennation angle in T4ES, and therefore could be used with confidence in future analyses of morphometry changes during functional postures.

The current *ICC* obtained from T4ES USI thickness ($ICC(3,3) = 0.995$) was well within the range of what has been previously reported for the trapezius and multifidus muscle. Using a similar *ICC(3,k)* model for lower-trapezius measures of T7-T9, O'Sullivan et al. (2007) reported between-day intra-rater $ICC(3,3) = 0.89-0.91$. Furthermore, lumbar multifidus thickness in rest and contraction has shown *ICC* values ranging from 0.93-1.00 in novice raters (Djordjevic et al., 2014). However, moderate intra-rater reliability was reported in middle-trapezius at T1 ($ICC(3,2) = 0.67$ (Bentman et al., 2010)). It has been suggested that the lower trapezius is more uniform in thickness (O'Sullivan et al., 2009), thus providing greater measures of reliability (O'Sullivan et al., 2007). This is opposed to the rapid changes in thickness when moving from middle- to upper-trapezius (O'Sullivan et al., 2009), and this lack of uniformity in muscle thickness could have resulted in lower reliability (Bentman et al., 2010). Similarly, Belavý et al., (2015) found the intra-rater lumbar ES thickness *ICCs* to vary between 0.57-0.87 depending on the level and side, with thicknesses of 3.18-4.94 cm reported.

The *SEM* as defined by Wagner et al. (2008) was the measurement error that indicated the within-subject variability across repeated trials, or an indication of precision (Djordjevic et al., 2014). The current thickness *SEM* (Table 4.3) showed precision values of 0.02 cm and 0.04 cm for USI and MRI, respectively. This was similar to the findings of Bentman et al. (2010) who found middle-trapezius thickness to be 1.0-1.1 cm thick with *SEM* of 0.1 cm. The *MDC* represented the magnitude of change necessary to exceed the measurement error (Wagner et al.,

2008), or how large a change needs to be for it to be considered a ‘real’ difference. Applying this rationale, the current results (Table 4.3) showed that any changes in thickness values greater than 0.08 cm for USI and 0.14 cm for MRI would be considered ‘actual changes’. These MDC ranges are comparable to those reported in both multifidus thickness ($MDC = 0.24$ cm (2.87 cm thick), Djordjevic et al., 2014; $MDC = 0.60-0.82$ cm (3.59-4.48 cm thick), Sions et al., 2015) and lumbar ES thickness ($MDC = 0.55-1.11$ cm (3.18-4.94 cm thick), Belavý et al., 2015).

The mean (SD) T4ES thickness measured from both USI (0.89 (0.34) cm) and MRI (0.88 (0.29) cm) was thicker than previously reported measures of lower-trapezius and rhomboids from T2-T5, and thinner than middle-trapezius measured from T1. For example, MRI measures from O’Sullivan et al. (2009) reported lower-trapezius at T5 to be 0.62 cm thick; whereas Bentman et al. (2010) reported USI thickness of middle-trapezius at T1 to be approximately 1.0-1.1 cm thick. The study by Jeong et al. (2016) was the closest in anatomical location, where those authors measured rhomboid major by USI between T2-T5 midway to the spine of the scapula and found the mean thickness of rhomboid major to be approximately 0.46-0.48 cm. Moving even further laterally, Yang et al. (2011) measured the muscle thickness of the interscapular region with USI in both males and females. Placing the ultrasound transducer close to the medial border of the scapula, the trapezius (0.33-0.52 cm), rhomboids (0.32-0.63 cm), and posterior serratus (0.22-0.40 cm) muscles were measured, with total thickness ranges from skin-to-bone of 1.5-2.0 cm (Yang et al., 2011). In the present study, the skin-to-bone depth was approximately 3-4 cm highlighting the feature of the ribcage, which reduced the space for soft tissue moving laterally from the midline. Given the function of the ES muscles as trunk extensors, compared to the function of trapezius and rhomboids as scapular mobilizers, it was

within reason the muscles responsible for the heavier trunk motion would be larger in size at that thoracic level.

For the pennation angle measures, both USI and MRI were considered to have excellent reliability (>0.962) (Table 4.4). Interestingly, the reliability was greater in USI than MRI, which was likely a result of the resolution limitation of the MRI processing described above. However, O'Sullivan et al. (2009) noted some of the muscle borders of trapezius that had very little fat surrounding the muscle tissue were harder to identify on MRI and easier to see in USI. As a result of better visualization of muscle borders from USI, O'Sullivan et al. (2009) have called to question the assumption of MRI as the gold standard for imaging all muscle tissue. In the present study, we still agree that MRI is the gold standard; however, given the greater reliability in USI for muscle angle, perhaps there is a trade off at the T4 level as to which imaging modality provides the 'best' measure, with suitable thickness measures coming from MRI, and higher-quality angle measures coming from USI.

The mean (*SD*) T4ES pennation angles (Table 4.4) were smaller than the pennation angles reported in the lumbar spine measured from USI, with the current average angle of T4ES being about 14° , compared to average lumbar ES pennation angles reported as 26° (McGill et al., 2000) and 20° (Harriss and Brown, 2015). It is well documented that flexing the lumbar spine reduces the fibre angle (Harriss and Brown, 2015; McGill et al., 2000; Singh et al., 2011), so it would make sense that the kyphotic (naturally flexed) curvature of the thoracic would result in a smaller fibre angle orientation. Recently, Bayoglu et al. (2017b) published a complete data set of morphological parameters for musculoskeletal modelling of the thoracic and cervical regions of the spine from 39 muscles, including pennation angle. However, as part of their measurement procedure from the cadaveric specimen, no pennation angles of less than 10° were recorded

(Bayoglu et al., 2017a), resulting in only 3/39 cervical/thoracic muscles having documented pennation angles (Bayoglu et al., 2017b). The pennation angles measured from USI in the present study fall within 1 *SD* of 10°, which confirmed the shallow angles from Bayoglu et al. (2017b). The difference in pennation angle between LES and T4ES likely stemmed from the functional role of these muscles. The oblique orientation of the lumbar extensor fibres allow for production of posterior shear forces to offset any anterior shear loading often associated with lifting with a flexed spine (Potvin et al., 1991). The fact that the T4ES pennation angles were shallower indicated that these muscles are not as capable of producing as much posterior shear force, likely due to anatomical requirements. As the trunk bends forward, the mass of the entire upper body is supported by the LES muscles, whereas at the T4 level only the mass of the head, neck, and some of the trunk will be resisted by the T4ES. The more inferiorly-directed orientation of the T4ES fibres would be indicative of providing compression forces, which could result in more of a stabilizing effort rather than a moment-generating one.

There were some limitations associated with this study. For example, only one image was taken per participant as there were time constraints surrounding use of the MR scanner, as such, this study was focused on measurement reliability as opposed to procedural reliability (location identification and image acquisition (Sions et al., 2015)). Specifically, this study was focused on intra-rater reliability, concerning the measurements of a single rater. However, it should be acknowledged that inter-rater reliability is also an important consideration and will be addressed in future studies. Another limitation involved using the software image reconstruction to align the parasagittal orientation of the USI and MRI. This may have resulted in some loss of image resolution which was reflected by the overall lower reliability of angle measures in MRI; however, this specific parasagittal view was required for measuring both the thickness and the

pennation angle of the muscle, thus the reconstruction technique could not be avoided. Future studies could look to analyze the CSA of T4ES from the transverse plane, with the potential to compare USI and MRI without requiring an image reconstruction method. Another potential drawback of this study was using a young healthy population, as the applicability of the results could be limited. However, it was important to establish a baseline level of criteria before starting to make any comparisons to clinical populations.

In conclusion this study demonstrated that the morphology of T4ES could be reliably and accurately measured from USI. Upcoming work from this thesis (Study #4: US-EMG) will use USI to measure change in thickness and fibre angle during active and passive postures concurrently with surface electromyography in order to determine how the structure of T4ES drives the functional aspects. Future work should look to track any morphological changes in ES structure across multiple lumbar and thoracic levels using either USI or MRI, as there is an identified need for comprehensive documentation of a healthy population in order to better understand the inter-relationship between spinal levels (Stokes et al., 2007). Overall, USI showed excellent intra-rater reliability and good agreement to MRI measures of T4ES thickness and pennation angle, signifying that USI can be used in lieu of MRI if required.

Chapter 5: Study #2: T4ES-MVC

5.1 T4ES-MVC Introduction

Normalization of EMG signals is the process of expressing the raw voltage (mV) of a given task as a percentage of the raw voltage associated with the muscle activity from a calibrated test contraction (Lehman & McGill, 1999). The normalization procedure is important for a number of reasons, such as improving the repeatability of the signal (Lehman, 2002), allowing for comparisons across muscles and between subjects, and for making the interpretation of the signal biologically relevant (De Luca, 1997; Lehman & McGill, 1999). There are a multitude of ways to normalize the EMG signal, such as using the peak or average of the task (Yang & Winter, 1984), or submaximal and maximal contractions (Burden, 2010). A common normalization technique in healthy participants is a MVC, where an isometric contraction of the muscle of interest is performed to the maximal capacity that the participant can generate, resulting in units expressed as %MVC (Burden, 2010; Lehman & McGill, 1999). The use of MVC to normalize the EMG signal has also been recommended as the conclusion of an extensive review (Burden, 2010) and has been endorsed by the *Journal of Electromyography and Kinesiology* (Merletti, 1999). Typical to the ES musculature, the MVC technique is a horizontal back extension performed while hanging over the edge of a table from prone (McGill, 1991), however this technique may not be appropriate for all levels of ES (Vera-Garcia et al, 2010).

Testing of different MVC techniques for select muscle groups has been previously reported across the body, including the trunk, and scapulo-thoracic region of the shoulder. For example, trunk MVC techniques have been investigated in the abdominals, latissimus dorsi, and ES at T9, L2, and L5 (Ng et al., 2002; Vera-Garcia et al., 2010). Ng et al. (2002) tested trunk

MVCs in all three cardinal planes using a locked dynamometer in upright standing. The pelvis and chest were restrained, and the dynamometer locked in three planes while participants performed maximal contractions for flexion, extension, and bilateral axial twist and lateral bend (Ng et al., 2002). The results of Ng et al. (2002) found multi-planar peaks for latissimus dorsi and L2ES, and concluded that multiple planes should be considered for MVCs. Vera-Garcia et al. (2010) tested nine different MVC techniques on six trunk muscles and found that ES muscles showed the largest activation during sagittal plane (extension) movement. Scapulo-thoracic MVC techniques have been analyzed specifically in latissimus dorsi (Beaudette et al., 2014; Park & Yoo, 2013), and trapezius muscles (Ekstrom et al., 2005), with a common result indicating no single test produced the highest level of activation. One region of the trunk that has implications from both a trunk and scapulo-thoracic perspective is the T4 level; however, normalization procedures for T4ES have not been assessed.

Typical scapulo-thoracic motion is produced by the trapezius and rhomboid muscle groups which rotate, elevate, and retract the scapula (Terry & Chopp, 2000). However, deep to these muscles towards the midline (paraspinal) are the ES muscle group. Specifically, the T4ES muscle is a region that remains relatively under-reported compared to LES studies. Previous research on T4ES has focused on posture-related changes during slumped sitting (Burnett et al., 2009; Caneiro et al., 2010; Edmondston et al., 2011; Nairn et al., 2013c) and prolonged sitting (Nairn et al., 2013b; Schinkel-Ivy et al. 2013); while others have looked at more functional patterns such as the flexion-relaxation phenomenon in sitting and standing (Ang et al., 2016), combinations of lumbar and thoracic movement (Nairn & Drake, 2014), and during sequencing of muscle timing patterns (Schinkel-Ivy & Drake, 2015a; Siu et al., 2016) and flexion/extension movements (Kienbacher et al., 2016). Common to the preceding studies was that T4ES was

considered part of either the cervico-thoracic complex or grouped strictly with the lumbar/thoraco-lumbar extensors. To date, no attention has been given on T4ES in the context of scapulo-thoracic integration. However, such an investigation could be important to the understanding of how T4ES functions during different arm and body postures given its proximity to the primary scapulo-thoracic muscles.

In order to begin to integrate thoracic spine behaviour with upper-extremity tasks, it is important to have established collection techniques in place, including normalization procedures. For T4ES, a normalization procedure has not been clearly established in the literature as the only description of a MVC for T4ES comes from Burnett et al. (2009). These authors described the MVC protocol as having the participant lying prone on a table and lifting their head, shoulder, and elbows above the table with manual resistance being applied to the upper arms (Burnett et al., 2009). However, recent work has shown axial twist (Nairn & Drake, 2014) and arm abduction with axial twist (Siu et al., 2016) to elicit high activation of T4ES, typical to the action of an arm raise targeting upper-trapezius (MacLean, 2005). Due to the proximity and observed concurrent activation of scapulo-thoracic and ES muscles, there should be concern for the potential of crosstalk between muscles, which occurs when surface electrodes pick up the EMG signal from overlapping or adjacent muscle (Winter, 2009). For the case of the deep T4ES muscle, the signal of recorded from surface EMG electrodes may be susceptible to crosstalk from the overlaying trapezius and rhomboid groups. The issue of crosstalk further highlights the need to test different postures for producing a maximum value at T4ES, as well as to analyze the surrounding musculature (e.g. rhomboid/trapezius) concurrently in order to see if there is possible crosstalk contamination.

Normalizing the EMG signal is important for interpretation of the signal, yet there remains a lack of information regarding normalization techniques for T4ES. However, the proximity of T4ES to the surrounding rhomboids and trapezius muscles could be a potential for crosstalk to occur when collecting EMG from surface electrodes. Therefore, the purpose of this study was to determine which MVC technique produced the largest value at the T4ES level with minimal interference from neighbouring muscles.

5.2 T4ES-MVC Methods

5.2.1 Participants

A total of 30 participants were recruited from the University population, 15 males and 15 females. The mean (*SD*) age, height, and weight of the males were 21.7 y (3.6), 1.77 m (0.09), and 18.98 kg (15.37), respectively; and of the females were 19.9 y (1.5), 1.62 m (0.05), and 56.25 kg (4.90), respectively. As per the **Common Methods 3.1: Participants** section, all participants were free of neck, back, and shoulder pain for at least one year prior to collection, and had not sought medical attention for those regions during that time. The University's Office of Research Ethics approved this study, and prior to data collection all participants obtained informed written consent.

5.2.2 Instrumentation

For the purpose of this study, electromyography was recorded and analyzed unilaterally from T4ES and MidTrap (Figure 5.1). Electrodes were placed on the dominant side, with four participants (two male, two female) being left-hand dominant. For T4ES, electrodes were placed

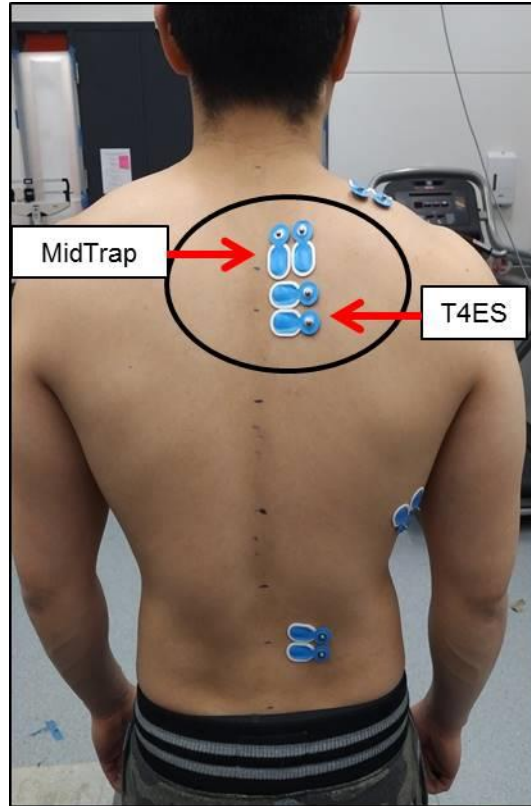


Figure 5.1. Electrode placement for the upper-thoracic erector spinae at the T4 level (T4ES) and the middle trapezius (MidTrap).

approximately 2.0-2.5 cm from the spinous process of T4 (Nairn & Drake, 2014), and MidTrap electrodes were a modification of Criswell (2011), which were placed at T3, and oriented in the direction of the MidTrap fibres. The modification comes from the fact that the MidTrap electrodes should be placed more laterally, next to the root of the scapula on the medial border (Criswell, 2011). This modification was done in order to assess MidTrap as close as T4ES as possible. The electrode and amplifier specifications can be found in the **Common Methods 3.3.1: Collection Specifications** section. Briefly, the electrodes used were disposable silver/silver-chloride with a centre-to-centre spacing of 2.5 cm (Ambu® Blue Sensor N, Ambu

A/S, Denmark). The EMG signals were differentially amplified (frequency response 10-1000 Hz, common mode rejection 115 dB at 60 Hz, input impedance 10 G Ω ; model AMT-8, Bortec, Calgary, Canada) and converted from an analog to digital signal at a rate of 2048 Hz (NDI First Principles, Northern Digital Inc., Canada).

5.2.3 Data Collection

Data collection of EMG consisted of the general steps outlined in the **Common Methods 3.3: Electromyography** section, and included electrode application, and the MVC trials. The skin was prepared by a shave and alcohol swab of the area in order to assist with electrode adherence to the skin (Konrad, 2006). After electrode placement, a series of eight MVC techniques were performed in a random order, but repeated two times consecutively (for a total of 16 active, yet static, trials). These MVC techniques were selected to target the T4ES muscle activation in multiple planes, and included thoracic extension (ThorExt), lumbar extension (LumbExt), abducted arm raise (Raise-Stand, Raise-Sit), rowing/pulling (Row-Stand, Row-Sit), and lateral pull down (LatPull-Stand, LatPull-Sit)., The different MVC techniques are shown in Figure 5.2A-H and explained in detail below and in the Glossary. A minimum 2 min rest break was given between each of the eight techniques to minimize any effects of fatigue (Vera-Garcia et al., 2010).

Each of the different MVC techniques targeted a different plane of motion as recommended by Ng et al. (2002). For example, sagittal plane motion was achieved by ThorExt and LumbExt, frontal plane by Raise- and LatPull-, and transverse plane from the Row- techniques. The ThorExt and LumbExt trials were sagittal plane movements and considered to be in the line of action of the T4ES muscle, as the ES are the spine extensors. Thoracic

extension (Figure 5.2A) was adapted from Burnett et al. (2009) where participants were prone on a table and instructed to lift their head, shoulders, and elbows just off the table. The LumbExt was performed according to McGill (1991) where manual resistance was applied downward as participants attempted to lift their torso to horizontal (Figure 5.2B). The Raise- technique (Figures 5.2C and 5.2D, respectively) is often used to target upper-trapezius (MacLean, 2005) and mid-trapezius (Criswell, 2011); however, recent evidence has shown large amounts of EMG activation being recorded from the T4ES electrode site during arm raise (abducted) posture (Siu et al., 2016). Rowing exercises (Row-Stand and Row-Sit, Figures 5.2E and 5.2F, respectively) were classified as transverse plane motion and have been shown to increase muscle activation of the middle trapezius and rhomboids (Ekstrom et al., 2003; Lehman et al., 2004). Finally, LatPull-Stand and LatPull-Sit was performed in the frontal plane (Figures 5.2G and 5.2H) and is often used to target latissimus dorsi (Park & Yoo, 2013). Each technique not in the sagittal plane was typically performed to target different muscles of the back and shoulder, whereas sagittal plane movement was designed to target ES. Therefore, by recording the maximum T4ES and MidTrap EMG from MVC techniques in other planes, it was possible to get an indication of potential crosstalk from the overlying muscles, such as trapezius and rhomboids.

5.2.4 Data Processing

Again, the EMG in this study was collected simultaneously from T4ES and MidTrap and processed according to the **Common Methods 3.3.3: Linear Envelope** section. In brief, raw EMG signals were first full-wave rectified and low-passed filtered with a 4th order dual-pass Butterworth filter using a frequency cut-off of 2.5 Hz to generate the linear envelope of the signal (Brereton & McGill, 1998). Peak EMG values from the linear envelope were recorded

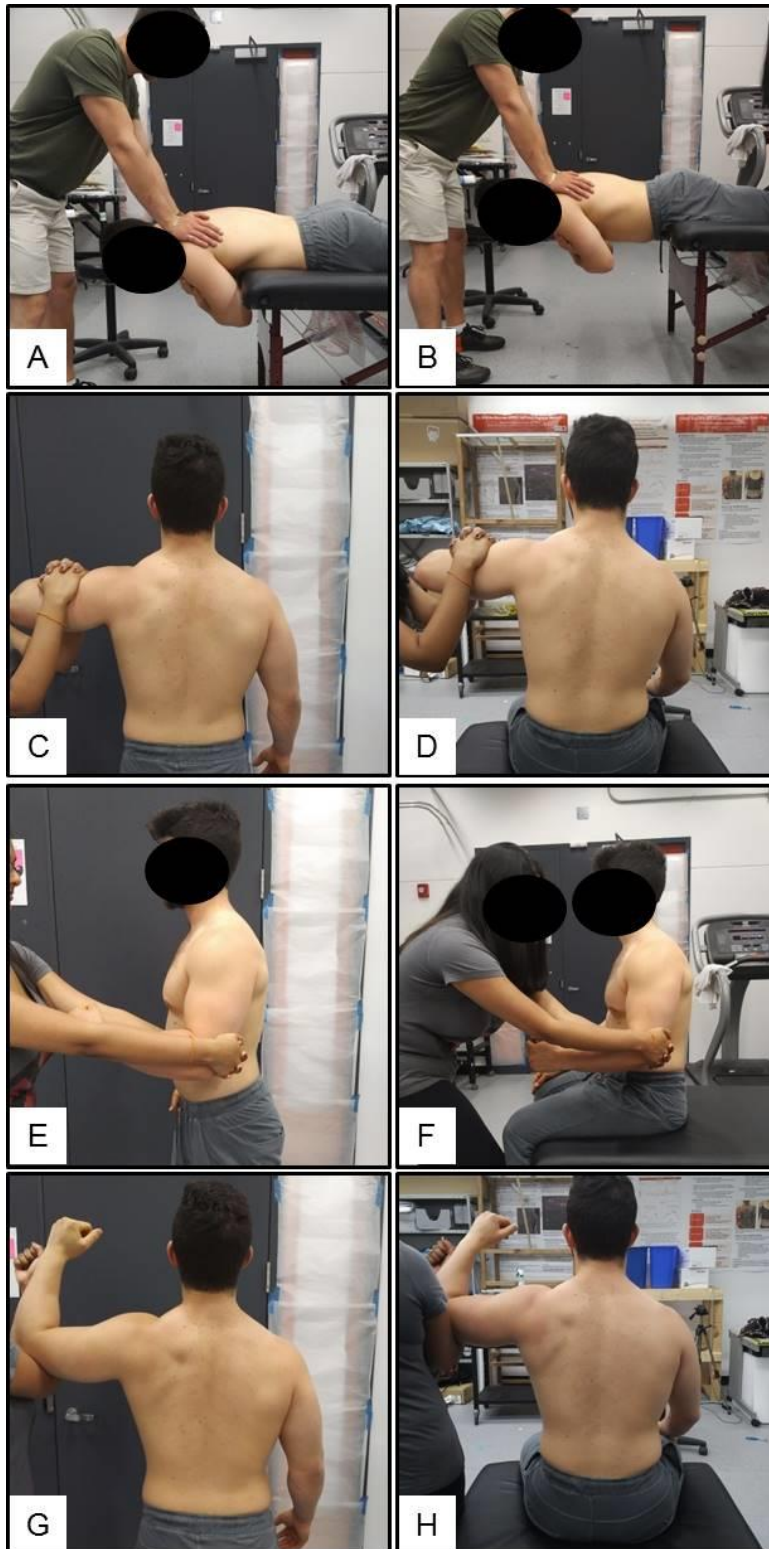


Figure 5.2. Representation of each MVC technique: ThorExt (A), LumbExt (B), Raise-Stand (C), Raise-Sit (D), Row-Stand (E), Row-Sit (F), LatPull-Stand (G), LatPull-Sit (H). Note: Care was taken to ensure no pressure was applied directly to the electrodes.

from the two repeats of each technique, and the average of the two peaks from each technique was taken (Park & Yoo, 2013). For T4ES, all techniques were then normalized to the ThorExt trial, resulting in the data being expressed as %ThorExt. This meant that any techniques that were above 100 %ThorExt indicated muscle activation larger than the ThorExt technique. Similarly, the MidTrap channel was normalized to the Raise-Stand trial, resulting in MidTrap being expressed as %Raise-Stand.

5.2.5 Statistical Analysis

Statistical analyses were run as per the **Common Methods 3.5: Statistical Analyses** section. In general, for both the T4ES and MidTrap muscle a 2×8 (Sex \times Technique) mixed-model ANOVA was run on each dependent measure (T4ES (%ThorExt), and MidTrap (%Raise-Stand)). If no Sex effects were present, male and female data were pooled and the ANOVA was re-run as one-way repeated measures ANOVA with the factor being Technique. If appropriate, post hoc tests were run using a series of Bonferroni correct *t*-tests and $\alpha = 0.05$ for all analyses.

5.3 T4ES-MVC Results

Results of the T4ES ANOVA did not reveal a main effect ($F(1,28) = 0.109, p = 0.743$) or interaction effect ($F(7,196) = 0.493, p = 0.839$) of Sex. The subsequent pooled ANOVA showed a main effect of Technique on T4ES %MVC ($F(7, 203) = 26.93, p < 0.0001$) with the ThorExt and Raise-Stand and Raise-Sit trials showing the largest values ($p < 0.002$) (Figure 5.3). These results indicated that ThorExt did in fact elicit a maximum activation of T4ES, yet there was still upwards of 20% more activation recorded from the Raise- techniques.

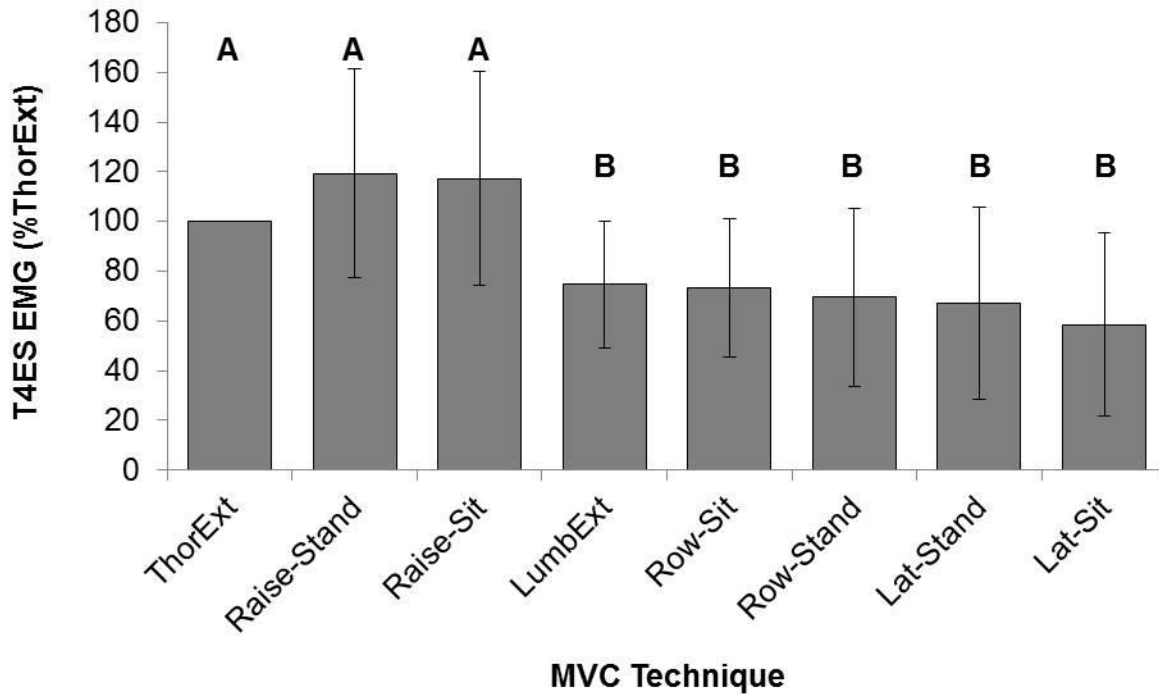


Figure 5.3. Results of the ANOVA (mean (*SD*)) highlighting the effect of Technique on T4ES (%ThorExt) ($p < 0.01$). Levels not connected by the same letter were considered significant at $p < 0.05$.

The initial MidTrap 2×8 ANOVA also showed no main effect of Sex ($F(1,28) = 2.72$, $p = 0.11$), and no interaction effect of Sex when adjusted for violations of Sphericity (see **Common Methods 3.5: Statistical Analyses** section) ($F(3.7,104.8) = 2.49$, $p = 0.052$). When male and female data were pooled, an effect of Technique on MidTrap EMG was revealed ($F(7,203) = 46.16$, $p < 0.0001$). These results showed that Raise-Stand and Raise-Sit were greater than all techniques ($p < 0.017$), with the exception of Raise-Stand and Row-Sit ($p = 0.11$) (Figure 5.4). Additionally, Row-Stand and Row-Sit showed EMG values that were not different from ThorExt ($p = 1.00$), yet these three techniques all produced larger activation than LumbExt, and both LatPull- techniques ($p < 0.010$) as shown in Figure 5.4. Overall, the MidTrap muscle showed the largest activation in the Raise- trials, followed by the Row- trials and ThorExt, highlighting the role of MidTrap as a scapular abductor and retractor.

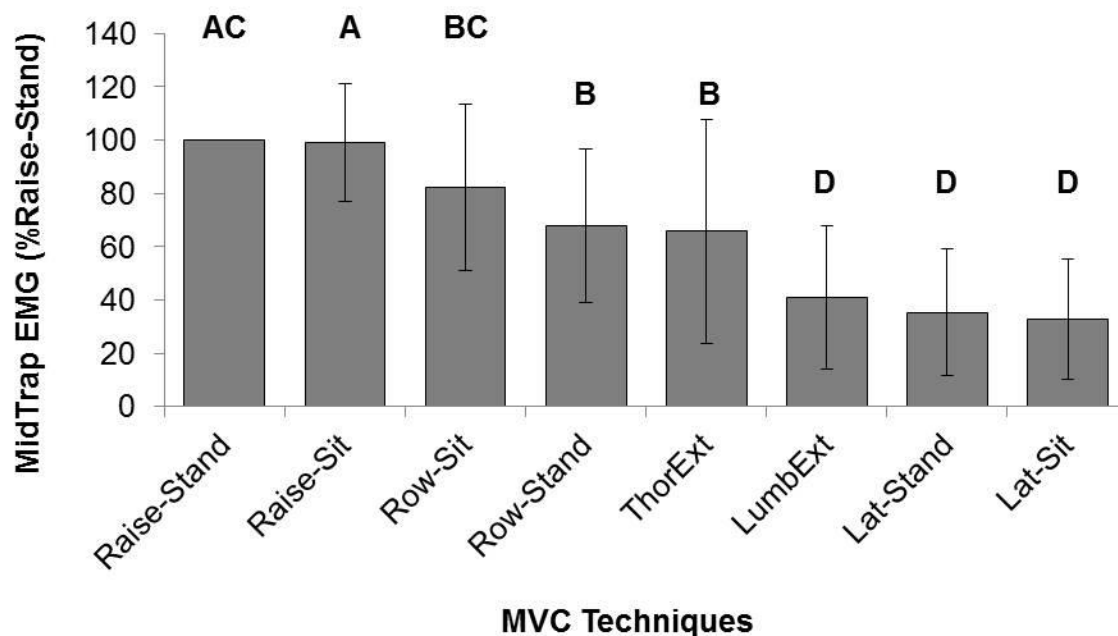


Figure 5.4. Results of the ANOVA (mean (*SD*)) highlighting the effect of MVC Technique on MidTrap (%Raise-Stand) ($p < 0.01$). Levels not connected by the same letter were considered significant at $p < 0.05$.

5.4 T4ES-MVC Discussion

This was the first study to test different MVC techniques in the T4ES musculature. Eight MVCs targeting T4ES in multiple planes were performed, with muscle activation recorded in T4ES as well as MidTrap for context. The results of T4ES showed the Raise- techniques had the largest absolute %ThorExt, though this was not statistically different from ThorExt (Figure 5.3). These suggested that ThorExt be recommended as the MVC of choice for T4ES, as this technique followed the muscle line of action as an extensor. However, caution must be taken when applying the T4ES to functional tasks such as overhead reaching, as the large level of activation during the Raise- techniques could be indicative of crosstalk from the trapezius and/or rhomboid muscle groups. This was supported by the fact that MidTrap showed the highest activation in the expected Raise- and Row- trials with mid-range activation coming from ThorExt (Figure 5.4). This would suggest that if the T4 level is the area of interest, then the

MidTrap muscle should also be tracked. If tasks involve any overhead or above-shoulder work, it is then recommended to use the maximum value obtained from either the extension or arm raise trials, and to group the T4ES location as a general Trap/Rhomboid/ES muscle grouping, rather than label it solely as T4ES.

The results of this study agreed with the findings of Vera-Garcia et al. (2010), who noted that while sagittal plane motion had the largest ES activation, the conventional lumbar-extension may not be appropriate for recruiting all levels of ES. Those authors found that a lower-trunk extension, where the lower-trunk was raised and the upper-trunk was secured had the highest activation of T9ES, whereas the traditional lumbar-extension of raising the upper-trunk activated L5ES the greatest (Vera-Garcia et al., 2010). The results of the current study also found ThorExt to show activations in T4ES that were larger than that obtained from LumbExt (Figure 5.3), showing that non-traditional sagittal-plane motion produced the highest activation in T4ES. This indicated that the sagittal plane should be used for an ES MVC, but the axis of rotation should be appropriate for the muscle. For example, LES techniques should pivot about the hips, whereas T4ES should pivot about the mid-chest.

Considering that ThorExt elicited high EMG activation from T4ES (Figure 5.3), whereas Raise- produced the highest MidTrap activation (Figure 5.4) suggested it was possible to collect the deeper ES muscle when moving in the sagittal plane; however, the large T4ES activity with upper-extremity motion (~120 % ThorExt in Raise-) highlighted the potential for muscle crosstalk. In the arm-elevated Raise- positions the majority of the EMG signal was likely coming from the trapezius and/or rhomboid area and not just the ES. Fuglevand (1992) modelled the motor unit action potential and showed that the surface EMG signal will be dominated by activity within a depth of 1.0-1.2 cm. From this, Ekstrom et al. (2005) concluded

they would have minimal crosstalk in their study of trapezius MVC tests as trapezius was the most superficial muscle at that region. Anecdotal results from Study #1: USI-MRI reported depths of approximately 3-4 cm from skin surface to bony landmark, with approximately 1 cm of ES thickness. This would imply the potential for all three muscle layers (trapezius, rhomboid, ES) to be within range of surface EMG electrodes.

One of the main reasons for the different activation recorded from T4ES and MidTrap likely resulted from the orientation of the electrodes. It is recommended to place the electrodes parallel to the muscle fibres to avoid reductions in amplitude of the EMG signal, as Vigreux et al. (1979) found that surface EMG electrode placement along the fibre orientation of the biceps (longitudinally) picked up twice as much signal as those electrodes placed transversally. In the current study, the physical locations of the EMG electrodes between T4ES and MidTrap were very similar, with the main difference being the orientation of the electrodes (Figure 5.1). The electrodes running longitudinally along the fibres at T4 were better able to detect the signal from the ThorExt compared to the perpendicular electrodes placed at T3 targeting MidTrap. However, the longitudinal orientation also picked up strong EMG signal during the Raise- techniques. This indicated that during sagittal-plane tasks with no overhead arm motion the T4ES could be recorded from surface EMG due to the electrode orientation; however, once upper-extremity movement occurred then muscle crosstalk was likely. This was further evidenced by the activation during the Row- technique, as high level of middle trapezius/rhomboid was expected (Ekstrom et al., 2003; Lehman et al., 2004). In the present study, the Row-Sit technique showed the third highest MidTrap activation (82 %Raise-Stand), which was larger than what was found in T4ES (73 %ThorExt). These findings highlighted the importance of electrode orientation and confirmed the ability to somewhat capture the muscle of

interest, as the MidTrap muscle was expected to be activated during Row, while the T4ES was expected to show high activation during extension techniques.

This study was not without limitations. For example, these results were reflective of a young, healthy (pain-free) population with unilateral muscle recordings, and it remains unclear if those experiencing neck, back, or shoulder pain would show similar bilateral activation patterns. However, for a clinical low-back pain population MVCs are not recommended as patients are generally unwilling or unable to exert themselves maximally (Dufour et al., 2013), thus a different protocol would need to be employed for a patient group. Additionally, while these motions were designed to target the scapulo-thoracic region of the spine, it was possible other techniques not tested here could have resulted in a “truer” maximum, particularly in the MidTrap channel. Nevertheless, the primary focus was T4ES and we were confident that the resulting EMG activation from ThorExt was reflective of the maximum for that muscle. In addition, though MidTrap was reported, the electrode location was not ideal for this muscle group. However it was important to have MidTrap activation in comparison to T4ES, and given the differences in activation level between T4ES and MidTrap during the MVCs (ThorExt and Raise-Stand, respectively), it was evident that we were recording separate activations from both channels. Another limitation comes from the issue of crosstalk between the ES and trapezius/rhomboid muscle groups, as this was unavoidable given the use of surface electrodes and the anatomical constraints in the thoracic region. Future study designs could look to quantify the amount of crosstalk either by using indwelling electrodes, or by employing cross-correlation techniques to assess the commonality of the signals being recorded by the electrodes (Winter et al., 1994).

In conclusion, this study assessed the surface EMG recording of T4ES from eight MVC techniques with the results showing the ThorExt and Raise techniques elicited the largest activation from the T4ES electrode site. There was a large difference between T4ES and MidTrap during the ThorExt technique when normalized to their respective values, which showed that although crosstalk may be present, ThorExt was able to effectively target the T4ES musculature. However, caution must be exerted when analyzing T4ES during overhead or pulling-tasks, as there was high likelihood of signal contamination coming from trapezius and/or rhomboid. In these overhead and/or pulling situations, the EMG signal from the T4ES channel was the result of contributions from not just T4ES, but also the scapulo-thoracic muscles. This ES/Rhomboid/Trap complex should then be analyzed as a whole and normalized to the largest activation (e.g. from Raise-Stand), as opposed to analyzing T4ES in isolation. As such, it was therefore recommended to perform ThorExt to normalize T4ES musculature in general, yet other techniques may want to be utilized depending on the specific task being assessed.

Chapter 6: Study #3: Flexi-MoCap

6.1 Flexi-MoCap Introduction

Sagittal plane spine angles of passive postures are important to measure in the workplace and clinic, but can be difficult to quantify. For example, sitting has been shown to increase lumbar spine flexion (Callaghan & McGill, 2001), which changes the line of action of the LES muscles such that they provide less resistance to the flexion-generated anterior shear force (McGill et al., 2000). Furthermore, increased trunk flexion angle has been identified as a known risk-factor for developing occupationally-related low back disorders (Marras et al., 1993), while prolonged exposures to lumbar flexion increase the loading on the passive structures (Beach et al., 2005). Additionally, analyses of slumped sitting have revealed differences in lumbar angle within low back pain patients (Dankaerts et al., 2006) and end-range of motion patterns in the thoracic spine (Nairn et al., 2013c), highlighting potential clinical relevance. While tracking lumbar and thoracic flexion angles using MoCap is considered the gold standard for external motion analysis, MoCap can be cumbersome if not impossible to use outside of specifically designed kinematic research spaces. The common challenges of using MoCap in clinics and/or workplaces include: the high cost of the equipment and software, insufficient unobstructed space, lack of time, and unavailable qualified personnel required to collect, process, and interpret the data. Likewise, it is important for clinicians, ergonomists, and on-site researchers to be able to quickly and effectively acquire data from patients or workers in a non-invasive/non-disruptive, low-cost manner, while maintaining the accuracy and repeatability of the measures.

One potential tool for quantifying different measures of sagittal plane spine angles is Flexi (Barrett et al., 2014). Briefly, Flexi is a malleable strip of metal coated in soft

rubber/plastic that can be contoured down the midline of the spine and retain its shape in the sagittal plane. The shape of Flexi is then traced onto a sheet of paper and marked at specific vertebral levels for further measurement analysis to yield sagittal plane spine angles. Different Flexi measures have been compared to both internal and external flexion/extension thoracic and lumbar spine angle measurements. Internal measures were radiographs (Greendale et al., 2011; Tillotson & Burton, 1991; Tran et al., 2016), and external measures have included inclinometers (Tillotson & Burton, 1991; Thompson & Eales, 1994), and Debrunner kyphometers (Greendale et al., 2011; Tran et al., 2016). However, these inclinometers and kyphometers are not the ‘gold standard’ of external measurements, so the true accuracy of Flexi remains unknown. To date, no Flexi sagittal plane angles have been compared directly to MoCap calculations.

Two different ways to measure sagittal plane spine angles include: creating a local coordinate system (LCS) from marker clusters at a tangent to the spine and calculating the angle between marker clusters (Schinkel-Ivy et al., 2014), and creating rigid segments between marker clusters by drawing straight lines between specific spinous processes and calculating the angle between intersecting lines (Claus et al., 2009). With Flexi, a tangential method has been previously described by Burton (1986) for the lumbar spine. Briefly, this tangential method involves two steps: using a ruler to draw tangents on the Flexi tracing at previously marked locations (e.g. T12, L4, and S2), and using a protractor to measure the angles formed by intersecting tangents (Tillotson & Burton, 1991). High intra-rater reliability of the Flexi tangential method in the lumbar spine was previously reported in upright standing, with $ICC = 0.90$ (Taweetanalarp & Purepong, 2015), and $ICC = 0.82$ (Youdas et al., 2006). However, compared to an inclinometer, discrepancy of up to 18° was found during lumbar extension (Tillotson & Burton, 1991), indicating some level of uncertainty when comparing Flexi lumbar

tangential angles to other external measurements. Furthermore, it remains unclear the accuracy and reliability of the Flexi tangential method when applied to the thoracic spine. The segmental method described above has been used for thoracic angles in sitting with electromagnetic sensors (Claus et al., 2009), and in both sitting (Nairn et al., 2013b; c) and standing (Nairn & Drake, 2014) using MoCap; however, the segmental angle has not been described using Flexi. To date, the Flexi tangential method has only been described in the lumbar spine and has yet to be implemented in the measurement of thoracic spine angles; whereas the segmental method has not been tested on a Flexi tracing.

The Flexi is not a new measurement tool, yet it can be considered novel due to its versatility of producing reliable metrics to describe the sagittal curvature of the spine in addition to the tangential method. For example, ratios of the length and width of the lumbar and thoracic spines were developed for tracking age-related clinical changes of kyphosis and lordosis (Cain et al., 1996; Milne & Lauder, 1974). These ratios have shown high inter-rater reliability ($ICC = 0.93-0.94$, Hinman, 2004) and intra-rater reliability ($ICC = 0.93$, Yanagawa et al., 2000) in the thoracic spine, yet lower inter-rater reliability in the lumbar spine in both relaxed and erect standing ($ICC = 0.60$ and 0.73 , respectively (Hinman, 2004)). Another Flexi angle calculated from trigonometric derivation (Hart & Rose, 1986) provides an angular representation of the thoracic and lumbar curves similar to a sagittal Cobb angle obtained from radiographs by taking the angle between endplates (Keynan et al., 2006). Hart and Rose (1986) found good correlation ($r = 0.87$) and high intra-rater reliability ($ICC = 0.97$) between the lumbar sagittal Cobb angle and this trigonometric Flexi angle, and concluded the simple Flexi tool could quantify the shape of the lumbar spine. Calculations of the same trigonometric Flexi angle have shown high inter-rater reliability in seated lumbar angles ($ICC = 0.89$, Link et al., 1990), and good intra-rater

reliability in lumbar angles in standing and sitting ($ICC = 0.79$ and 0.86 , respectively, Bennett et al., 1989). Though reliable, these additional characterizations of the sagittal curvature of the spine are not a replacement for the tangential and segmental measures commonly obtained from MoCap. In order to determine the feasibility of using Flexi over MoCap for the same measures, it was important to test the reliability of the Flexi measure, especially in the thoracic spine. As such, the reliability of thoracic tangential and all segmental Flexi angles remains unclear.

Given the versatility and high reliability of Flexi measurements in determining the sagittal shape of the thoracic and lumbar spine, it still remained unclear how Flexi-measured angles and gold standard MoCap-calculated angles compared to one another, specifically in terms of the tangential and segmental methods. Therefore, the purpose of this study was twofold: to determine the level of agreement between Flexi and MoCap methods of measuring thoracic and lumbar sagittal plane spine angles, and to determine the intra-rater reliability of angles calculated from Flexi tracings. In essence, can Flexi measures match those of MoCap quality?

6.2 Flexi-MoCap Methods

6.2.1 Participants

Twenty participants (10 male, 10 female) were recruited for this study from a university population. The mean (SD) age, weight, and height were (25.3 (2.7) y, 73.40 (12.61) kg, and 1.75 (0.10) m respectively. All participants were free from neck, back, and shoulder pain at the time of collection, and had not missed any time from school or work, nor sought medical or healthcare treatment due to injury in those regions, for at least one year prior to collection. The

study was approved by the institution's Research Ethics Board and informed consent was obtained from the participants prior to collection.

6.2.2 Data Collection

The spinous processes at C7, T6, T12, and S2 (at level of posterior-superior iliac spines) were palpated while the participants were standing, and the skin just lateral to the spinous process was marked with permanent black marker. A total of 18 trials were then conducted in a random order with Flexi tracings taken from each trial. The trials included three repeats of three different spine postures (upright, flexed, and slumped) performed while sitting and standing. The trials were named Upright-Sit, Flex-Sit, Slump-Sit, Upright-Stand, Flex-Stand, and Slump-Stand, with the appropriate repeat number (1, 2, or 3).

Participants were instructed to move into the specific posture and hold statically while a 1 m Flexi was contoured down their spine (Figure 6.1A). Non-permanent marker was used on the Flexi tool to record the corresponding location of the 4 spinous process levels previously palpated and marked. Carefully and immediately the Flexi was transferred to a 60.96 cm x 91.44 cm sheet of chart paper. The shape of the Flexi (captured spine curvature) was traced and the four spinous process levels were marked with a small dot on the tracing. Then the markings were wiped off the Flexi, and the procedure was repeated until all 18 trials were completed. The Flexi was straightened out between each trial so as not to influence the next contouring and tracing of the Flexi.

Following the 18 trials with Flexi tracings, four passive-reflective motion capture clusters, consisting of five-markers per cluster (Schinkel-Ivy & Drake, 2015b), were applied over the previously palpated 4 spinous process levels (Figure 6.1B) for all 20 participants. This four-

cluster set was chosen on the basis of Schinkel-Ivy and Drake (2015b) which suggested this array for capturing sagittal plane motion of the thoracic spine. The same 18 trials were then repeated in a new random order. A MoCap system (Vicon MX, Vicon Systems Ltd., Oxford, UK) sampled at 50 Hz was used to collect 5 s of static kinematic data in each of the 18 postures.

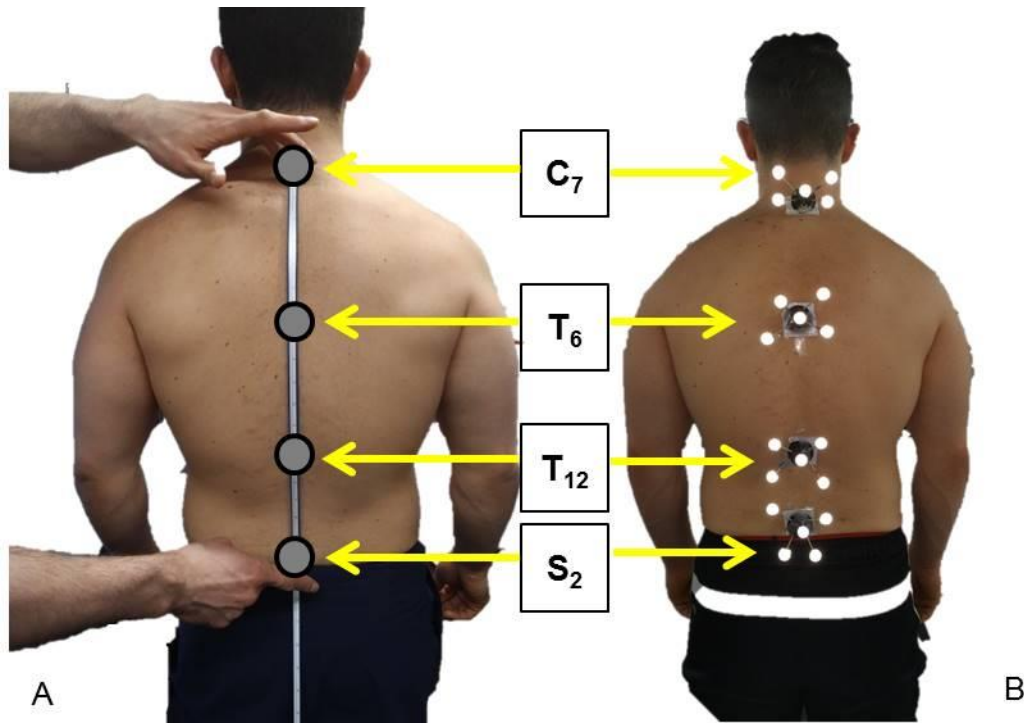


Figure 6.1. Photo showing the flexible ruler (A) and optoelectronic motion capture marker clusters (B). The locations of the palpated vertebrae are labelled with the arrows.

For a subset of 10 participants (7 Female, 3 Male), an additional randomized set of 18 trials were completed where Flexi and MoCap were collected simultaneously. This was done to confirm the reliability of collecting Flexi and MoCap separately. The MoCap clusters were removed and re-applied approximately 2.5 cm to the right of the spinous processes, and Flexi was placed the same distance to the left of the spinous processes. This small shift in position

permitted simultaneous capture of both MoCap and Flexi data, with the assumption of equal bilateral muscle mass distribution. When the participant had moved to the specific posture the Flexi was contoured down the spine and held by the researcher during the static 5 s of MoCap data recording. The Flexi was then carefully removed and immediately transferred and traced as previously described.

6.2.3 Data Processing

6.2.3.1 Flexible Ruler

A total of five sagittal plane spine angles (four thoracic, one lumbar) were measured directly on the tracing: two segmental and three tangential (Figure 6.2). In the segmental method, thoracic segments were defined as lines connected between adjacent landmarked spinous processes (dots), resulting in lines from C7-T6, T6-T12, and T12-S2, with the intersection of adjacent segments being measured as MidSeg and LowSeg (Figure 6.2A). For the tangential method, the tangents to the Flexi tracings were drawn from each of the four landmarked spinous processes (dots), and the intersection of C7-T6, T6-T12, and T12-S2 were used to define the UpTTan, LowTTan, and LumbTan angles, respectively (Figure 6.2B). All Flexi angles were measured on a single tracing using a protractor with 1° increments, and were measured by 0.5° where angles fell between the 1° increments.

6.2.3.2 Motion Capture

Motion capture marker data were first labelled using Vicon Nexus software (v. 1.6.1, Vicon Systems Ltd., Oxford, UK) then remaining processing was completed using Visual3D

(v5.02 C-Motion Inc., Germantown, USA). Kinematic data were low-pass filtered with a dual-pass, 4th order Butterworth filter with a 2.5 Hz cut-off rate as determined by residual analysis previously run on similar movement patterns (Nairn et al., 2013b). For the segmental method, the MoCap clusters were used to define the endpoints of the rigid segments created between adjacent clusters, and angles were calculated between adjacent rigid segments (Nairn et al., 2013b). For example, the marker cluster at C7 was used as the proximal endpoint, and the marker cluster at T6 as the distal endpoint for one of the rigid segments. The cluster at T6 was then used as the proximal endpoint, and the cluster at T12 as the distal endpoint for the next rigid

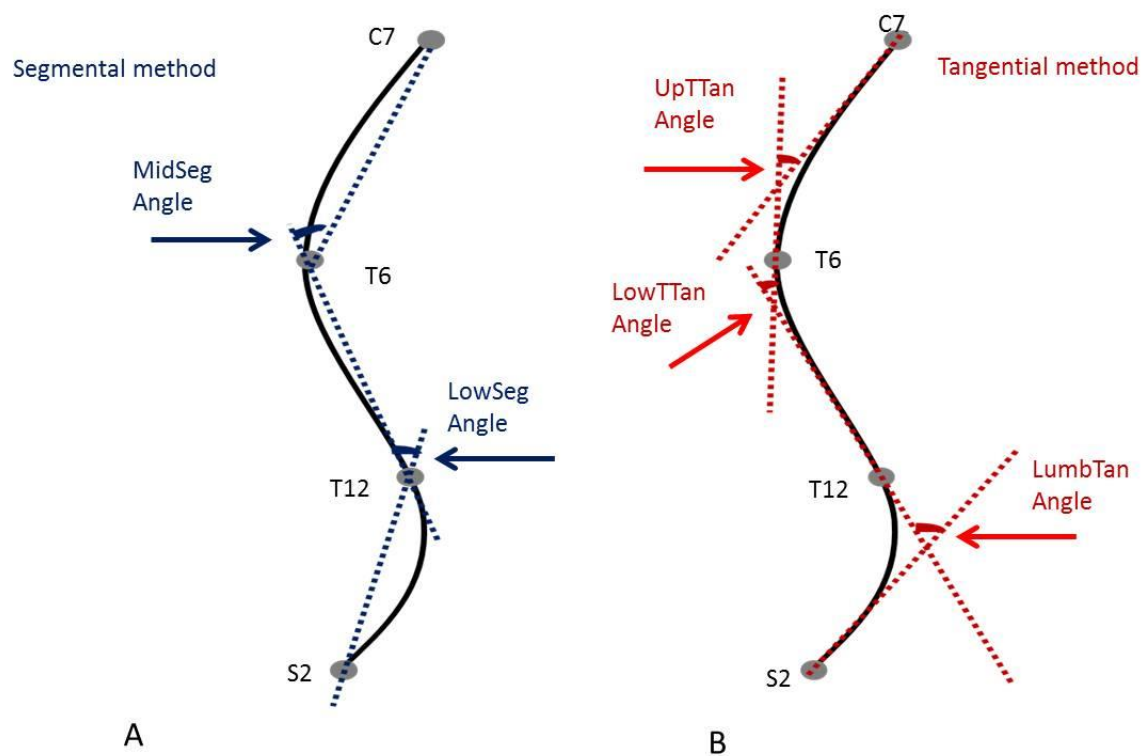


Figure 6.2. Representation of a flexible ruler tracing (solid black line) with the angles drawn. The grey circles are the specific spinous processes. The segmental method (A) is represented by the blue lines that connect the spinous process points, and the angles between these lines are MidSeg and LowSeg. The tangential method (B) is represented by the red angles between the tangent lines, shown as UpTTan, LowTTan, and LumbTan angles.

segment. The intersection of these two rigid segments was the MidSeg angle (Figure 6.2A). Equivalent tangential angles were calculated according to Schinkel-Ivy et al. (2014), and were defined as the angles between adjacent clusters. Briefly, this method defined a LCS for each of the MoCap clusters, and the sagittal angles were taken between the vertical components of the LCS of adjacent clusters. Since the orientation of the LCS was dependent on the cluster, and the orientation of the cluster depended on the curvature of the spine, the LCS was generated at the tangent to the curve. For example, the angle between the vertical components of the LCS in the cluster at C7 and the cluster at T6 resulted in the UpTTan angle (Figure 6.2B).

6.2.4 Data Analysis

6.2.4.1 Bland-Altman

To measure the agreement between Flexi and MoCap angles, the Bland-Altman graphical approach was used to plot the individual difference between the methods as a function of the average between the two methods (Altman & Bland, 1983; Bland & Altman, 1986). This method is preferred over strict comparison of means and correlation analyses to determine if two methods of measurement agree (Altman & Bland, 1983). Included on the Bland-Altman plot is the MeanDiff between the methods, and the Upper and Lower LoA, which is a 95% confidence interval about the MeanDiff calculated from the standard deviation (*SD*) using Equations 6.1 and 6.2 (Bland & Altman, 1986). The LoA indicates where 95% of the differences between the two measurements will lie (Bland & Altman, 1986), and values outside of the LoA can be considered outliers. Appropriate levels of agreement based on \bar{d} and LoA were determined *a priori* and outlined below.

$$\text{Equation 6.1: Upper LoA} = \text{MeanDiff} + 1.96 * SD$$

$$\text{Equation 6.2: Lower LoA} = \text{MeanDiff} - 1.96 * SD$$

6.2.4.2 Statistics

All statistical analyses were performed using IBM SPSS Statistics v.22 (SPSS Inc., Chicago, IL). The reliability of each recorded angle was analyzed using the intraclass correlation coefficient model $ICC(3,k)$, which gives an indication of the consistency of the ratings when one person takes all the measurements and the mean is taken (Shrout and Fleiss, 1979). For this case, $k=3$ as three repeats of each condition were measured, resulting in the model $ICC(3,3)$ being used. To test for differences in the means between the methods, the average of the three repeats from each of the trials was used in the ANOVAs. Separate 2×2 mixed-model ANOVAs were conducted on each angle in each of the six postures, with the factors being Sex and Method. Significant F -tests were further analyzed pairwise using a series of Bonferroni corrected t -tests, and all significant p -values were set to $\alpha = 0.05$. Where sex differences were found in a given angle, the Bland-Altman plot and the ICC calculations were performed separately for each sex for that angle. With the subset of 10 participants who performed the simultaneous collection of Flexi and MoCap angles, a one-way ANOVA (factor: Method) tested for differences between the angles recorded, while the reliability and Bland-Altman analyses were performed the same way as described above. In addition, the Bland-Altman information was used to assess the presence of any systematic (fixed) bias, and any proportional bias that may be present within the two systems (Ludbrook, 2002). The fixed bias is present if a t -test of the mean difference significantly differs from zero, and proportional bias is present if the slope of the regression of the difference on the average is significantly different from zero (Ludbrook, 2002). Proportional

bias indicates that the measures do not agree over the entire range, for example, a positive slope would imply that the magnitude of differences measured between Flexi and MoCap increases as the average angle increases.

6.2.4.3 Overall Acceptability Criteria

To determine overall whether or not the measured Flexi angle was acceptable in comparison to the calculated MoCap angle, the following five criteria were established: an *ICC* value greater than 0.800, a MeanDiff less than or equal to 5° with a *p*-value greater than 0.05, and the upper and lower LoA within +/- 10°. The *ICC* threshold of 0.800 was chosen as the threshold for ‘excellent’ reliability (Swinscow, 1997) while the MeanDiff was arbitrarily chosen as half the value of the LoA. The 20° range in LoA was chosen as a conservative range of observation-based posture assessment, where 30° increment has been suggested as the optimal range for minimizing error in observing sagittal plane trunk angles (NIOSH 2014). To summarize, there needed to be a reliable measure with a small, non-significant mean difference that fell within a set range. In cases where four of the five criteria were met for a given angle, consideration was made for acceptability if an outlier was present.

6.3 Flexi-MoCap Results

The main findings from the primary analysis (n=20) and the subset analysis (n=10) were similar, in that the segmental method showed the highest level of acceptability between Flexi and MoCap methods (Tables 6.1 and 6.2). This indicated that Flexi and MoCap measured separately (n=20) were appropriate for interpretation, as similar results were found when measured simultaneously (n=10); thus, only the results of the primary analysis (n=20) will be presented

and discussed further. Additional data are presented in Appendix B. Specifically, the mean (*SD*) angles for each Flexi and MoCap condition are presented in Tables B1 and B2, and Figures B1-B30 shows each Bland-Altman plot, with the systematic and proportional bias reported in Table B3-B8.

Specifically, the MidSeg angle showed the best agreement between the two methods as this angle met all five of the criteria in Upright-Stand (Figure 6.3), Flex-Stand, and Flex-Sit. Additionally, four of the five criteria were met in MidSeg Slump-Stand and this was also deemed acceptable (Table 6.1). For the MidSeg Slump-Stand posture, the upper LoA was 11.9° yet the actual largest difference between measures was 9.1°, therefore this Flexi measure was considered acceptable. These results showed that Flexi measurements of the MidSeg angle were most similar to the gold standard MoCap calculated angles.

Table 6.1. Summary of the angles and postures from the main analysis that were deemed acceptable (n=20). The shaded cell indicates where the Limit of Agreement was violated, yet the maximum difference was under 10°.

	Stand Upright MidSeg (n=20)	Stand Flex MidSeg (n=20)	Stand Slump MidSeg (n=20)	Sit Flex MidSeg (n=20)
Mean Difference	-0.3°	0.4°	2.1°	0.3°
Upper LoA	8.2°	7.6°	11.9° max=9.1°	7.0°
Lower LoA	-8.8°	-6.8°	-7.8°	-6.5°
<i>p</i> -value	0.790	0.625	0.081	0.718
<i>ICC</i> _{flexi}	0.913	0.927	0.926	0.908
<i>ICC</i> _{mocap}	0.965	0.982	0.979	0.993

Table 6.2. Summary of the angles and postures from the subset analysis that were deemed acceptable (n=10). Where the Limit of Agreement was violated, the maximum value obtained is presented.

	Stand Upright	Stand Flex	Stand Slump	Sit Upright	Sit Flex	LowSeg	Sit Slump
	LowSeg (n=10)	LowSeg (n=10)	LowSeg (n=10)	MidSeg (n=10)	MidSeg (n=10)	LowSeg (n=10)	MidSeg (n=10)
Mean Difference	1.4°	1.1°	0.9°	2.8°	-0.1°	1.2°	1.8°
Upper LoA	9.9°	9.8°	11.8° max [†] =4.8°	12.6° max=9.3°	4.5°	8.6°	6.8°
Lower LoA	-7.2°	-7.6°	-9.9°	-7.0°	-4.7°	-6.2°	-3.2°
p-value	0.347	0.446	0.602	0.109	0.913	0.333	0.048
ICC _{flexi}	0.863	0.879	0.915	0.886	0.914	0.807	0.955
ICC _{mocap}	0.955	0.996	0.962	0.953	0.991	0.981	0.993

[†]Maximum value with the lone outlier removed.

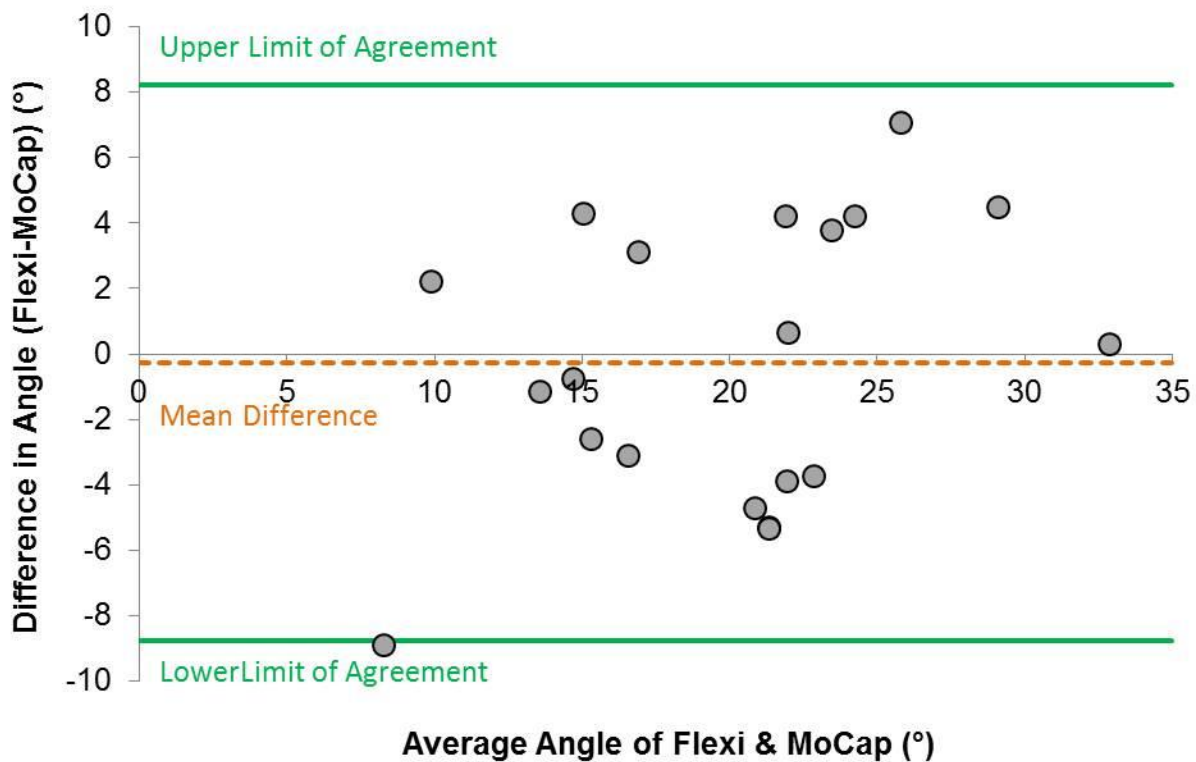


Figure 6.3. Bland-Altman plot of the MidSeg angle in Upright-Stand. This flexicurve angle was considered 'acceptable'.

Sex differences were found in six of the ANOVA analyses: four LumbTan angle differences and two LowSeg differences ($F(1,18) > 4.70, p < 0.044$). Main effects of Sex on the LumbTan angle were found in Slump-Sit, Upright-Stand, and Slump-Stand, where females had significantly greater lordosis than males by up to 12.4° ($p < 0.03$). The LumbTan Upright-Sit angle showed an interaction effect of Sex by Method as shown in Figure 6.4. The LowSeg angle in Upright-Sit and Slump-Sit also revealed an interaction effect of Sex by Method, where males showed up to 10.4° less lordosis than females with Flexi measurements ($p < 0.040$). These sex differences did not impact the overall results of which measures were considered acceptable, as the reported values within sexes did not meet the overall level of acceptability criteria of having a reliable measure with a small, non-significant mean difference that fell within a set range.

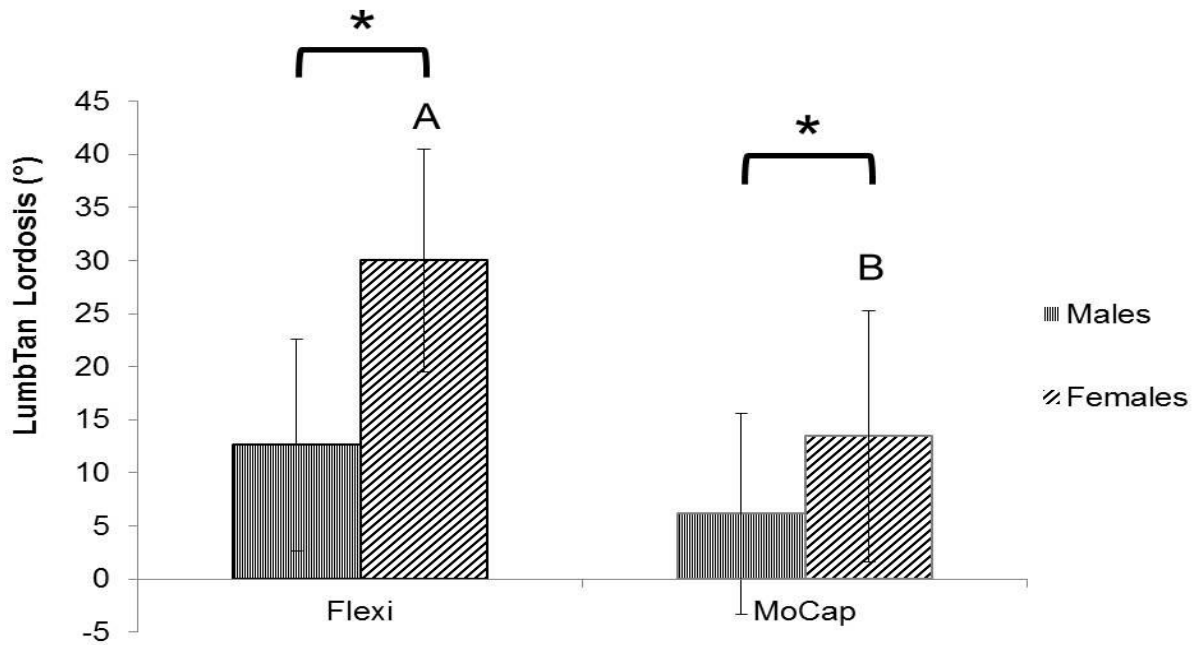


Figure 6.4. Interaction effect of Sex (Males and Females) and Method (Flexi and MoCap) on LumbTan lordosis angle. Asterisks (*) represent a difference between Sex for each Method ($p < 0.024$). Unmatched lettering between females represent a difference in Method ($p = 0.001$).

Though none of the Flexi tangential angles showed an acceptable agreement with the MoCap angles, there were notable results in the UpTTan angle. For example, with the UpTTan Upright-Stand angle there was a small, non-significant mean difference (MeanDiff = 1.6°, $p = 0.498$); however, there was a large range in the LoA (Lower LoA = -18.9°, Upper LoA = 22.1°), as shown in Figure 6.5. Similar results of non-significant mean differences with a large upper and lower LoA were also found in UpTTan Upright-Sit.

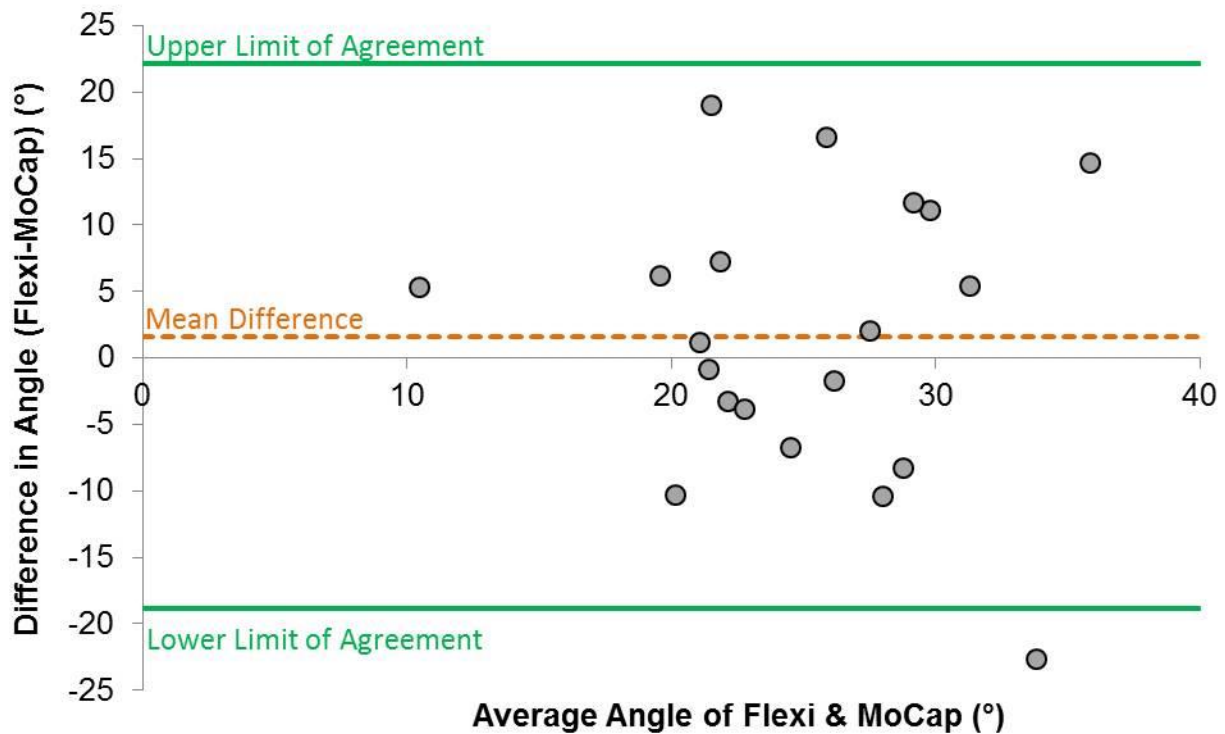


Figure 6.5. Bland-Altman plot of the UpTTan angle in Upright-Stand (n = 20). This Flexi angle was considered ‘not acceptable’ because of the large Limits of Agreement.

6.4 Flexi-MoCap Discussion

This study compared two segmental and three tangential sagittal spine angles obtained from Flexi measurements to those same angles calculated from MoCap. In general, the segmental method showed acceptable agreement between the Flexi and MoCap methods as the

MidSeg angle met 5/5 or 4/5 of the criteria in each Stand- posture as well Flex-Sit as summarized in Table 6.1. The findings of the subset analysis (n=10) supported the results of the primary analysis. Overall, caution should be used when using the tangential method to obtain angles from Flexi, as these thoracic and lumbar angles, particularly in the lower regions, showed minimal agreement with the MoCap angles.

The LumbTan angles obtained from Flexi were comparable to previously reported literature. For example, Flexi angles from Burton (1986) reported maximum seated lumbar flexion angles from 20 healthy participants (characteristics unknown) to be 20.3°, which was comparable to the present study mean (*SD*) of 18.8° (7.7). Also in seated flexion, Youdas et al. (1996) reported lumbar Flexi angles in 45 asymptomatic males (31°) and 45 asymptomatic females (22.9°). These values were slightly larger in absolute terms compared to the present study (Males: 22.3° (6.2); Females: 15.4° (7.8)); however, the relative difference between sexes was similar. Additionally, in upright standing Youdas et al. (1996) reported males and females having lordosis angles of 37.5° and 52.7°, respectively, which was similar to the current study with males and females having lordosis angles of 34.6° (7.1) and 47.6° (11.7), respectively.

Comparing the MoCap tangential angles, Schinkel-Ivy et al. (2014) used two clusters located at T3 and T9 in addition to the T6 cluster to determine tangential angles. The standing flexion tangential angles from the thoracic spine (T3 relative to T6 and T6 relative to T9) were reported as 23.7° (4.6) and 20.1° (5.8), respectively, and the Lumbar angle (L1 relative to L5) was 17.9° (11.2) (Schinkel-Ivy et al., 2014). In the present study, the UpTTan and LowTTan angles were 37.78° (10.40) and 26.35° (11.79), respectively, with the LumbTan angle being 29.37° (11.89). It was likely that the current values obtained were larger than those obtained

from Schinkel-Ivy et al. (2014) due to the differences in marker setup, as the closer spacing of the clusters in Schinkel-Ivy et al. (2014) would result in smaller angles.

Despite minor methodological differences in the MoCap segmental method, the thoracic angles obtained in the current study were comparable to what has been previously reported (Nairn & Drake, 2014). Additional clusters were used to further partition the thoracic spine into upper-, mid-, and lower-thoracic regions, and instead of peak angle the range of motion was reported at each region (Nairn & Drake, 2014). The mid- and lower-thoracic range of motion in standing flexion described by Nairn and Drake (2014) were reported as 11.76° and 35.34° , respectively. In the present study, the range of motion could be represented as the flexion angle minus the upright angle, and in this case would be 13.14° and 37.55° for the MidSeg and LowSeg, respectively. The mid-thoracic angle from Nairn and Drake (2014) was defined as the angle between segments T5-T8 and T9-T12 which was similar to the MidSeg angle of the current study, between segments C7-T6 and T6-T12 (Figure 6.2A). Additionally, the lower-thoracic angle from Nairn and Drake (2014) was defined as the angle between segments T9-T12 and L1-PSIS and is most similar to the LowSeg angle in the present study, between segments T6-T12 and T12-S2 (Figure 6.2A). These segments were similarly defined across both studies and produced similar MoCap angles accordingly.

Caution must be taken when interpreting absolute tangential angles measured from Flexi, as these did not agree with MoCap angles. For example, in upright sitting the current results showed that Flexi over-estimated lumbar lordosis compared to MoCap by 6.5° and 16.5° in males and females, respectively. Furthermore, there is evidence to suggest that Flexi measures do not entirely agree with lordotic curves in the spine. This discrepancy in lordotic measures was shown by Tillotson and Burton (1991) who found poor agreement between Flexi angles and

inclinometer measures during lumbar extension, and Hinman (2004) who found lower reliability in lumbar ratio measures compared to thoracic ratio measures. Likewise, this disagreement might not be limited to the lumbar spine, as Harrison et al. (2005) found poor agreement between Flexi tangential calculations and radiographic images in the cervical spine. Future work should investigate normalized Flexi measures, such as a percentage of max flexion in order to determine if the relative changes of the tangential angles are similar to those obtained from MoCap.

This study was not without its limitations, both from the perspective of using MoCap and Flexi. The results of the current study were limited to a passive-reflective MoCap system with a specific marker cluster set, albeit this marker set was based on previously published research that focused on thoracic spine motion (Schinkel-Ivy et al., 2014; 2015b). It is likely that other motion capture systems, such as electromagnetic and active-marker optoelectronic systems, would show similar results, though it is possible that there may be different marker configurations that could strengthen the comparison between the two methods. In terms of Flexi, one of the drawbacks was the inability to calculate a global angle from the segmental method, e.g. segment relative to vertical, as the position of the spine in space cannot be captured. Another setback of the Flexi tool is it is only able to capture angles in one plane, without three-dimensional or co-planar analyses. These drawbacks tend to limit the overall use of Flexi when analyzing thoracic angles, depending on the application. A limitation of the Bland-Altman method was that the criteria for the LoA acceptability were arbitrarily set, and the level of acceptability will vary depending on the methods being compared. As such, it was important to set the acceptable limits *a priori* in order to reduce the subjectivity of the analysis. Another limitation stemmed from using static postures only, as Flexi measures did not allow for monitoring dynamic postures. However, the applicability of static passive postures, such as

those outlined in the current study, remains an important consideration in the workplace and clinical settings.

To the authors' knowledge, this was the first study to use the Flexi tangential method in the thoracic spine, to calculate a segmental angle using Flexi, and to compare these Flexi angles to those obtained via gold standard MoCap. The overall acceptability between the methods was based on criteria both statistically and graphically, with results showing the segmental method to have a good level of agreement between the methods, specifically the MidSeg angle. This suggested that Flexi could be used as an alternative to MoCap if segmental thoracic angles were the variable of interest. Therefore, Flexi could prove useful in quantifying sagittal-plane thoracic spine angles for on-site data collections such as with industrial and office workers and/or healthcare professionals (e.g. nurses during a hospital shift).

Chapter 7: Study #4: USI-EMG

7.1 USI-EMG Introduction

The T4ES musculature could play an important role in the load trade-off between the shoulder and low back region during functional tasks, as this location interfaces with the scapulothoracic muscles responsible for connecting the scapula to the thorax (Peat, 1986). During active contraction and passive motion, changes in muscle morphology such as muscle thickness and fibre pennation angle play a key role in how that muscle will function over a variety of demands. For example, pennation angles of the muscle fibres dictate the force transmission onto the tendon (Kawakami et al., 2000), with larger angles increasing the force generating capacity along the tendon (Maganaris & Baltzopoulos, 1999). Additionally, muscle thickness and pennation angle have been shown to be related to each other (Kawakami et al., 2000), as the angle of the fibres (θ) affects the change in fibre length (Herbert & Gandevia, 1995). Pennation angle and fibre length can then be related to two-dimensional muscle thickness by: Muscle thickness = Fascicle length * $\sin \theta$ (Dieterich et al., 2014). Muscle contractions have been shown to decrease fibre length and increase pennation angle (Narici et al., 1996), which could lead to changes in muscle thickness. The results from Study #1: USI-MRI found that in supine posture, T4ES was relatively thinner (0.8 cm) and had a shallower pennation angle (14°) compared to reported LES thickness (3.88 cm, Belavý et al., 2015) and angles (25.7° , McGill et al., 2000). This contribution was important as it highlighted potential functional differences throughout ES levels, as a reduction in ES pennation angle shifts the line of action towards creating compression force and away from posterior shear force (Macintosh et al., 1993). As changes in muscle structure can alter the general function of that muscle, the next step is to

understand how the structure of T4ES will react throughout a number of functional Active and Passive postures. Knowing how the structure of T4ES changes could help in understanding how the loads are traded-off between the shoulders and low back based on the function of the intermediary (thoracic) region. For example, different arm and body postures along with varying levels of contraction will alter pennation angle, and thereby the amount of force that can be generated in a given compression or shear direction. However, these changes in the T4 region and their potential implications remain unclear.

One of the relatively recent applications of USI in trunk muscles has been to relate changes in morphology to muscle activity/function, with varying results being found. For example, linear regression has shown LES thickness at L1 was related to upright extension force ($R^2 = 0.60$), whereas pennation angle was not ($R^2 = 0.17$) (Desmoulin & Milner, 2007). Furthermore, lumbar multifidus thickness was measured in prone posture from rested and contracted states while performing contralateral arm lifts, and found no significant increases in muscle thickness (Teyhen et al., 2012). In terms of relating changes of morphometry from USI to different levels of EMG activity, Hodges et al. (2003) was considered the first to address this issue directly. In the abdominal wall, USI and fine-wire needle electrodes were used to record muscle activation from EO and internal oblique (IO), and TransAb during ramped isometric contractions (Hodges et al., 2003). In general, a linear relationship was found between EMG and changes in thickness up to about 30 %MVC in all muscles except for EO ($R^2 = 0.23$), which did not get thicker despite increasing in activation (Hodges et al., 2003). Similarly, McMeeken et al., (2004) found a linear relationship between TransAb activation and thickness during a ramped abdominal drawing-in maneuver ($R^2 = 0.87$); whereas no clear relationships between thickness changes and surface EMG recordings were found during abdominal hollowing and brace

techniques in IO ($r = 0.14$) and EO ($r = -0.22$) (Brown & McGill, 2010). Mixed results of EO and EMG have also been reported by John and Beith (2007) who found stronger relations during trunk rotation than abdominal drawing-in, indicating the importance of accounting for functionality of the muscle when interpreting USI thickness changes as a level of muscle contraction.

Specific to changes in lumbar muscle thickness and pennation angle measured by USI, there are relatively few studies that have also included EMG recording. Kiesel et al., (2007) was the first to examine the relationship between lumbar multifidus thickness changes and EMG recorded from fine-wire electrodes. During contralateral arm raises from prone with varying degrees of weight, strong correlation coefficients were found ($r = 0.79$) with EMG values ranging from 20-35 %MVC (Kiesel et al., 2007). Also in multifidus, however with surface electrodes, Djordjevic et al., (2015) found significant weak correlations between thickness and EMG ($r = 0.37$). In a study that correlated both LES thickness and pennation angle to %MVC during light and moderate contractions, Cuesta-Vargas and Gonzalez-Sanchez (2013) found strong positive correlations ($r = 0.731$ to 0.907) between variables of the same contraction (e.g. moderate contractions to moderate contractions), but weak negative relations between different variables of different contraction intensities (e.g. moderate contractions to light contractions) ($r = -0.314$ to -0.109). Finally, increasingly demanding extension tasks from Harriss and Brown (2015) found LES fibre pennation angle to increase as the level of EMG increased at L1 ($r = 0.89$) and L3 ($r = 0.90$). There remain few insights into the relationship between morphology and muscle activation in the lumbar spine, and to date there has yet to be a similar analysis in the thoracic spine, which could play an important role in understanding how forces are transmitted through the thoracic to the lumbar spine.

The findings from Study#1: USI-MRI showed that USI was reliable and accurate for measuring T4ES morphology such as thickness and pennation angle. Additionally, the results of Study #2: T4ES-MVC indicated large activation of T4ES in active MVC postures such as arm raise and thoracic extension during maximum effort trials. Furthermore, passive postures, such as those exhibited in Study #3: Flex-MoCap have shown a reduction of T4ES activity when moving from upright to slump or full-flexion (Ang et al., 2016; Caneiro et al., 2010; Nairn et al., 2013c). However, it remains unclear how the muscle activation patterns found during functional active and passive postures are related to the underlying structural changes of T4ES. Therefore, the purpose of this study was twofold: to determine the relationship between changes in morphology and muscle activation in T4ES, and to see if there was an effect of different active and passive postures on these changes.

7.2 USI-EMG Methods

7.2.1 Participants

The same 30 participants from Study #2: T4ES-MVC were used for this collection, with ethical and recruitment considerations highlighted in the **Common Methods 3.1: Participants** section. Briefly, the mean (*SD*) age, height, and weight of these participants were 20.8 (2.8) y, 1.69 (0.10) m, and 67.1 (15.6) kg, respectively.

7.2.2 Instrumentation

Surface EMG was collected from T4ES according to the **Common Methods 3.3: Electromyography** section and Study #2: T4ES-MVC (see Figure 5.1). Briefly, the T4 spinous

process was palpated from C7, the skin was prepared, and electrodes were placed unilaterally on the dominant side approximately 2-2.5 cm from the midline, with a ground electrode placed over the clavicle.

Ultrasound images were recorded as outlined in the **Common Methods 3.2: Ultrasound Imaging** section. Briefly, a Mindray DP-6900 system with a linear transducer (model 75L60EA, 7.5 MHz, Shenzhen Mindray Bio-medical Electronics Co., Ltd., Nanshan, P.R. China) was used to acquire b-mode images at the T4 level on the side opposite to the EMG electrodes. Prior to any image recordings, the transducer was placed over the skin on the area to be recorded and marker was used on the skin to denote the top, bottom, left, and right sides of the transducer so placement could be repeated between trials. Similar methods of simultaneous unilateral collection of USI and EMG have been reported in LES (Harriss & Brown, 2015) and the abdominal wall (Brown & McGill, 2010).

7.2.3 Data Collection

After electrode placement, Study #2: T4ES-MVC was performed to determine which MVC maximum should be used for subsequent analyses. This was followed by the current study's USI-EMG trials.

A total of 15 trials were recorded for analysis, by which six were designated as Passive, eight as Active, and one Prone (rest/calibration). The Passive postures assumed were the same as Study #3: Flexi-MoCap, and included Upright-Stand, Upright-Sit, Flex-Stand, Flex-Sit, Slump-Stand, and Slump-Sit. With these Passive postures, participants were instructed to move to the final position and hold statically while remaining relaxed. Once the participant was static, the ultrasound transducer was coated with transmission gel, placed over the skin within the

previously marked area, and verbal indication was provided to an assistant to begin a 5 s recording of the EMG. During this 5 s, the USI was frozen on-screen and saved automatically to a USB key as a Dicom file for offline processing. For the Active postures, these were similar to the MVCs from Study #2: T4ES-MVC which were: ThorExt, LumbExt, Raise-Stand, Raise-Sit, Row-Stand, Row-Sit, LatPull-Stand, and LatPull-Sit. Participants were instructed to perform these contractions at a submaximal-level against manual resistance, with the exception of ThorExt and LumbExt, where no resistance was applied. The ThorExt and LumbExt trials were performed against body weight with no additional resistance as the collection assistant present was required to support the legs of the participant during the extension motion. The recording of the data for the Active trials was similar to that of the Passive ones. The transducer was initially placed over the skin, and the participants were instructed to begin their light contraction against the manual resistance. Once the contraction had started, 5 s recording was initiated and the USI was saved during that 5 s window. The Prone trial was performed on a therapy table where participants lay prone with their arms at their sides and their heads turned to the side the EMG electrodes were on. Within this position a 5 s recording of EMG data was taken and the USI was saved. For all participants, Upright-Stand, Upright-Sit, and Prone were collected first, while the remaining trials were all presented in a different random order for each participant.

7.2.3 Data Processing

There were a total of 450 EMG trials and subsequent USIs that were collected (30 participants x 15 postures). Due to instrumentation issues with the EMG system, data from four participants (1 Male, 3 Female) were removed from EMG analyses, yet these participants' USI data were retained. Of the remaining 390 EMG trials (including Prone), an additional 7 separate

trials (1.79%) were removed due to EMG artefact. With the USIs, Prone was used as a reference and not analyzed separately, resulting in 420 USIs for analysis. Of those 420 USIs, four images (0.95%) were excluded due to image quality.

Initial USI and EMG processing was performed offline as outlined in the **Common Methods 3.2: Ultrasound Imaging** section and Study #1: US-MRI; and Study #2: T4ES-MVC, respectively. In short, USI thickness measures were taken between the transverse process and echogenic fascial border (Bentman et al., 2010; Watanabe et al., 2014), and pennation angle measures were taken with respect to the skin (Harriss & Brown, 2015; McGill et al., 2000) as illustrated in Study #1: USI-MRI, Figure 4.3C. With the EMG signal, the linear envelope was generated by full-wave rectification and passing the signal through a 4th order low-pass Butterworth filter with a 2.5 Hz cut-off frequency (Brereton & McGill, 1998; Brown & McGill, 2010). For context, the thickness of rhomboid major and trapezius were also measured in each of the postures. For these muscles, the transverse process superior to the T4ES measurement was identified, and the thickness measures were taken between the fascial borders of each muscle.

All USI and EMG measures were then normalized to a respective reference value (Brown & McGill, 2010; Whittaker et al., 2007). Ultrasound thickness and pennation angles were normalized to a percentage of change from Prone (Equation 7.1), where 100% change indicated the thickness or pennation angle doubled in value from the Prone trial.

$$\text{Equation 7.1: \%Change} = \left(\frac{\text{Muscle}_{\text{task}} - \text{Muscle}_{\text{prone}}}{\text{Muscle}_{\text{prone}}} \right) \times 100\%$$

This USI normalization resulted in the dependent variables %ThickChange and %AngleChange. For EMG normalization, the results of Study#2: T4ES-MVC concluded that ThorExt (sagittal plane) was the recommended MVC technique to use; as such, all extensor MVCs were used (ThorExt and LumbExt) to ensure the maximum extension value was obtained. The maximum value was taken from across the four Extension trials (two Thor, two Lumb) and this absolute maximum was used to normalize the 15 trials to %MVC. From the 5 s of data collection for each trial, the middle 3 s were averaged and used for statistical input. These normalization techniques of comparing USI as a percent change from rest, and EMG as a %MVC of the linear envelope have been reported in previous literature relating USI and EMG to one another (Brown & McGill, 2010).

7.2.5 Statistical Analyses

A combination of correlation and inferential statistics were used for analyses. To determine the relationship between EMG (%MVC) and T4ES morphometry (%Change) across the postures, Pearson's r values were calculated on the following pairings: %MVC-%ThickChange, %MVC-%AngleChange, and %ThickChange-%AngleChange. These analyses were performed on all postures combined, Active and Passive postures only and each posture individually. Correlation values were considered as follows: very weak: 0-0.199; weak: 0.200-0.399; moderate: 0.400-0.599; strong: 0.600-0.799; and very strong: 0.800-1.000. To test for differences between postures separate ANOVAs were run on each dependent measure (%MVC, %ThickChange, %AngleChange). The EMG data were analyzed using a 2 x 15 mixed-model ANOVA with the factors Sex and Posture, which included Prone. For the USI measures, a 2 x 14 mixed-model ANOVA was run, with Prone being excluded as this measure was incorporated

into the normalization process. For all analyses, $\alpha = 0.05$, and significant F -statistics were further analyzed pairwise using Bonferroni-corrected t -tests. If sex differences were not present in the ANOVA, the correlation analysis was run with combined male/female data, and the ANOVA was re-run as a one-way repeated measures ANOVA.

7.3 USI-EMG Results

There were no interaction or main effects of Sex found on EMG ($F(14,280) = 0.99, p = 0.464$; $F(1,20) = 0.88, p = 0.360$, respectively) or USI ($F(13,212) < 1.15, p > 0.313$; $F(1,24) < 2.15, p > 0.156$, respectively) measures, thus male and female data were combined for all analyses. A representative USI from each posture is shown in Figure 7.1A-P, which highlights the borders of T4ES, rhomboid major, and trapezius. Appendix C provides the raw pennation angle and thickness measurements from each posture for each muscle, including rhomboid and trapezius.

7.3.1 Correlation

When all postures were analyzed together a weak positive correlation was found for each of the pairings; however, this relationship became much more diluted when the individual postures are analyzed separately. For example, across all postures the r (95% C.I.) for EMG-%ThickChange, was $r = 0.297$ (0.207-0.388), $p < 0.01$ (Figure 7.2); EMG-%AngleChange was $r = 0.265$ (0.140-0.391), $p < 0.01$ (Figure 7.3); and %ThickChange-%AngleChange was $r = 0.378$ (0.285-0.468), $p < 0.001$ (Figure 7.4). On the contrary, the EMG-%ThickChange pairings showed no significant correlations for any posture on its own or for combined just Active and Passive postures ($r = -0.355$ to 0.345 , Tables 7.1 & 7.2), indicating no clear relationship between

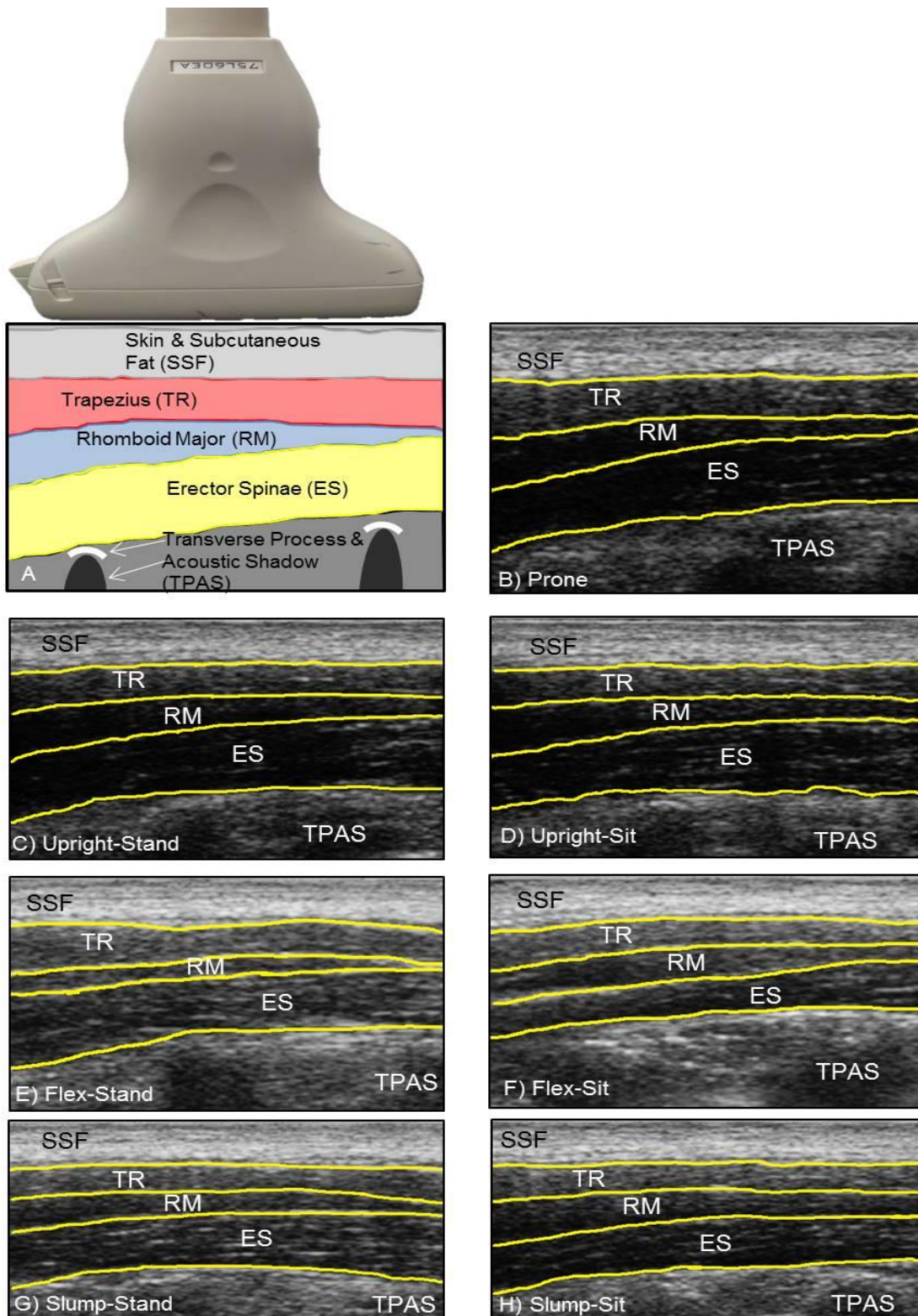


Figure 7.1. (A-H). Representation of transducer and the visible layers (A), including: skin and subcutaneous fat (SSF), trapezius (TR), rhomboid major (RM), erector spinae (ES), and the transverse process and acoustic shadow it creates (TPAS). Postures include: Prone (B), Upright-Stand (C), Upright-Sit (D), Flex-Stand (E), Flex-Sit (F), Slump-Stand (G), and Slump-Sit (H).

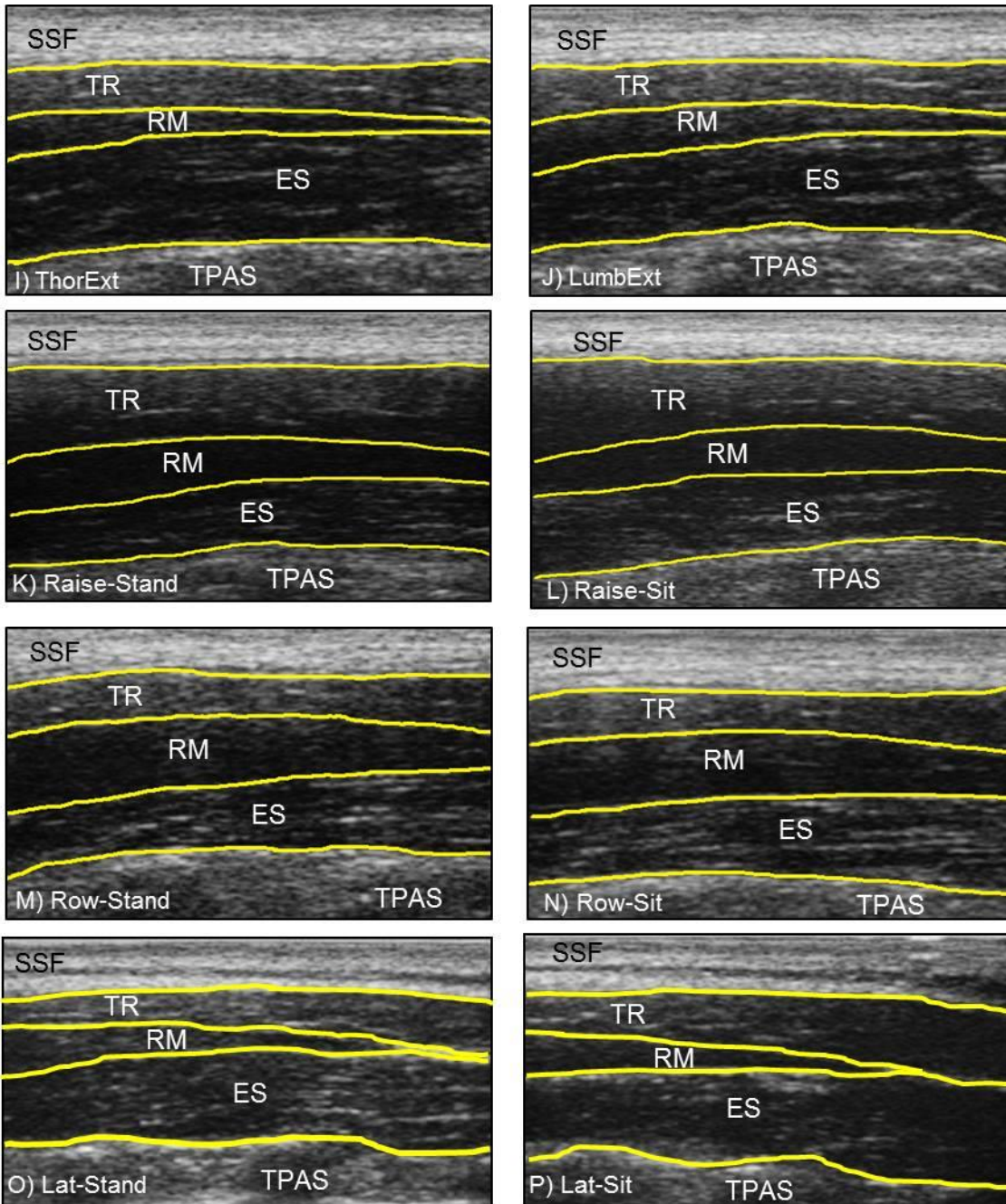


Figure 7.1. [cont'd] (I-P). Images showing: skin and subcutaneous fat (SSF), trapezius (TR), rhomboid major (RM), erector spinae (ES), and the transverse process and acoustic shadow it creates (TPAS). Postures include: ThorExt (I), LumbExt (J), Raise-Stand (K), Raise-Sit (L), Row-Stand (M), Row-Sit (N), Lat-Stand (O), and Lat-Sit (P).

muscle activation and thickness change. With EMG-%AngleChange, Active postures showed a very weak relationship across all Active postures (Table 7.1), and a moderate relationship was found in Raise-Stand and Row-Sit (Table 7.1). Weak-to-moderate relationships were also found between %ThickChange-%AngleChange throughout the Active and Passive postures (Tables 7.1 & 7.2). Overall, there was no clearly defined relationship found between muscle activation and muscle morphometry from T4ES.

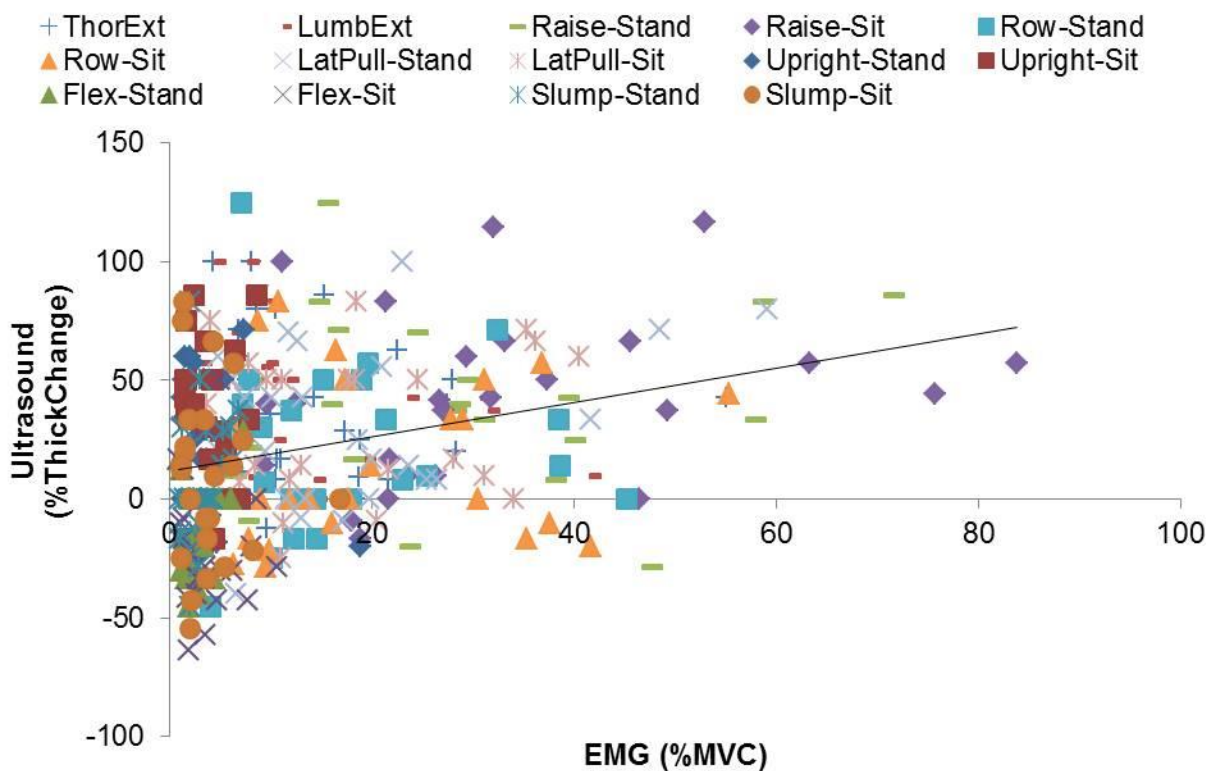


Figure 7.2. Correlation of EMG to %ThickChange for all postures and all participants combined (n = 354). $r = 0.297$, $p < 0.01$.

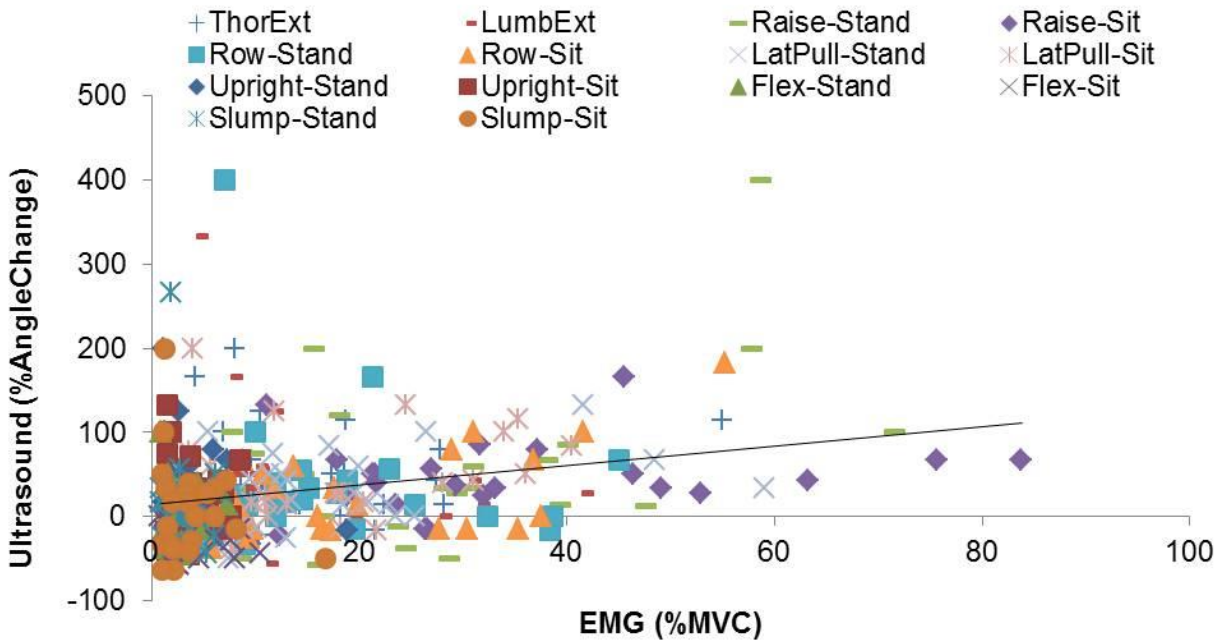


Figure 7.3. Correlation of EMG to %AngleChange for all postures and all participants combined (n = 354). $r = 0.265$, $p < 0.01$.

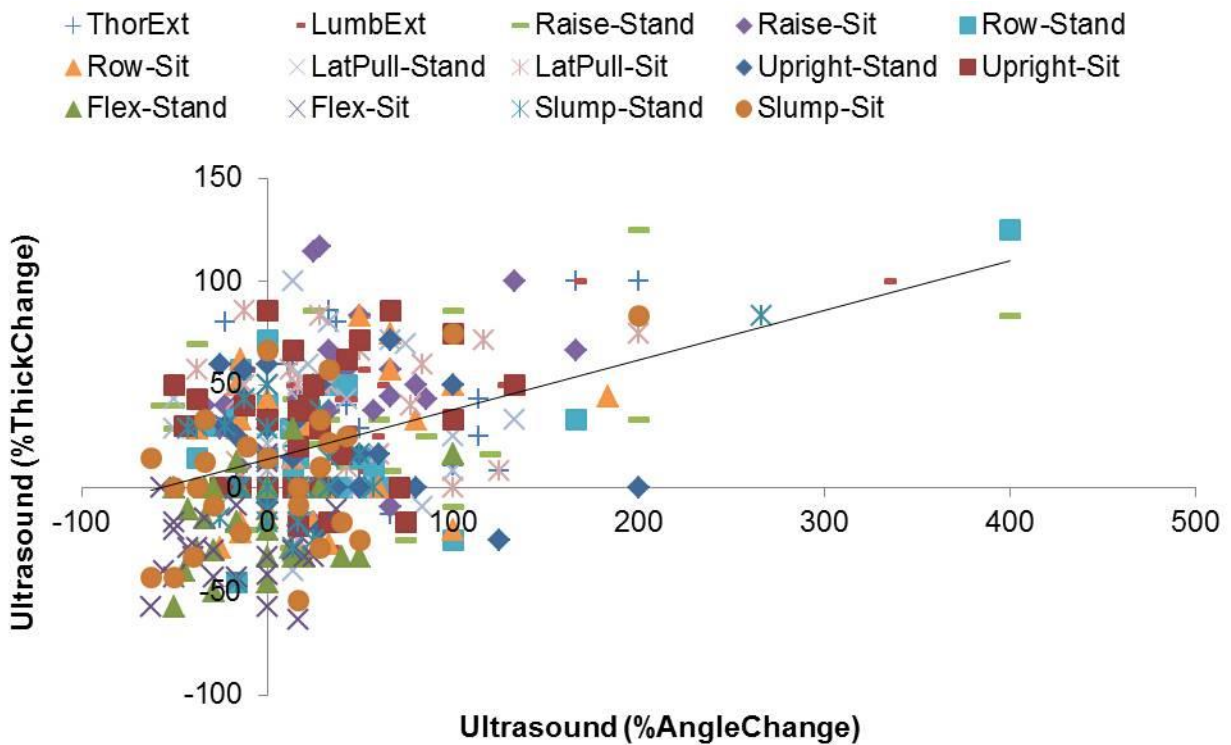


Figure 7.4. Correlation of %AngleChange to %ThickChange for all postures and all participants combined (n = 416). $r = 0.378$, $p < 0.001$.

Table 7.1. Summary of correlation analyses for each of the Active postures. Significant correlations are designated by shaded cells with bold font.

Active Postures	%MVC vs. %Thick (<i>r</i> (95% C.I.))	%MVC vs. % Angle (<i>r</i> (95% C.I.))	%Angle vs %Thick (<i>r</i> (95% C.I.))
ThorExt	<i>r</i> = -0.150 (-0.477-0.127)	<i>r</i> = 0.009 (-0.467-0.440)	<i>r</i> = 0.281 (-0.246-0.592)
LumbExt	<i>r</i> = -0.355 (-0.590- -0.049)	<i>r</i> = -0.276 (-0.489-0.001)	<i>r</i> = 0.479 (-0.010-0.674)
Raise- Stand	<i>r</i> = 0.177 (-0.258-0.590)	<i>r</i> = 0.437 (-0.114-0.700)	<i>r</i> = 0.253 (-0.294-0.510)
Raise-Sit	<i>r</i> = 0.264 (-0.024-0.542)	<i>r</i> = 0.341 (-0.010-0.642)	<i>r</i> = 0.218 (-0.088-0.506)
Row-Stand	<i>r</i> = 0.045 (-0.324-0.464)	<i>r</i> = -0.084 (-0.343-0.429)	<i>r</i> = 0.470 (-0.489-0.782)
Row-Sit	<i>r</i> = 0.087 (-0.308-0.475)	<i>r</i> = 0.536 (-0.092-0.810)	<i>r</i> = 0.261 (-0.132-0.542)
LatPull- Stand	<i>r</i> = 0.320 (-0.166-0.593)	<i>r</i> = 0.308 (-0.072-0.622)	<i>r</i> = 0.040 (-0.249-0.304)
LatPull-Sit	<i>r</i> = 0.069 (-0.315-0.419)	<i>r</i> = 0.227 (-0.173-0.664)	<i>r</i> = 0.141 (-0.282-0.472)
All Active Postures	<i>r</i> = 0.115 (-0.019-0.248)	<i>r</i> = 0.188 (0.008-0.359)	<i>r</i> = 0.296 (0.138-0.420)

7.3.2 Analysis of Variance

The results of the one-way ANOVA of Posture on EMG activation showed a significant effect ($F(14, 294) = 27.74, p < 0.001$). Post-hoc analysis revealed that none of the Passive postures (including Prone) were different from any other Passive posture ($p = 1.00$), yet all were lower than any Active postures ($p < 0.006$) (Figure 7.5). Additionally, Figure 7.5 highlights

Raise-Sit showing the largest activation, which was significantly higher than LumbExt ($p = 0.045$) and Row-Stand ($p = 0.010$).

An effect of Posture on %ThickChange was also found ($F(13, 325) = 19.88, p < 0.001$). With %ThickChange, the only difference between Upright and any Active postures was Raise-Sit showing a greater change than Upright-Stand ($p = 0.033$), and both Flex-Stand and Flex-Sit reduced their thickness compared to all other trials ($p < 0.046$) (Figure 7.6). Additionally, the Slump postures showed less %ThicknessChange compared to Raise, LumbExt, and Lat-Sit ($p < 0.046$) (Figure 7.6). The only %ThickChange difference in Active postures was found between

Table 7.2. Summary of correlation analyses for each of the Passive postures. Significant correlations are designated by shaded cells with bold font.

Passive Postures	%MVC vs. %Thick (r (95% C.I.))	%MVC vs. %Angle (r (95% C.I.))	%Angle vs %Thick (r (95% C.I.))
Upright-Stand	r = -0.288 (-0.586-0.216)	r = -0.178 (-0.406-0.410)	r = -0.204 (-0.521-0.203)
Upright-Sit	r = -0.075 (-0.526-0.348)	r = -0.083 (-0.477-0.370)	r = 0.142 (-0.225-0.431)
Flex-Stand	r = 0.339 (-0.273-0.730)	r = 0.018 (-0.370-0.507)	r = 0.221 (-0.241-0.504)
Flex-Sit	r = -0.065 (-0.418-0.253)	r = -0.343 (-0.622- -0.013)	r = 0.089 (-0.246 -0.399)
Slump-Stand	r = 0.345 (0.032-0.739)	r = -0.126 (-0.392-0.375)	r = 0.426 (-0.437-0.760)
Slump-Sit	r = -0.094 (-0.365-0.270)	r = -0.209 (-0.484-0.316)	r = 0.471 (-0.064-0.742)
All Passive Postures	r = -0.008 (-0.147-0.148)	r = -0.137 (-0.255-0.033)	r = 0.344 (0.161-0.485)

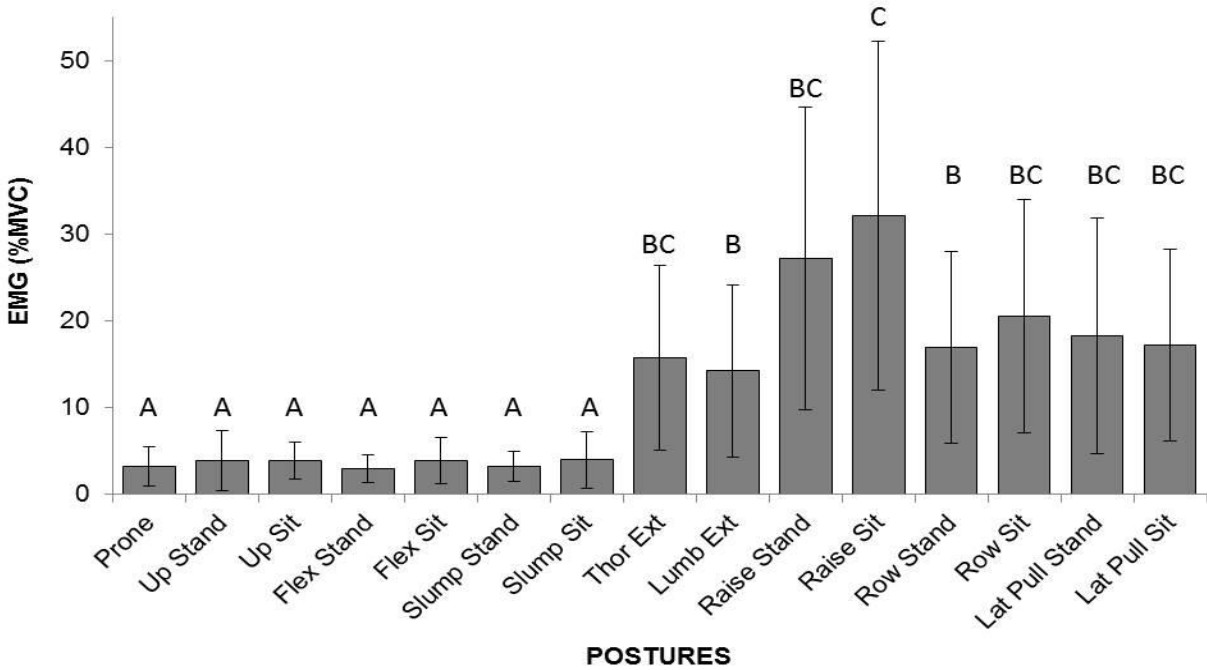


Figure 7.5. Summary of EMG ANOVA results for all postures. Levels not connected by the same letter are statistically different ($p < 0.045$).

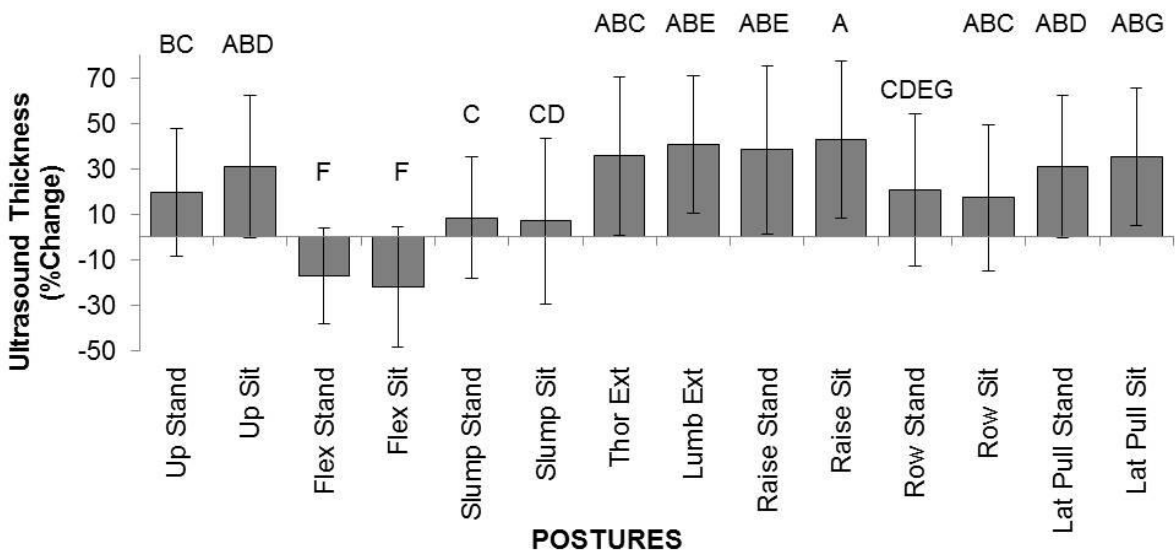


Figure 7.6. Summary of ultrasound thickness (%change) results for all postures. Levels not connected by the same letter are statistically different ($p < 0.046$).

Raise-Sit and Row-Stand ($p = 0.014$). In general, the %ThicknessChange was more distinguishable amongst the Passive postures, as Flex- Stand and Flex-Sit were the only postures by which the muscle got thinner. Furthermore, there was not a single Active posture that was dominating the thickness changes. Finally, there was also an effect of Posture on %AngleChange ($F(13, 325) = 6.86, p < 0.001$) as shown in Figure 7.7. The Upright postures both showed a greater change in angle compared to the Flex postures ($p < 0.026$); however, these changes were not different than any other Active or Passive posture ($p > 0.905$) (Figure 7.7). The pennation angle in both Flex-Stand and Flex-Sit postures decreased relative to Prone, and was significantly lower than the Thor and LumbExt ($p < 0.004$), and LatPull ($p < 0.039$) postures as highlighted in (Figure 7.7).

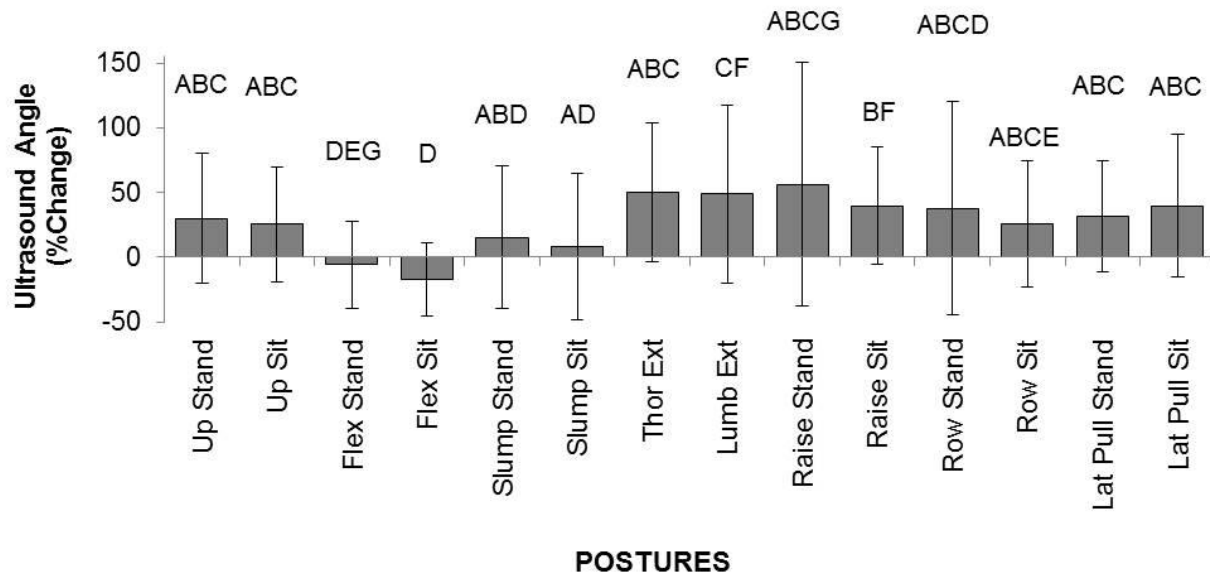


Figure 7.7. Summary of ultrasound thickness (%change) results for all postures. Levels not connected by the same letter are statistically different ($p < 0.045$).

The Slump postures showed slight increases in pennation angle from prone; however these were not statistically different amongst the other Passive postures ($p > 0.890$). Both Slump postures also showed lower pennation changes compared to LumbExt ($p < 0.045$), and Slump-Sit also showed less of a change compared to Raise-Sit ($p = 0.036$) (Figure 7.7). Additionally, there were no differences found in the %AngleChange increase between any of the Active postures, ($p = 1.00$). Overall, the %AngleChange differences showed that there was not a clear change in pennation angle during Active postures, while the Flex postures displayed a significant reduction in pennation angle compared to all other postures.

7.4 USI-EMG Discussion

This was the first study to examine the relationship between muscle activation and changes in morphology in T4ES in both active and passive postures. In general, there were weak-to-moderate positive correlations across all postures in each measure (EMG-%ThickChange, EMG-%AngleChange, %ThickChange-%AngleChange); however, this relationship was less clear when considering each posture on own. Additionally, there was no clear Active posture producing the largest muscle activation, though the EMG was greater in all Active postures compared to Passive postures. The lack of clear increases in EMG was also reflected in the thickness and pennation angles changes, which were generally not different between Active postures, or between Active and Upright Passive postures. There were however, more distinguishable changes within the Passive postures, especially in the Flex postures which showed a reduction in thickness and pennation angle (Figure 7.6 & 7.7). Considering the unclear relationship between EMG and changes in morphometry, as well as a lack of clear differences between Active postures, it can be concluded that USI alone cannot determine the level of T4ES

contraction or be used to distinguish between other multi-directional movements. However, USIs of T4ES could be potentially used to characterize different Passive postures such as Flexion and Slump, as well as be used to discriminate between postures that involve an active contraction compared to those that are passive in nature.

Muscle activity was generally more correlated to changes in angle rather than changes in thickness, as there were moderate relationships found between EMG-%AngleChange for Raise-Stand ($r = 0.437$) and Row-Sit ($r = 0.536$), and a weak relationship in all Active postures ($r = 0.188$). Conversely, no significant correlations were found in any of the EMG-%ThickChange comparisons, as shown in Table 7.1 & 7.2. This could partly be explained by the simplified two-dimensional representation of muscle thickness as a function of fascicle length and angle (Dieterich et al., 2014): Muscle thickness = Fascicle length * $\sin \theta$. As a pennated muscle contracts the fibre lengths shorten (Henriksson-Larsén et al., 1991), which can change the thickness as a result of the corresponding change in angle. However, it is possible to have fibre shortening (e.g. contraction) and angle increases without changes to the thickness, as has been shown in human gastrocnemius (Narici et al, 1996). For a given angle, the fibres have to be shortened enough to affect the thickness. For example, a thickness of 1.0 cm at a 10° angle implies a fibre length of 5.76 cm. If the muscle contracts to a fibre length of 3.0 cm at a 19.5° angle, the thickness remains at 1.0 cm. This relationship could also explain the muscle getting thinner with a narrower angle during Flex-Stand and Flex-Sit (Figures 7.6 & 7.7), as the fibres are stretched and lengthened, the angle could decrease such that the thickness is reduced. The fact that the pennation angle is dictated by the contraction implies that thickness alone may not be adequate to detect muscle contraction of T4ES from USI; therefore pennation angle should also be considered when using USI on T4ES.

A lack of relationship between changes in muscle thickness and muscle activity has also been reported in the EO muscle (Brown & McGill, 2010; Ferreira et al., 2004, 2011; Hodges et al., 2003; Rabello et al. 2015; Whittaker et al., 2013) and gluteus minimus muscle (Dieterich et al., 2015). For example, using fine-wire EMG in gluteus minimus (Dieterich et al., 2015), and surface EMG on EO (Brown & McGill, 2010), both groups reported a negative relationship between thickness and muscle activity ($r = -0.66$ to -0.22), indicating that the muscle was thinner at maximum activation. Additionally, individual instances of EO becoming thinner during muscle contractions recorded by fine-wire EMG have also been reported (Ferreira et al., 2011; Hodges et al., 2003; John & Beith, 2007). One possible mechanism for the findings of EO involves the transmission of forces through the connective tissue between abdominal layers (Brown & McGill, 2008; 2010). Using surface EMG to estimate muscle force, and USI to record IO aponeurosis and rectus abdominis tendinous intersection, Brown and McGill (2008) found that the abdominal wall produced and resisted forces in a number of competing directions. As a result, as a muscle shortens and thickens, an opposing force will be directly applied against the shortening force of an adjacent muscle with perpendicular fibres (Brown & McGill, 2010). In turn, this will limit the amount of shortening (hence thickening) if the adjacent muscle is active (Brown & McGill, 2010). Similarly in gluteus minimus, Dieterich et al. (2014) suggested a similar mechanism in that this muscle could not thicken due to pressure from the superficial gluteus medius muscle. In the present study, a similar negative relationship was found during ThorExt ($r = -0.150$) and LumbExt ($r = -0.355$), as these were the only Active postures that showed a negative, albeit not statistically significant, EMG-%ThickChange relationship (Table 7.1), which indicated that the high EMG recordings were occurring with minimal amount of muscle thickness changes. It is plausible that the complex interactions found within T4ES

stemmed from the interaction between the rhomboid and trapezius muscles. As the rhomboid and trapezius muscles attach the scapula to the axial skeleton, they act to balance the abductor force applied on the scapula by the rotator cuff (Peat, 1986). As a result of these competing forces for a given postural demand, it was likely the thickness of T4ES was affected by the contraction of the surrounding muscles, especially given the already-limited space of that region. If the superficial muscles thicken first, there will be no room for the deep ES to also thicken, further supporting the importance of pennation angle and not simply relying on thickness changes for relating USIs to EMG. This would imply that the order by which the muscles were activated would have an effect on which muscles could thicken. However, as noted by Whittaker et al. (2013), it is important to understand that the underlying changes in morphology represent the combined influences of biomechanical and neuromuscular factors, meaning that USI cannot be represented as the sole source of information about muscle activity.

The results from the ANOVAs showed that body position alone can alter morphology and subsequent function without changing muscle activation in T4ES, particularly in the Passive postures. This was evidenced by the low level of muscle activity in each of the Passive postures (Figure 7.5), with both increased (Upright) and decreased (Flex) thickness and pennation angle (Figure 7.6 & 7.7). Similar changes in lumbar ES thickness have been reported by Watanabe et al. (2004). Using USI to measure thickness at each lumbar vertebral level (L1-L5), Watanabe et al. (2004) found ES thickness to decrease in seated flexion and increase in seated extension compared to seated upright. Presently, in T4ES the muscle also got thinner during the Flex trials, with indication that Slump thickness was between Upright and Flex (Figure 7.6). Regarding changes in pennation angle, McGill et al. (2000) were the first to show *in vivo* that full lumbar flexion reduced the pennation angle of LES at L3 during standing. Changes in LES

angle with flexion was also confirmed by Harriss and Brown (2015), who found that pennation angles in upright sitting were greater than prone, whereas flexed sitting showed smaller angles than prone. These patterns of changes in LES angle were similar to T4ES in the present study (Figure 7.7). Furthermore, natural reductions in lumbar lordosis due to ageing have shown corresponding reductions in LES pennation angle when comparing young and old populations (Singh et al., 2011). Naturally occurring changes in spine curvature also have implications for the thoracic spine. For example, using an optimization model, Briggs et al. (2007) looked at the effects of natural kyphosis on spinal loading and found those with high kyphosis had increased net compression and shear muscle forces acting at the T2-T5 section. In addition, the overall shear forces were low in T2-T5, highlighting that compression was the predominant force in this upper-thoracic region (Briggs et al., 2007). The results of the current study support the notion of lower shear forces in the upper-thoracic as the mean (*SD*) pennation angles in Upright were 7.5° (1.9), indicating that by nature the T4ES are not designed to resist large shear forces.

Additionally, the pennation angle changes were not different between Upright and any Active postures (Figure 7.7). This is important as decreased pennation angle results in increased compression as the vertical component of the muscle vector increases (Macintosh et al., 1993), indicating that a smaller angle compromises the amount of posterior shear force generated (Harriss & Brown, 2015). When the ES are contracted, the pennation angles are increased; thereby creating a protective mechanism as the muscles contribute more to posterior shear (Harriss & Brown, 2015). In the case of the thoracic spine, further increases in kyphosis (e.g. flexion or slump, compared to upright), resulted in a decreased pennation angle (Figure 7.7), which would then require even greater muscle force to resist anterior shear forces if required. However, the pennation angles in T4ES not increasing from Upright during the Active postures

further indicates the role of T4ES in primarily generating compression rather than in resisting anterior shear forces. Overall, the implications were that Passive postures resulting in increased flexion could place T4ES at higher internal loading as a result of a reduction in pennation angle, thereby contributing to overall injury risk if external loading were to occur during one of these passive-flexed postures.

This study has some limitations that need to be accounted for. For instance, symmetry was assumed as EMG and USI were collected unilaterally at the same time. This could be a reason for the lower correlations as there could be variations in EMG recorded from one side and the actual morphological changes on the other due to unequal or varying levels of contraction. However, due to the surface EMG electrode placement, some adjustments needed to be made, and similar unilateral recordings have been performed in the lumbar (Harriss & Brown, 2015) and abdominal (Brown & McGill, 2010) muscles. Another concern that arose from surface EMG was the likelihood of crosstalk between muscles; however, based on the results of Study #2: T4ES-MVC we were confident that we were able to primarily collect T4ES, with some additional recordings from trapezius/rhomboids. Similar to Brown and McGill (2010) who used surface EMG to collect from deep abdominal muscles, our electrodes were aligned with the direction of the fibres, and placed so that the desired muscles were most superficial to the skin (e.g. away from the muscle bellies of trapezius/rhomboid). This resulted in electrode placement parallel to the midline of the spine, and placed as medially as possible (~2-2.5 cm) to avoid the muscle bellies of trapezius and rhomboid, which are typically collected between the scapula and the midline (Jeong et al., 2016). Another limitation comes from the fact that USI is a two-dimensional image of a three-dimensional structure; therefore it is possible to have changes occurring out of plane (Hodges et al., 2003). This could primarily include changes in

mediolateral thickness; however, as ES are the primary extensors, the function is in the sagittal plane anyway, so one would expect noticeable changes from this view. In the future, transverse-plane USI measures such as CSA could provide additional information about the underlying structural changes of T4ES.

Future directions could possibly shed light on the low relationships found, and the potential for clinical usage of USI in passive postures. For example, using indwelling electrodes for the deep T4ES, along with targeted contractions at fixed trunk/spine positions, could potentially strengthen the observable relationship between muscle activity and morphology changes. Additionally, those with low back pain have shown a reduction in thickness during a contraction in multifidus (Djordjevic et al., 2015; Kiesel et al., 2008), but it remains unclear what changes there would be in T4ES with thoracic spine pain individuals. In light of what answers are still unknown, the results of the current study have revealed the potential for further analyses of the T4ES.

In conclusion, the interaction and association between muscle activation and changes in thickness and pennation angle in T4ES appears to be complex. During passive postures such as flexion, this region behaved similar to LES in that the muscle became thinner and showed a decrease in pennation angle. This implied that changes in morphometry from passive postures can alter the force-generating capabilities, and further supported the notion to avoid full-flexion postures not just in the lumbar region, but also the thoracic region. However, during active postures that involved sub-maximal contractions of varying trunk and arm motions, there was no clear relationship between thickness changes and muscle activation. This thickness behaviour was similar to other muscles that are layered, such as EO and gluteus minimus, indicating the influence of the surrounding structures on how T4ES functions. Therefore, it is recommended

that USI is not used to determine the level of muscle activity amongst active postures; however, in passive postures such as flexion and slump, changes in thickness and pennation angle could potentially be used to distinguish these postures from upright or other active contractions.

Chapter 8: General Discussion

The General Discussion section presented here is split into six sections. The first two sections present the general and specific contributions from the research, respectively, followed by general limitations. The specific research questions and hypotheses are then re-visited, followed by future directions and a general conclusion summarizes the body of work.

8.1 General Contributions

The overall purpose of this dissertation was to assess the structure and function of the T4ES musculature. The structure component was achieved by measuring thickness and pennation angle from USI and MRI, whereas the functional component was addressed primarily by T4ES EMG activity. Five studies in total were presented (N=86), with the final one being limited to a pilot application study.

Taken together, the results of these studies have contributed to the overall methodology concerning thoracic spine research, as well as highlighting important structure and function changes of T4ES, which could impact the trade-off between shoulder and low back loading. Generally, T4ES was relatively thin and had a shallower angle compared to reported LES, which implied a primary function of generating compression forces rather than posterior shear forces, which could contribute to the overall stability of that region. From an industry perspective, often the shoulder and low back are looked at in terms of a trade-off in loading, which could be influenced by arm and body posture alone (Cudlip et al., 2015; Lee et al., 2012). Clinical implications include the ability to use USI to discriminate between static postures that require minimal muscle activation in an un-injured population, with potential to identify abnormal

muscle behaviour in a clinical population. As a whole, the analysis of T4ES directly may be limited by the arm and body positioning of the task, specifically if postures involve overhead or above-shoulder tasks. As such, it might be important to consider the T4 region as a unit involving muscle contributions not just from T4ES, but also rhomboid and trapezius. Knowing the total muscle activation from the T4 level, and how those activation profiles change throughout a variety of arm and body positions, could help in understanding the trade-off between shoulder and low back loading through the thoracic spine.

8.2 Specific Contributions

One of the main findings was that USI was a reliable and valid tool for measuring thickness and pennation angle of T4ES. This was important as it allowed for further analysis of T4ES structure during a range of Active and Passive static postures. Additionally, the thickness and pennation angles recorded were the first *in vivo* measurements of T4ES, which contributed to the database of structural information from young, healthy participants. This contribution of general morphological information of T4ES was important as it provided a reference for future work in assessing effects of pathology and intervention, as well as providing context for changes between different spinal levels (Stokes et al., 2007).

Two of the primary measures in biomechanics research are EMG and kinematics, as these provide information regarding the muscle activation and underlying movement patterns. Methodologies concerning these measures are important to consider, and were addressed in Study #2: T4ES-MVC and Study #3: Flexi-MoCap. In terms of EMG, it is important to normalize the raw signal to some reference value, usually a MVC, in order to garner meaningful information (Lehman & McGill, 1999). Testing of different MVC techniques on T4ES had yet

to be done, and these results confirmed that sagittal plane (ThorExt) elicited the highest activation. However, there were also large amounts of activation recorded from the T4ES channel during arm raise trials, which indicated the likelihood of crosstalk from the underlying rhomboid and trapezius muscles. Therefore, a major conclusion was that muscle activation from trapezius and rhomboid must be considered and acknowledged for in the T4ES electrodes, especially during overhead work. This implied that if a task was being analyzed that involved large upper extremity motions then the muscles should be assessed as a grouping that includes ES/rhomboid/trapezius, where the MVC would be taken from the absolute maximum. If the task was fairly static or did not require much arm elevation, then T4ES could be analyzed using the ThorExt MVC to normalize. With kinematics, MoCap is considered the gold standard, yet it is not always available and/or accessible to interested parties such as clinicians or on-site researchers. A simple pen-and-paper tool (Flexi) had been used for a multitude of ways to represent sagittal plane spine angles, including a tangential representation of the lumbar angle. A “segmental” method for measuring sagittal plane spine angles from Flexi was proposed in this dissertation, and this method showed high reliability and validity when compared to the gold standard MoCap, specifically in the MidSeg region. Taken together, the overall contributions from Study #2: T4ES-MVC and Study #3: Flexi-MoCap were towards improving methodological considerations for recording the thoracic spine.

The basis for Study #4: USI-EMG incorporated some aspect from each of the preceding studies. Previously validated USI (Study #1: USI-MRI) was used to assess the changes in thickness and pennation angle from the same postures used in Study #2: T4ES-MVC and Study #3: Flexi-MoCap. These results revealed a complex interaction between morphological changes in T4ES and the relationship to the EMG recorded. However, notable changes in thickness and

pennation angle were found between Upright, Flex, and Slump, regardless of the minimal muscle activation, which implied USI could be used to distinguish between these postures based on morphology alone.

The final study was a pilot study to look at possible applications of T4ES. In Study #5: Application-Pilot, T4ES activation was measured during two breathing tasks. One of the tasks was normal breathing after running on a treadmill until exhaustion, while the other task was a maximum voluntary ventilation task, where participants breathed heavily into a paper bag. In general, the treadmill trial required greater perceived effort and showed a larger peak HR with no substantial changes in T4ES EMG. This suggested that T4ES did not play a major role in respiration, yet further analysis could elucidate these findings further.

8.3 General Limitations

Specific limitations from each study were presented in the individual study chapters. However, there were some limitations that were applicable across all or most studies. These general limitations included: a young, healthy (uninjured) population, the use of static postures, and a narrowly-focused spine region.

The population used throughout this dissertation were university-aged and free of neck, back, and shoulder pain, which could limit the applicability across clinical groups and the elderly. There is recent evidence to suggest that a LBP population and elderly adults would show different muscle morphological changes. For example, Djordjevic et al., (2015) found that during contraction, relative changes in lumbar multifidus thickness were smaller in LBP compared to non-LBP individuals. Additionally, Singh et al. (2011) noted a decrease in pennation angle of LES in older adults (> 65 y) compared to younger adults (20-35 y). However,

measures of LES pennation angle and multifidus thickness in younger, pain-free populations have already been determined in the literature, thus providing a baseline for comparison to different populations. In T4ES, baseline measures of muscle morphology were not yet reported for any population, so this was an important first step to establish.

The postures adopted throughout the current studies were limited to being static in nature. The reason for this was because of the equipment used to collect the data, specifically USI and Flexi. Regarding USI, dynamic tasks would provide a challenge for maintaining transducer placement on the participant as they moved through a dynamic range of motion. With Flexi, by nature the tool can only provide a “snapshot” of information and cannot produce a time series of spine angles. However, information about a static posture can still prove useful. For example, knowledge of changes of spine angles and muscle characteristics at end-ranges of motion or worst-case-scenario types of postures could provide information on injury risk at a given instant in time.

Broader applications directly to the shoulder or low back areas could be limited by the focus being narrowly on the T4 region. This region was chosen because of the interface between the scapulo-thoracic junction of the shoulder and the axial skeleton, where muscles such as rhomboids and trapezius attach to both; however, this region in isolation may not provide direct information about the loading at the shoulder or the low back. Yet before expanding the protocol to include shoulder and low back information, it was still important to gain an understanding of what the general characteristics of the T4 region were. Knowing the characteristics of the T4 region would provide a reference point for future studies to compare against.

8.4 Hypotheses Revisited

Study #1: USI-MRI

Research Question: Is USI a reliable and accurate way to measure thickness and pennation angle in T4ES?

Hypothesis #1: Ultrasound imaging will be reliable and accurate for measuring morphometry of T4ES

Hypothesis #1 Re-visited: Accepted. Based on high reliability and precision with low measurement error, and good agreement via Bland-Altman analysis, USI is reliable and accurate for T4ES.

Study #2: T4ES-MVC

Research Question: What MVC technique provides that maximum activation from T4ES?

Hypothesis #2: Thoracic extension will show the largest value.

Hypothesis #2 Re-visited: Accepted. Though arm raise techniques showed the absolute highest numeric values, these were not statistically different from thoracic extension. The combination of the anatomical function (e.g. ES as extensors), and the activation of T4ES during thoracic extension with minimal contribution from the MidTrap region showed that thoracic extension was properly targeting T4ES.

Study #3: Flexi-MoCap

Research Question: Is a flexible ruler a reliable tool for measuring thoracic spine sagittal plane angles in passive postures, and how do these angles compare to those obtained from optoelectronic motion capture?

Hypothesis #3: The Flexi angles will show high reliability and good agreement to MoCap angles.

Hypothesis #3 Re-visited: Rejected. Not all measures showed high reliability and good agreement to MoCap. Specifically, the segmental method, specifically the MidSeg region (apex at T6), showed high reliability and good agreement compared to MoCap. Absolute measures of the tangential method from Flexi are not recommended, whereas the segmental method could be a viable replacement for MoCap.

Study #4: USI-EMG

Research Questions: What is the relationship between changes in morphometry and muscle activation at T4ES? Are any of these changes different across active and passive postures?

Hypothesis #4: The relationship between EMG and changes in morphometry will show a strong positive relationship.

Hypothesis #4 Re-visited: Rejected. No relationship was found between change in thickness and EMG activity, and few weak-to-moderate correlations were found for EMG and changes in pennation angle.

Hypothesis #5: Changes in EMG and morphometry will be reflected across the different postures, specifically, Active postures will show greater increase in thickness pennation angle compared to Passive postures.

Hypothesis #5 Re-visited: Rejected. Some changes between Active and Postures were found, but not what was fully expected. For example, thickness changes showed significant reduction in Flex and Slump compared to most Active postures; however, Upright and the Active posture showed no thickness differences. Changes were more notable within the Passive postures, particularly in Flex and Slump compared to Upright.

8.5 Future Directions

Now that collection techniques and baseline measures have been recorded for thoracic spine characteristics, future work could further advance the knowledge of this spine region as well as address the issues outlined in Section 9.3 General Limitations. For example, differences in T4ES structure and function in a clinical population could be present based on what is known in the low back musculature. Future studies should look at T4ES morphology in a LBP and shoulder-pain group to see if there are any compensatory effects, as well as in those with thoracic spine pain to see if there are any relationships to pain location and changes in the musculature. Furthermore, ES muscle thickness and pennation angle should be measured along the spine from thoracic to lumbar in order to see how the muscle changes structure over the length of the spine. For example, USI could be used to determine where the ES muscles are superficial and would less impact by surrounding muscles, as this could improve surface EMG collection techniques from the thoracic spine. In addition, indwelling electrodes should be used in the T4 region for the three muscles involved (trapezius, rhomboid, T4ES) as this would provide a true indication of the amount of electrical activity produced by the specific muscles in various postures, and eliminate crosstalk as a potential confounder.

The ultimate goal of the understanding gained from these works is the contribution toward improving biomechanical models in order to truly assess the force transmission from the shoulder to the low back. By segmenting the thoracic spine into a subset of regions, along with knowledge of inertial properties of these regions, the reaction forces and moments could be tracked along the thoracic regions to the lumbar spine. The results from this body of work suggest that the T4 region may not be the ideal location for where to assess the force transmission due to the complex interaction with the scapulothoracic musculature, and perhaps

moving down to the T6-T8 region may provide meaningful information relating to the ES in particular, as the muscle becomes more uniform in nature with less overlap from the superficial musculature.

8.6 General Conclusions

Overall, measurement techniques of USI and Flexi were reliable and comparable in nature to the “gold standards” of MRI and MoCap, respectively. Additionally, including a thoracic extension trial as part of the MVC protocol was recommend if recording surface EMG from T4ES. However, if overhead tasks are being performed, then it was recommended to analyze the T4ES/rhomboid/trapezius region as whole, instead of reporting as an individual muscle group. The T4ES region showed complex changes in morphometry during Active and Passive postures, likely as a result of being deep to the rhomboids and trapezius. Nevertheless, distinguishable changes in morphometry were exhibited in Passive postures, particularly Flex and Slump compared to Upright. Therefore it can be recommended that Flexi and USI could be used in place of MoCap and EMG if the intent is to analyze different components of Passive postures. This could be especially useful in a clinical setting, where access to these pieces of equipment may be more readily available, allowing for potential savings on resources such as time, space, money, and personnel.

References

- Agur, A. M. R., & Dalley, A. F. (2009). *Grant's atlas of anatomy* (12th ed.). Philadelphia: Lippincott Williams & Wilkins.
- Altman, D. G., & Bland, J. M. (1983). Measurement in medicine: the analysis of method comparison studies. *The Statistician*, 32(3), 307-317.
- Andriacchi, T., Schultz, A., Belytschko, T., & Galante, J. (1974). A model for studies of mechanical interactions between the human spine and rib cage. *Journal of Biomechanics*, 7(6), 497–507.
- Ang, C., Nairn, B. C., Schinkel-Ivy, A., & Drake, J. D. M. (2016). Seated maximum flexion: An alternative to standing maximum flexion for determining presence of flexion-relaxation? *Journal of Back and Musculoskeletal Rehabilitation*, 29(2), 249–258.
- Barrett, E., McCreesh, K., & Lewis, J. (2014). Reliability and validity of non-radiographic methods of thoracic kyphosis measurement: a systematic review. *Manual Therapy*, 19(1), 10-17.
- Bayoglu, R., Geeraedts, L., Groenen, K. H. J., Verdonshot, N., Koopman, B., & Homminga, J. (2017a). Twente spine model: A complete and coherent dataset for musculo-skeletal modeling of the lumbar region of the human spine. *Journal of Biomechanics*, 53, 111–119.
- Bayoglu, R., Geeraedts, L., Groenen, K. H. J., Verdonshot, N., Koopman, B., & Homminga, J. (2017b). Twente spine model: A complete and coherent dataset for musculo-skeletal modeling of the thoracic and cervical regions of the human spine. *Journal of Biomechanics*, 58, 52–63. <https://doi.org/10.1016/j.jbiomech.2017.04.003>

- Beach, T. A. C, Parkinson, R. J., Stothart, J. P., & Callaghan, J. P. (2005). Effects of prolonged sitting on the passive flexion stiffness of the in vivo lumbar spine. *The Spine Journal*, 5, 145-154.
- Beaudette, S. M., Unni, R., & Brown, S. H. M. (2014). Electromyographic assessment of isometric and dynamic activation characteristics of the latissimus dorsi muscle. *Journal of Electromyography and Kinesiology: Official Journal of the International Society of Electrophysiological Kinesiology*, 24(3), 430–436.
- Belavý, D. L., Armbrecht, G., & Felsenberg, D. (2015). Real-time ultrasound measures of lumbar erector spinae and multifidus: reliability and comparison to magnetic resonance imaging. *Physiological Measurement*, 36(11), 2285–2299. <https://doi.org/10.1088/0967-3334/36/11/2285>
- Bentman, S., O’Sullivan, C., & Stokes, M. (2010). Thickness of the middle trapezius muscle measured by rehabilitative ultrasound imaging: description of the technique and reliability study. *Clinical Physiology and Functional Imaging*, 30(6), 426–431. <https://doi.org/10.1111/j.1475-097X.2010.00960.x>
- Bland, J. M., & Altman, D. G. (1986). Statistical methods for assessing agreement between two methods of clinical measurement. *The Lancet*, 1(8476), 307-310.
- Brereton, L. C., & McGill, S. M. (1998). Frequency response of spine extensors during rapid isometric contractions: effects of muscle length and tension. *Journal of Electromyography and Kinesiology*, 8(4), 227-232.
- Briggs, A. M., van Dieën, J. H., Wrigley, T. V., Greig, A. M., Phillips, B., Lo, S. K., & Bennell, K. L. (2007). Thoracic kyphosis affects spinal loads and trunk muscle force. *Physical Therapy*, 87(5), 595–607. <https://doi.org/10.2522/ptj.20060119>

- Bronner, S., Agraharasamakulam, S., & Ojofeitimi, S. (2010). Reliability and validity of electrogoniometry measurement of lower extremity movement. *Journal of Medical Engineering & Technology*, *34*(3), 232–242. <https://doi.org/10.3109/03091900903580512>
- Brown, S. H. M., & McGill, S. M. (2008). An ultrasound investigation into the morphology of the human abdominal wall uncovers complex deformation patterns during contraction. *European Journal of Applied Physiology*, *104*(6), 1021–1030.
- Brown, S. H. M., & McGill, S. M. (2010). A comparison of ultrasound and electromyography measures of force and activation to examine the mechanics of abdominal wall contraction. *Clinical Biomechanics (Bristol, Avon)*, *25*(2), 115–123. <https://doi.org/10.1016/j.clinbiomech.2009.10.001>
- Burden, A. (2010). Review. How should we normalize electromyograms obtained from healthy participants? What we have learned from over 25 years of research. *Journal of Electromyography and Kinesiology*, *20*, 1023-1035.
- Burnett, A., O’Sullivan, P., Caneiro, J. P., Krug, R., Bochmann, F., & Helgestad, G. W. (2009). An examination of the flexion-relaxation phenomenon in the cervical spine in lumbo-pelvic sitting. *Journal of Electromyography and Kinesiology*, *19*(4), e229-236.
- Burton, A. K. (1986). Regional lumbar sagittal mobility; measurement by flexicurves. *Clinical Biomechanics*, *1*(1), 20-26.
- Buxton, R. B. (2002). *Introduction to functional magnetic resonance imaging: Principles and techniques*. Cambridge: Cambridge University Press.
- Caine, M. P., McConnel, A. K., & Taylor, D. (1996). Assessment of spinal curvature: an evaluation of the flexicurve and associated means of analysis. *International Journal of Rehabilitation Research*, *19*(3), 271-278.

- Callaghan, J. P., & McGill, S. M. (2001). Low back joint loading and kinematics during standing and unsupported sitting. *Ergonomics*, *44*(3), 280-294.
- Caneiro, J. P., O'Sullivan, P., Burnett, A., Barach, A., O'Neil, D., Tveit, O., & Olafsdottir, K. (2010). The influence of different sitting postures on head/neck posture and muscle activity. *Manual Therapy*, *15*(1), 54–60. <https://doi.org/10.1016/j.math.2009.06.002>
- Claus, A. P., Hides, J. A., Moseley, G. L., & Hodges, P. W. (2009). Is 'ideal' sitting posture real? Measurement of spinal curves in four sitting postures. *Manual Therapy*, *14*(4), 404-408.
- Cotter, B. D., Nairn, B. C., & Drake, J. D. M. (2014). Should a standing or seated reference posture be used when normalizing seated spine kinematics? *Journal of Biomechanics*, *47*(10), 2371–2377. <https://doi.org/10.1016/j.jbiomech.2014.04.023>
- Criswell, E (ed). (2011). *Cram's introduction to surface electromyography* (2nd ed). Sudbury, MA: Jones and Bartlett Publishers.
- Cudlip, A. C., Callaghan, J. P., & Dickerson, C. R. (2015). Effects of sitting and standing on upper extremity physical exposures in materials handling tasks. *Ergonomics*, *58*(10), 1637-1646.
- Cuesta-Vargas, A. I., & Gonzalez-Sanchez, M. (2013). Relationship of moderate and low isometric lumbar extension through architectural and muscular activity variables: a cross sectional study. *BMC Medical Imaging*, *13*, 38. <https://doi.org/10.1186/1471-2342-13-38>
- Dankaerts, W., O'Sullivan, P. B., Burnett, A., & Straker, L. (2006). Differences in sitting postures are associated with nonspecific chronic low back pain disorders when patients are subclassified. *Spine*, *31*(6), 698-704.
- Davis, P. R. (1959). The medial inclination of the human thoracic intervertebral articular facets. *Journal of Anatomy*, *93*(1), 68–74.

- Davis, K., & Marras, W. (2005). Load spatial pathway and spine loading: how does lift origin and destination influence low back response? *Ergonomics*, *48*(8), 1031-1046.
- de Looze, M. P., van Greuningen, K., Rebel, J., Kingma, I., & Kuijer, P. P. F. M. (2000). Force direction and physical load in dynamic pushing and pulling. *Ergonomics*, *43*(3), 377-390.
- De Luca, C. J. (1997). The use of surface electromyography in biomechanics. *Journal of Applied Biomechanics*, *13*, 135-163.
- Delp, S. L., Suryanarayanan, S., Murray, W. M., Uhlir, J., & Triolo, R. J. (2001). Architecture of the rectus abdominis, quadratus lumborum, and erector spinae. *Journal of Biomechanics*, *34*(3), 371–375.
- Desmoulin, G., & Milner, T. (2007). Lumbar mechanics from ultrasound imaging. *Canadian Acoustics*, *35*(2), 61–68.
- Dieterich, A. V., Pickard, C. M., Strauss, G. R., Deshon, L. E., Gibson, W., & McKay, J. (2014). Muscle thickness measurements to estimate gluteus medius and minimus activity levels. *Manual Therapy*, *19*(5), 453–460. <https://doi.org/10.1016/j.math.2014.04.014>
- Djordjevic, O., Djordjevic, A., & Konstantinovic, L. (2014). Interrater and intrarater reliability of transverse abdominal and lumbar multifidus muscle thickness in subjects with and without low back pain. *The Journal of Orthopaedic and Sports Physical Therapy*, *44*(12), 979–988. <https://doi.org/10.2519/jospt.2014.5141>
- Djordjevic, O., Konstantinovic, L., Miljkovic, N., & Bijelic, G. (2015). Relationship Between Electromyographic Signal Amplitude and Thickness Change of the Trunk Muscles in Patients With and Without Low Back Pain. *The Clinical Journal of Pain*, *31*(10), 893–902. <https://doi.org/10.1097/AJP.0000000000000179>

- Dolan, P., Adams, M. A., & Hutton, W. C. (1988). Commonly adopted postures and their effect on the lumbar spine. *Spine*, *13*(2), 197–201.
- Dufour, J. S., Marras, W. S., & Knapik, G. G. (2013). An EMG-assisted model calibration technique that does not require MVCs. *Journal of Electromyography and Kinesiology*, *23*(3), 608–613. <https://doi.org/10.1016/j.jelekin.2013.01.013>
- Edmondston, S. J., Aggerholm, M., Elfving, S., Flores, N., Ng, C., Smith, R., & Netto, K. (2007). Influence of posture on the range of axial rotation and coupled lateral flexion of the thoracic spine. *Journal of Manipulative and Physiological Therapeutics*, *30*(3), 193–199. <https://doi.org/10.1016/j.jmpt.2007.01.010>
- Edmondston, S. J., Sharp, M., Symes, A., Alhabib, N., & Allison, G. T. (2011). Changes in mechanical load and extensor muscle activity in the cervico-thoracic spine induced by sitting posture modification. *Ergonomics*, *54*(2), 179–186.
- Ekstrom, R. A., Donatelli, R. A., & Soderberg, G. L. (2003). Surface electromyographic analysis of exercises for the trapezius and serratus anterior muscles. *The Journal of Orthopaedic and Sports Physical Therapy*, *33*(5), 247–258.
- Ekstrom, R. A., Soderberg, G. L., & Donatelli, R. A. (2005). Normalization procedures using maximum voluntary isometric contractions for the serratus anterior and trapezius muscles during surface EMG analysis. *Journal of Electromyography and Kinesiology*, *15*(4), 418–428.
- Faber, G. S., Kingma, I., Kuijer, P. P. F. M., van der Molen, H. F., Hoozemans, M. J. M., Frings-Dresen, M. H. W., & van Dieën, J. H. (2009). Working height, block mass and one- vs. two-handed block handling: the contribution to low back and shoulder loading during masonry work. *Ergonomics*, *52*(9), 1104–1118.

- Ferreira, P. H., Ferreira, M. L., & Hodges, P. W. (2004). Changes in recruitment of the abdominal muscles in people with low back pain: ultrasound measurement of muscle activity. *Spine*, *29*(22), 2560–2566.
- Ferreira, P. H., Ferreira, M. L., Nascimento, D. P., Pinto, R. Z., Franco, M. R., & Hodges, P. W. (2011). Discriminative and reliability analyses of ultrasound measurement of abdominal muscles recruitment. *Manual Therapy*, *16*(5), 463–469.
- Fleiss, J. L. (1981). *Statistical Methods for Rates and Proportions*. Wiley.
- Fuglevand, A. J., Winter, D. A., Patla, A. E., & Stashuk, D. (1992). Detection of motor unit action potentials with surface electrodes: influence of electrode size and spacing. *Biological Cybernetics*, *67*(2), 143–153.
- Greendale, G. A., Nili, N. S., Huang, M. -H., Seeger, L., & Karlamangla, A. S. (2011). The reliability and validity of three non-radiological measures of thoracic kyphosis and their relations to the standing radiological Cobb angle. *Osteoporosis International*, *22*(6), 1897-1905.
- Gregersen, G. G., & Lucas, D. B. (1967). An in vivo study of the axial rotation of the human thoracolumbar spine. *The Journal of Bone and Joint Surgery. American Volume*, *49*(2), 247–262.
- Grenier, S. G., & McGill, S. M. (2008). When exposed to challenged ventilation, those with a history of LBP increase spine stability relatively more than healthy individuals. *Clinical Biomechanics (Bristol, Avon)*, *23*(9), 1105–1111.
- Harriss, A. B., & Brown, S. H. M. (2015). Effects of changes in muscle activation level and spine and hip posture on erector spinae fiber orientation. *Muscle & Nerve*, *51*(3), 426–433. <https://doi.org/10.1002/mus.24309>

- Harrison, D. E., Haas, J. W., Cailliet, R., Harrison, D. D., Holland, B., & Janik, T. J. (2005). Concurrent validity of flexicurve instrument measurements: sagittal skin contour of the cervical spine compared with lateral cervical radiographic measurements. *Journal of Manipulative and Physiological Therapeutics*, 28(8), 597-603.
- Hart, D. L., & Rose, S. J. (1986). Reliability of a noninvasive method for measuring the lumbar curve. *The Journal of Orthopaedic and Sports Physical Therapy*, 8(4), 180-184.
- Henriksson-Larsén, K., Wretling, M. L., Lorentzon, R., & Oberg, L. (1992). Do muscle fibre size and fibre angulation correlate in pennated human muscles? *European Journal of Applied Physiology and Occupational Physiology*, 64(1), 68–72.
- Herbert, R. D., & Gandevia, S. C. (1995). Changes in pennation with joint angle and muscle torque: in vivo measurements in human brachialis muscle. *The Journal of Physiology*, 484(Pt 2), 523–532.
- Hides, J. A., Richardson, C. A., & Jull, G. A. (1995). Magnetic resonance imaging and ultrasonography of the lumbar multifidus muscle. Comparison of two different modalities. *Spine*, 20(1), 54–58.
- Hinman, M. R. (2004). Interrater reliability of flexicurve postural measures among novice users. *Journal of Back and Musculoskeletal Rehabilitation*, 17(1), 33-36.
- Hodges, P. W., & Gandevia, S. C. (2000). Changes in intra-abdominal pressure during postural and respiratory activation of the human diaphragm. *Journal of Applied Physiology (Bethesda, Md.: 1985)*, 89(3), 967–976.
- Hodges, P. W., Gandevia, S. C., & Richardson, C. A. (1997). Contractions of specific abdominal muscles in postural tasks are affected by respiratory maneuvers. *Journal of Applied Physiology (Bethesda, Md.: 1985)*, 83(3), 753–760.

- Hodges, P. W., Pengel, L. H. M., Herbert, R. D., & Gandevia, S. C. (2003). Measurement of muscle contraction with ultrasound imaging. *Muscle & Nerve*, 27(6), 682–692.
- Hoozemans, M. J. M., Kuijer, P. P. F. M., Kingma, I., van Dieën, J. H., de Vries, W. H. K., van der Woude, L. H. V., ... Frings-Dresen, M. H. W. (2004). Mechanical loading of the low back and shoulders during pushing and pulling activities. *Ergonomics*, 47(1), 1-18.
- Kremkau, F. W. (2011). *Sonography principles and instruments*. 8th ed. St. Louis, MO: Elsevier/Saunders.
- Jeong, J. R., Ko, Y. J., Ha, H. G., & Lee, W. H. (2016). Reliability of rehabilitative ultrasonographic imaging for muscle thickness measurement of the rhomboid major. *Clinical Physiology and Functional Imaging*, 36(2), 134–138.
- John, E. K., & Beith, I. D. (2007). Can activity within the external abdominal oblique be measured using real-time ultrasound imaging? *Clinical Biomechanics (Bristol, Avon)*, 22(9), 972–979. <https://doi.org/10.1016/j.clinbiomech.2007.07.005>
- Kamen, G. (2004). Electromyographic kinesiology. In D. G. E. Robertson, G. E. Caldwell, J. Hamill, G. Kamen, & S. N. Whittlesey (Eds.), *Research methods in biomechanics* (pp. 163-181). Champaign, IL: Human Kinetics.
- Kawakami, Y., Ichinose, Y., Kubo, K., Ito, M., Imai, M., & Fukunaga, T. (2000). Architecture of Contracting Human Muscles and Its Functional Significance. *Journal of Applied Biomechanics*, 16(1), 88–97. <https://doi.org/10.1123/jab.16.1.88>
- Kienbacher, T., Fehrmann, E., Habenicht, R., Koller, D., Oeffel, C., Kollmitzer, J., ... Ebenbichler, G. (2016). Age and gender related neuromuscular pattern during trunk flexion-extension in chronic low back pain patients. *Journal of Neuroengineering and Rehabilitation*, 13, 16. <https://doi.org/10.1186/s12984-016-0121-1>

- Kiesel, K. B., Uhl, T. L., Underwood, F. B., Rodd, D. W., & Nitz, A. J. (2007). Measurement of lumbar multifidus muscle contraction with rehabilitative ultrasound imaging. *Manual Therapy, 12*(2), 161–166. <https://doi.org/10.1016/j.math.2006.06.011>
- Kiesel, K. B., Uhl, T., Underwood, F. B., & Nitz, A. J. (2008). Rehabilitative ultrasound measurement of select trunk muscle activation during induced pain. *Manual Therapy, 13*(2), 132–138. <https://doi.org/10.1016/j.math.2006.10.003>
- Koppenhaver, S. L., Hebert, J. J., Fritz, J. M., Parent, E. C., Teyhen, D. S., & Magel, J. S. (2009). Reliability of rehabilitative ultrasound imaging of the transversus abdominis and lumbar multifidus muscles. *Archives of Physical Medicine and Rehabilitation, 90*(1), 87–94. <https://doi.org/10.1016/j.apmr.2008.06.022>
- Laursen, B. & Schibye, B. (2002). The effect of different surfaces on biomechanical loading of shoulder and lumbar spine during pushing and pulling of two-wheeled containers. *Applied Ergonomics, 33*, 167-174.
- Lee, Y.-J., Hoozemans, M. J. M., & van Dieën, J. H. (2012). Effects of pushing height on trunk posture and trunk muscle activity when a cart suddenly starts or stops moving. *Work, 41*, 3189-3195.
- Lehman, G. J., & McGill, S. M. (1999). The importance of normalization in the interpretation of surface electromyography: a proof of principle. *Journal of Manipulative and Physiological Therapeutics, 22*(7), 444–446.
- Lehman, G. J. (2002). Clinical considerations in the use of surface electromyography: Three experimental studies. *Journal of Manipulative & Physiological Therapeutics, 25*(5), 293–299. <https://doi.org/10.1067/mmt.2002.124423>

- Lehman, G. J., Buchan, D. D., Lundy, A., Myers, N., & Nalborczyk, A. (2004). Variations in muscle activation levels during traditional latissimus dorsi weight training exercises: An experimental study. *Dynamic Medicine : DM*, 3, 4. <https://doi.org/10.1186/1476-5918-3-4>
- Liebsch, C., Graf, N., Appelt, K., & Wilke, H. J. (2017). The rib cage stabilizes the human thoracic spine: An *in vitro* study using stepwise reduction of rib cage structures. *PLoS ONE*, 12(6), e0178733.
- Link, C. S., Nicholson, G. G., Shaddeau, S. A., Birch, R., & Gossman, M. R. (1990). Lumbar curvature in standing and sitting in two types of chairs: relationship of hamstring and hip flexor muscle length. *Physical Therapy*, 70(10), 611-618.
- Ludbrook, J. (2002). Statistical techniques for comparing measurers and methods of measurement: a critical review. *Clinical and Experimental Pharmacology and Physiology*, 29(7), 527-536.
- Macintosh, J. E., & Bogduk, N. (1987). The morphology of the lumbar erector spinae. *Spine*, 12(7), 658-666.
- Macintosh, J. E., & Bogduk, N. (1991). The attachments of the lumbar erector spinae. *Spine*, 16(7), 783-792.
- Macintosh, J. E., Bogduk, N., & Pearcy, M. J. (1993). The effects of flexion on geometry and actions of the lumbar erector spinae. *Spine*, 18(7), 884-893.
- Maciukiewicz, J. M., Lang, A. E., Vidt, M. E., Grenier, S. G., & Dickerson, C. R. (2017). Characterization of cashier shoulder and low back muscle demands. *International Journal of Industrial Ergonomics*, 59, 80-91.

- Maganaris, C. N., & Baltzopoulos, V. (1999). Predictability of in vivo changes in pennation angle of human tibialis anterior muscle from rest to maximum isometric dorsiflexion. *European Journal of Applied Physiology and Occupational Physiology*, 79(3), 294–297.
- Marras, W. S., Lavender, S. A., Leurgans, S. E., Fathallah, F. A., Ferguson, S. A., Allread, W. G., & Rajulu, S. L. (1995). Biomechanical risk factors for occupationally related low back disorders. *Ergonomics*, 38(2), 377–410.
- Marras, W. S., Lavender, S. A., Leurgans, S. E., Rajulu, S. L., Allread, W. G., Fathallah, F. A., & Ferguson, S. A. (1993). The role of dynamic three-dimensional trunk motion in occupationally-related low back disorders. The effects of workplace factors, trunk position, and trunk motion characteristics on risk of injury. *Spine*, 18(5), 617–628.
- McGill, S. M., Cholewicki, J., & Peach, J. P. (1997). Methodological considerations for using inductive sensors (3SPACE ISOTRAK) to monitor 3-D orthopaedic joint motion. *Clinical Biomechanics*, 12(3), 190–194. [https://doi.org/10.1016/S0268-0033\(97\)00063-6](https://doi.org/10.1016/S0268-0033(97)00063-6)
- McGill, S. M., Hughson, R. L., & Parks, K. (2000). Changes in lumbar lordosis modify the role of the extensor muscles. *Clinical Biomechanics (Bristol, Avon)*, 15(10), 777–780.
- McGill, S. M., Sharratt, M. T., & Seguin, J. P. (1995). Loads on spinal tissues during simultaneous lifting and ventilatory challenge. *Ergonomics*, 38(9), 1772–1792.
- McLean, L. (2005). The effect of postural correction on muscle activation amplitudes recorded from the cervicobrachial region. *Journal of Electromyography and Kinesiology: Official Journal of the International Society of Electrophysiological Kinesiology*, 15(6), 527–535.
- McMeeken, J. M., Beith, I. D., Newham, D. J., Milligan, P., & Critchley, D. J. (2004). The relationship between EMG and change in thickness of transversus abdominis. *Clinical Biomechanics (Bristol, Avon)*, 19(4), 337–342.

- Mendis, M. D., Wilson, S. J., Stanton, W., & Hides, J. A. (2010). Validity of real-time ultrasound imaging to measure anterior hip muscle size: a comparison with magnetic resonance imaging. *The Journal of Orthopaedic and Sports Physical Therapy*, *40*(9), 577–581. <https://doi.org/10.2519/jospt.2010.3286>
- Merletti, R. (1999). Standards for reporting EMG data. *Journal of Electromyography & Kinesiology*, *9*(1), III.
- Milne, J. S., & Lauder, I. J. (1974). Age effects in kyphosis and lordosis in adults. *Annals of Human Biology*, *1*(3), 327-337.
- Nairn, B. C., Azar, N. R., & Drake, J. D. M. (2013a). On-Site Observations of Spine Angle Data During Prolonged Office Sitting While Performing Computer-Aided Drafting Work: A Case Study. *IIE Transactions on Occupational Ergonomics and Human Factors*, *1*(1), 76–81. <https://doi.org/10.1080/21577323.2012.708700>
- Nairn, B. C., Azar, N. R., & Drake, J. D. M. (2013b). Transient pain developers show increased abdominal muscle activity during prolonged sitting. *Journal of Electromyography and Kinesiology*, *23*(6), 1421–1427.
- Nairn, B. C., Chisholm, S. R., & Drake, J. D. M. (2013c). What is slumped sitting? A kinematic and electromyographical evaluation. *Manual Therapy*, *18*(6), 498–505.
- Nairn, B. C., & Drake, J. D. M. (2014). Impact of lumbar spine posture on thoracic spine motion and muscle activation patterns. *Human Movement Science*, *37*, 1–11.
- Narici, M. V., Binzoni, T., Hiltbrand, E., Fasel, J., Terrier, F., & Cerretelli, P. (1996). In vivo human gastrocnemius architecture with changing joint angle at rest and during graded isometric contraction. *The Journal of Physiology*, *496*(Pt 1), 287–297.

- Nelson-Wong, E., & Callaghan, J. P. (2010). Is muscle co-activation a predisposing factor for low back pain development during standing? A multifactorial approach for early identification of at-risk individuals. *Journal of Electromyography and Kinesiology*, *20*, 256-263.
- Nelson-Wong, E., Gregory, D. E., Winter, D. A., & Callaghan, J. P. (2008). Gluteus medius muscle activation patterns as a predictor of low back pain during standing. *Clinical Biomechanics*, *23*, 545-553.
- Ng, J. K.-F., Kippers, V., Parnianpour, M., & Richardson, C. A. (2002). EMG activity normalization for trunk muscles in subjects with and without back pain. *Medicine and Science in Sports and Exercise*, *34*(7), 1082–1086.
- NIOSH (2014). Observation-based posture assessment: review of current practice and recommendation for improvement. By Lowe, B. D., Weir, P. L., Andrews, D. M. Cincinnati, OH: U.S. Department of Health and Human Services, Centres for Disease Control and Prevention, National Institute for Occupational Safety and Health, DHHS (NIOSH) Publication No. 2014-131.
- Nitz, W. (2006). Principles of magnetic resonance imaging and magnetic resonance angiography. In P. Reimer, P. M. Parizel, & F.-A. Stichnoth, (Eds.), *Clinical MR imaging. A practical approach* (pp. 1-53). Berlin, Germany: Springer.
- Oda, I., Abumi, K., Cunningham, B. W., Kaneda, K., & McAfee, P. C. (2002). An in vitro human cadaveric study investigating the biomechanical properties of the thoracic spine. *Spine*, *27*(3), E64-70.
- O’Sullivan, C., Bentman, S., Bennett, K., & Stokes, M. (2007). Rehabilitative ultrasound imaging of the lower trapezius muscle: technical description and reliability. *The Journal*

- of Orthopaedic and Sports Physical Therapy*, 37(10), 620–626.
- O’Sullivan, C., Meaney, J., Boyle, G., Gormley, J., & Stokes, M. (2009). The validity of Rehabilitative Ultrasound Imaging for measurement of trapezius muscle thickness. *Manual Therapy*, 14(5), 572–578. <https://doi.org/10.1016/j.math.2008.12.005>
- O’Sullivan, P. B. (2000). Lumbar segmental “instability”: clinical presentation and specific stabilizing exercise management. *Manual Therapy*, 5(1), 2–12.
- Panjabi, M. M., Takata, K., Goel, V., Federico, D., Oxland, T., Duranceau, J., & Krag, M. (1991). Thoracic human vertebrae. Quantitative three-dimensional anatomy. *Spine*, 16(8), 888–901.
- Park, S., & Yoo, W. (2013). Comparison of exercises inducing maximum voluntary isometric contraction for the latissimus dorsi using surface electromyography. *Journal of Electromyography and Kinesiology*, 23(5), 1106–1110.
- Peat, M. (1986). Functional anatomy of the shoulder complex. *Physical Therapy*, 66(12), 1855–1865.
- Potvin, J. R., McGill, S. M., & Norman, R. W. (1991). Trunk muscle and lumbar ligament contributions to dynamic lifts with varying degrees of trunk flexion. *Spine*, 16(9), 1099–1107.
- Punnett, L., & Wegman, D. H. (2004). Work-related musculoskeletal disorders: the epidemiologic evidence and the debate. *Journal of Electromyography and Kinesiology*, 14, 13-23.
- Rabello, L. M., Gagnon, D., da Silva, R. A., Paquette, P., & Larivière, C. (2015). External abdominal oblique muscle ultrasonographic thickness changes is not an appropriate surrogate measure of electromyographic activity during isometric trunk contractions.

- Journal of Back and Musculoskeletal Rehabilitation*, 28(2), 229–238.
- Radwin, R. G., Marras, W. S., & Lavender, S. A. (2002). Biomechanical aspects of work-related musculoskeletal disorders. *Theoretical Issues in Ergonomics Science*, 2(2), 153-217.
- Rajabi, R., Doherty, P., Goodarzi, M., & Hemayattalab, R. (2008). Comparison of thoracic kyphosis in two groups of elite Greco-Roman and freestyle wrestlers and a group of non-athletic participants. *British Journal of Sports Medicine*, 42(3), 229–232; discussion 232.
- Schinkel-Ivy, A., & Drake, J. D. M. (2015a). Sequencing of superficial trunk muscle activation during range-of-motion tasks. *Human Movement Science*, 43, 67–77.
- Schinkel-Ivy, A., & Drake, J. D. M. (2015b). Which motion segments are required to sufficiently characterize the kinematic behaviour of the trunk? *Journal of Electromyography and Kinesiology*, 25(2), 239-246.
- Schinkel-Ivy, A., Pardisnia, S., & Drake, J. D. M. (2014). Head and arm positions that elicit maximal voluntary trunk range-of-motion measures. *Journal of Applied Biomechanics*, 30(6), 689-696.
- Schinkel-Ivy, A., Nairn, B. C., & Drake, J. D. M. (2013). Investigation of trunk muscle co-contraction and its association with low back pain development during prolonged sitting. *Journal of Electromyography and Kinesiology*, 23(4), 778–786.
- Shrout, P. E., & Fleiss, J. L. (1979). Intraclass correlations: uses in assessing rater reliability. *Psychological Bulletin*, 86(2), 420-428.
- Silvestri, G., Schinkel-Ivy, A., & Drake, J. D. M. (2013). Assessment of trunk muscle co-contraction during typical occupational movement tasks. *Occupational Ergonomics*, 11(4), 165–176. <https://doi.org/10.3233/OER-140216>

- Singh, D. K. A., Bailey, M., & Lee, R. Y. W. (2011). Ageing modifies the fibre angle and biomechanical function of the lumbar extensor muscles. *Clinical Biomechanics (Bristol, Avon)*, 26(6), 543–547. <https://doi.org/10.1016/j.clinbiomech.2011.02.002>
- Sions, J. M., Velasco, T. O., Teyhen, D. S., & Hicks, G. E. (2015). Reliability of Ultrasound Imaging for the Assessment of Lumbar Multifidi Thickness in Older Adults with Chronic Low Back Pain. *Journal of Geriatric Physical Therapy (2001)*, 38(1), 33–39.
- Siu, A., Schinkel-Ivy, A., & Drake, J. D. (2016). Arm position influences the activation patterns of trunk muscles during trunk range-of-motion movements. *Human Movement Science*, 49, 267–276. <https://doi.org/10.1016/j.humov.2016.07.010>
- Smith, M. D., Chang, A. T., & Hodges, P. W. (2016). Balance recovery is compromised and trunk muscle activity is increased in chronic obstructive pulmonary disease. *Gait & Posture*, 43, 101–107.
- Soderberg, G. L. (1992). Recording techniques. In Soderberg, G. L. (ed.), *Selected Topics in Surface Electromyography for Use in the Occupational Setting: Expert Perspectives* (pp. 23-41). Rockville, MD: US Department of Health and Human Services, Public Health Service, Publication No. 91-100.
- Soderberg, G. L., & Knutson, L. M. (2000). A guide for use and interpretation of kinesiological electromyographic data. *Physical Therapy*, 80(5), 485-498.
- Stokes, M., Hides, J., Elliott, J., Kiesel, K., & Hodges, P. (2007). Rehabilitative ultrasound imaging of the posterior paraspinal muscles. *The Journal of Orthopaedic and Sports Physical Therapy*, 37(10), 581–595. <https://doi.org/10.2519/jospt.2007.2599>
- Swinscow TDV. (1997). *Statistics at Square One*, BMJ Publishing, 1997.

- Tan, A. L., Wakefield, R. J., Conaghan, P. G., Emery, P., & McGonagle, D. (2003). Imaging of the musculoskeletal system: magnetic resonance imaging, ultrasonography and computed tomography. *Best Practice & Research. Clinical Rheumatology*, *17*(3), 513–528.
- Taweetanalarp, S., & Purepong, N. (2015). Comparison of lumbar spinal angle between normal body mass index and overweight young adults. *Journal of Physical Therapy Science*, *27*(7), 2343-2346.
- Terry, G. C., & Chopp, T. M. (2000). Functional Anatomy of the Shoulder. *Journal of Athletic Training*, *35*(3), 248–255.
- Teyhen, D. S., Childs, J. D., Stokes, M. J., Wright, A. C., Dugan, J. L., & George, S. Z. (2012). Abdominal and lumbar multifidus muscle size and symmetry at rest and during contracted States. Normative reference ranges. *Journal of Ultrasound in Medicine: Official Journal of the American Institute of Ultrasound in Medicine*, *31*(7), 1099–1110.
- Teyhen, D. S., George, S. Z., Dugan, J. L., Williamson, J., Neilson, B. D., & Childs, J. D. (2011). Inter-rater reliability of ultrasound imaging of the trunk musculature among novice raters. *Journal of Ultrasound in Medicine: Official Journal of the American Institute of Ultrasound in Medicine*, *30*(3), 347–356.
- Thompson, S. B. N., & Eales, W. (1994). Clinical consideration and comparative measures of assessing curvature of the spine. *Journal of Medical Engineering & Technology*, *18*(4), 143-147.
- Tillotson, K. M., & Burton, A. K. (1991). Noninvasive measurement of lumbar sagittal mobility. An assessment of the flexicurve technique. *Spine*, *16*(1), 29-33.
- Tortora, G. J. (2004). *Principles of human anatomy* (10th ed.). New Jersey: John Wiley & Sons

- Tran, T. H., Wing, D., Davis, A., Bergstrom, J., Schousboe, J. T., Nichols, J. F., & Kado, D. M. (2016). Correlations among four measures of thoracic kyphosis in older adults. *Osteoporosis International*, 27(3), 1255-1259.
- Van, K., Hides, J. A., & Richardson, C. A. (2006). The use of real-time ultrasound imaging for biofeedback of lumbar multifidus muscle contraction in healthy subjects. *The Journal of Orthopaedic and Sports Physical Therapy*, 36(12), 920–925.
- Vasavada, A., Ward, S. R., Delp, S., & Lieber, R. L. (2011). Architectural Design and Function of Human Back Muscles. In H. N. Herkowitz, S. R. Garfin, F. J. Eismont, G. R. Bell, & R. A. Balderston, *Rothman-Simeone The Spine E-Book: Expert Consult* (pp. 57–72). Elsevier Health Sciences.
- Vera-Garcia, F. J., Moreside, J. M., & McGill, S. M. (2010). MVC techniques to normalize trunk muscle EMG in healthy women. *Journal of Electromyography and Kinesiology*, 20(1), 10–16.
- Vigreux, B., Cnockaert, J. C., & Pertuzon, E. (1979). Factors influencing quantified surface EMGs. *European Journal of Applied Physiology and Occupational Physiology*, 41(2), 119–129.
- Vincent, W. J. (2005). *Statistics in kinesiology* (3rd ed.). Champaign, IL: Human Kinetics.
- Wallwork, T. L., Hides, J. A., & Stanton, W. R. (2007). Intrarater and interrater reliability of assessment of lumbar multifidus muscle thickness using rehabilitative ultrasound imaging. *The Journal of Orthopaedic and Sports Physical Therapy*, 37(10), 608–612.
- Wang, S., & McGill, S. M. (2008). Links between the mechanics of ventilation and spine stability. *Journal of Applied Biomechanics*, 24(2), 166–174.

- Watanabe, K., Miyamoto, K., Masuda, T., & Shimizu, K. (2004). Use of ultrasonography to evaluate thickness of the erector spinae muscle in maximum flexion and extension of the lumbar spine. *Spine*, *29*(13), 1472–1477.
- Watkins, R., Watkins, R., Williams, L., Ahlbrand, S., Garcia, R., Karamanian, A., ... Hedman, T. (2005). Stability provided by the sternum and rib cage in the thoracic spine. *Spine*, *30*(11), 1283–1286.
- Whittaker, J. L., McLean, L., Hodder, J., Warner, M. B., & Stokes, M. J. (2013). Association between changes in electromyographic signal amplitude and abdominal muscle thickness in individuals with and without lumbopelvic pain. *The Journal of Orthopaedic and Sports Physical Therapy*, *43*(7), 466–477. <https://doi.org/10.2519/jospt.2013.4440>
- Whittaker, J. L., Teyhen, D. S., Elliott, J. M., Cook, K., Langevin, H. M., Dahl, H. H., & Stokes, M. (2007). Rehabilitative ultrasound imaging: understanding the technology and its applications. *The Journal of Orthopaedic and Sports Physical Therapy*, *37*(8), 434–449.
- Willems, J. M., Jull, G. A., & J, K.-F. N. (1996). An in vivo study of the primary and coupled rotations of the thoracic spine. *Clinical Biomechanics (Bristol, Avon)*, *11*(6), 311–316.
- Winter, D. A. (2009). *Biomechanics and motor control of human movement* (4th ed.). New Jersey: John Wiley & Sons, Inc.
- Winter, D. A., Fuglevand, A. J., & Archer, S. E. (1994). Crosstalk in surface electromyography: Theoretical and practical estimates. *Journal of Electromyography and Kinesiology*, *4*(1), 15–26. [https://doi.org/10.1016/1050-6411\(94\)90023-X](https://doi.org/10.1016/1050-6411(94)90023-X)
- Worsley, P. R., Kitsell, F., Samuel, D., & Stokes, M. (2014). Validity of measuring distal vastus medialis muscle using rehabilitative ultrasound imaging versus magnetic resonance imaging. *Manual Therapy*, *19*(3), 259–263. <https://doi.org/10.1016/j.math.2014.02.002>

- Yanagawa, T. L., Maitland, M. E., Burgess, K., Young, L., & Hanley, D. (2000). Assessment of thoracic kyphosis using the flexicurve for individuals with osteoporosis. *Hong Kong Physiotherapy Journal*, 18(2), 53-57.
- Yang, J. F., & Winter, D. A. (1984). Electromyographic amplitude normalization methods: improving their sensitivity as diagnostic tools in gait analysis. *Archives of Physical Medicine and Rehabilitation*, 65(9), 517-521.
- Youdas, J. W., Garrett, T. R., Harmsen, S., Suman, V. J., & Carey, J. R. (1996). Lumbar lordosis and pelvic inclination of asymptomatic adults. *Physical Therapy*, 76(10), 1066-1081.
- Youdas, J. W., Hollman, J. H., & Krause, D. A. (2006). The effects of gender, age, and body mass index on standing lumbar curvature in persons without current low back pain. *Physiotherapy Theory and Practice*, 22(5), 229-237.
- Zech, A., Steib, S., Hentschke, C., Eckhardt, H., & Pfeifer, K. (2012). Effects of localized and general fatigue on static and dynamic postural control in male team handball athletes. *Journal of Strength and Conditioning Research*, 26(4), 1162-1168.

Appendix A: Study #5: Application-Pilot

A.1 Application-Pilot Introduction

Challenged breathing has been associated with increased muscle activation in TransAb (Hodges & Gandevia, 2000) and LES (Wang & McGill, 2008), as well as an increase in lumbar stability in those with LBP (Grenier & McGill, 2008), and a decrease in balance recovery in those with COPD (Smith et al., 2016). However, the application/function of T4ES during challenged breathing remains unclear. Therefore, the purpose of this pilot study was to assess T4ES activation during two challenged breathing tasks. This application pilot was included as a first-glance into the efficacy of using T4ES in a real-world application.

A.2 Application-Pilot Methods

A total of 16 participants (9 male, 7 female) were collected and analyzed for this study, with recruitment and ethical considerations outlined in the **Common Methods 3.1: Participants** section. The combined mean (*SD*) age, height, and weight was 21.5 y (3.7), 1.7 m (0.08), and 69.68 kg (13.82), respectively. Participants also completed the International Physical Activity Questionnaire (Long version), where 12/16 were considered to have “High” physical activity, 2/16 “Moderate”, and 1/16 reported “Low” levels of physical activity. In addition to EMG that was recorded from T4ES as outlined in the **Common Methods 3.3: Electromyography** section, participants were also instrumented with a Polar M400 heart rate (HR) monitor (Polar Electro, Kempele, Finland) which continuously recorded HR throughout the collection.

Two different challenged breathing tasks were assessed, one “involuntary” and one “voluntary”. The “involuntary” task consisted of participants running on a treadmill with increasing speed until exhaustion. Based on the protocol established by Zech et al., (2012), the

treadmill grade was fixed at 1.5%, and began at 5 km/h. After the first 3 min the speed increased by 3 km/h, and by 2 km/hr after every subsequent 3 min interval (Zech et al., 2012). The treadmill used in the current study was in mph, thus the speeds were 3.1 mph, 5.0 mph, 6.2 mph, 7.5 mph, and 8.7 mph through the first 15 minutes. Participants were instructed to run until they could run no more, and verbal encouragement was provided throughout. The “voluntary” challenged breathing task was a maximum voluntary ventilation (MVV) task, where participants were instructed to breathe in and out with deep breaths as fast as possible (Wang & McGill, 2008). To ensure safety (e.g. reduce risk of hyperventilation), this MVV was done with the aid of a brown paper bag. Both the treadmill and MVV tasks were counter-balanced across participants and EMG was recorded during the MVV, yet not during the treadmill task.

The outcome measures for this pilot study were peak HR during the treadmill and MVV, the rating of perceived exertion (RPE, from 6-20 Borg scale) immediately following the treadmill and MVV tasks, and the average T4ES activation immediately before and after the treadmill task. In addition, the average T4ES activation before, during, and after the MVV task was reported. For the purpose of this pilot study, inferential statistics were not run, yet descriptive (mean (*SD*)) values were presented.

A.3 Application-Pilot Results and Discussion

Overall, the treadmill run resulted in increased HR and RPE without much increase in EMG activation immediately after the tasks (Figures A.1, A.2, A.3) (mean (*SD*) pre-test HR was 88.7 BPM (16.1)). However, Figure A.3 showed that the MVV resulted in an increase in T4ES activation. Considering there was no substantial increase in muscle activation during the “involuntary” challenged breathing (treadmill), these data supported the notion offered by

McGill et al., (1995) that the major roles of thoracic spine musculature are for moment production rather than for assistance of breathing. Additionally, it was unclear if the increased EMG during the MVV was a result of the breathing task, or the fact that participants had to lift their arms to their face to hold the bag to breathe into. This further implied that T4ES did not appear to play a large role in involuntary breathing, yet changes in posture with forced ventilation could influence the EMG signal.

In conclusion, the treadmill protocol was able to bring the participants to exhaustion, though there was no clear impact on T4ES activity. This had implications on the application of T4ES, and supported the thought that T4ES could provide more of a stabilizing function as a whole.

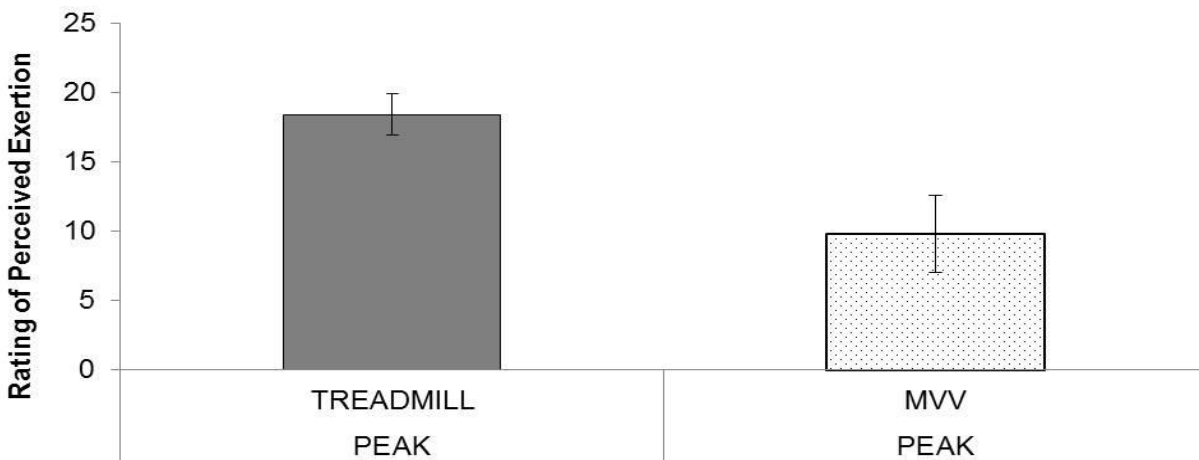


Figure A.1. Mean (*SD*) rating of perceived exertion after the treadmill task and maximum voluntary ventilation (MVV) task.

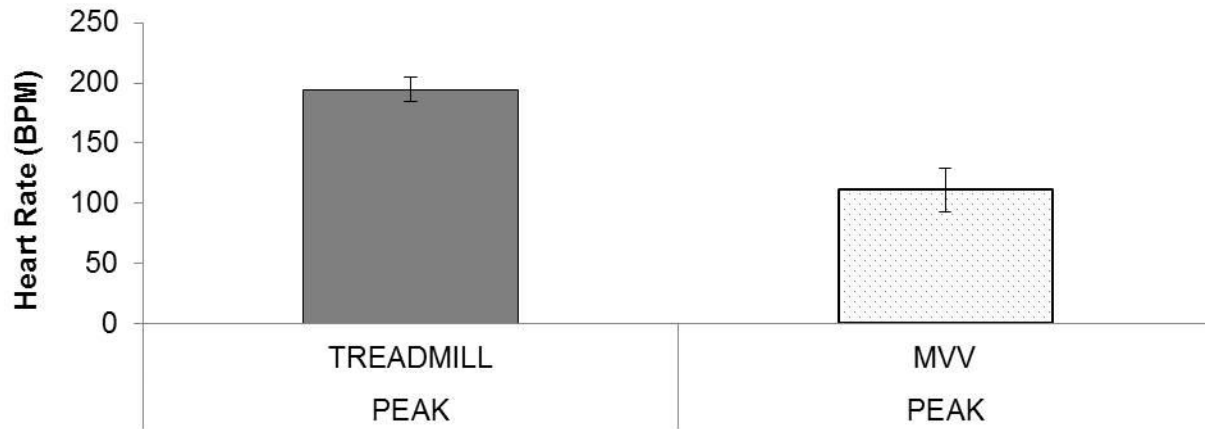


Figure A.2. Mean (*SD*) peak heart rate (BPM) after the treadmill task and maximum voluntary ventilation (MVV) task.

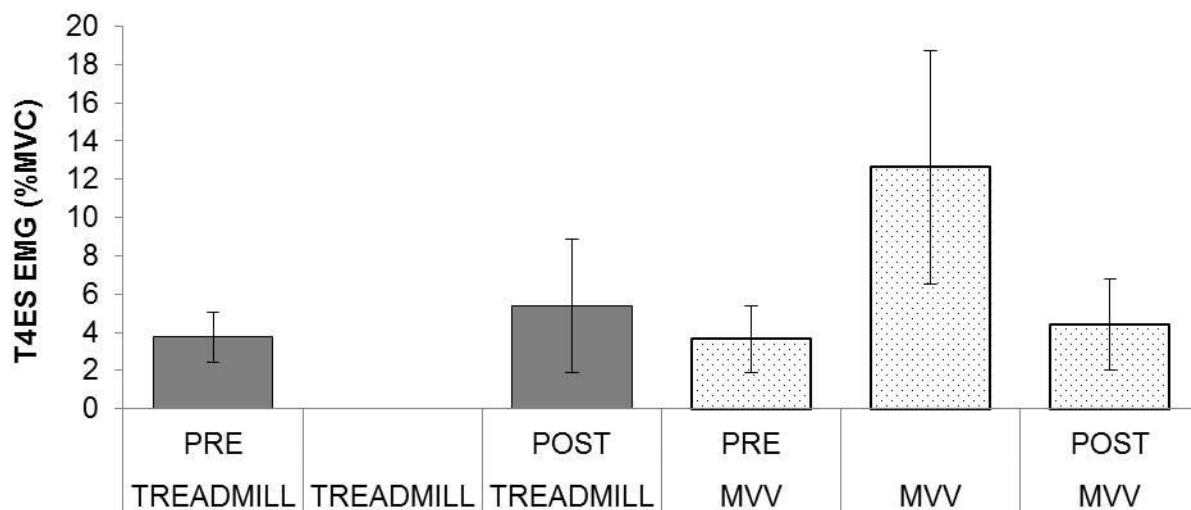


Figure A.3. Mean (*SD*) of T4ES activation (%MVC) before and after the treadmill task, and before, during, and after the maximum voluntary ventilation (MVV) task.

Appendix B: Flexi-MoCap Additional Results

Table B1. Mean (*SD*) Flexi angles recorded from each region and posture. (n=20)

Flexi Angles	Upright- Stand	Flex- Stand	Slump- Stand	Upright- Sit	Flex- Sit	Slump- Sit
UpTTan	25.90° (7.51)	30.33° (6.97)	30.52° (7.68)	26.42° (7.14)	35.23° (7.21)	26.72° (5.71)
MidSeg	19.77° (7.16)	33.58° (4.15)	30.69° (6.64)	18.37° (7.29)	37.52° (4.44)	30.43° (5.90)
LowTTan	8.93° (8.50)	32.71° (5.25)	23.83° (9.27)	8.17° (9.14)	34.79° (5.67)	29.68° (7.34)
LowSeg	-18.93° (10.37)	24.99° (4.70)	-5.06° (9.90)	-9.58° (11.25)	26.13° (3.99)	16.93° (9.99)
Lumbar	-41.12° (11.56)	18.96° (8.20)	-36.98° (10.34)	-21.31° (13.37)	18.82° (7.71)	0.26° (15.71)

Table B2. Mean (*SD*) MoCap angles recorded from each region and posture. (n=20)

MoCap Angles	Upright- Stand	Flex- Stand	Slump- Stand	Upright- Sit	Flex- Sit	Slump- Sit
UpTTan	24.29° (8.07)	37.78° (10.40)	24.95° (8.59)	22.16° (10.13)	46.58° (9.36)	16.83° (9.19)
MidSeg	20.03° (5.74)	33.17° (5.07)	28.61° (4.71)	18.41° (5.81)	37.23° (5.38)	25.02° (5.96)
LowTTan	4.17° (11.27)	26.35° (11.79)	17.58° (11.01)	2.94° (12.38)	26.66° (11.46)	14.80° (11.34)
LowSeg	-9.44° (6.46)	28.12° (4.49)	2.85° (9.05)	-3.91° (7.11)	28.50° (4.28)	15.71° (7.96)
Lumbar	-24.36° (10.42)	29.37° (11.89)	-17.90° (13.26)	-9.80° (7.11)	29.46° (11.39)	12.94° (13.60)

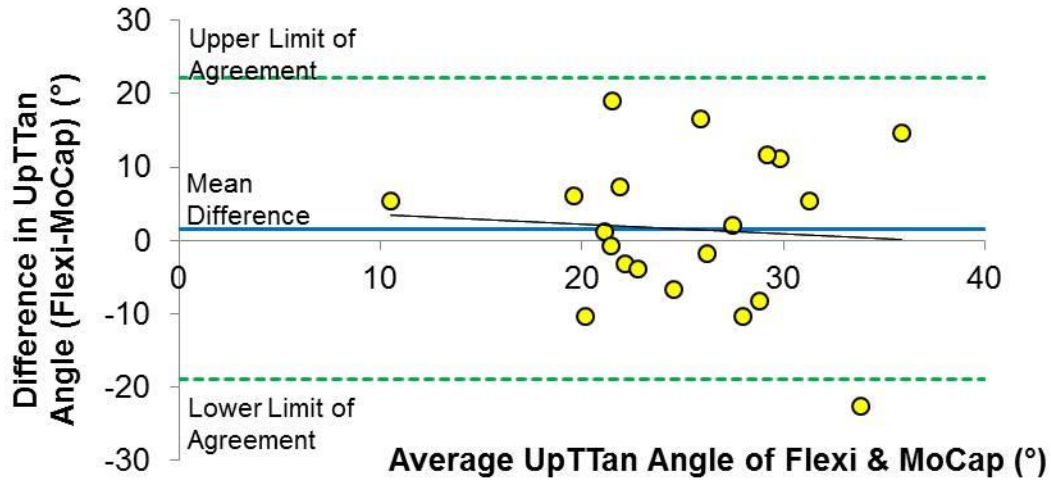


Figure B1. Bland-Altman plot for the UpTTan angle in Upright-Stand.

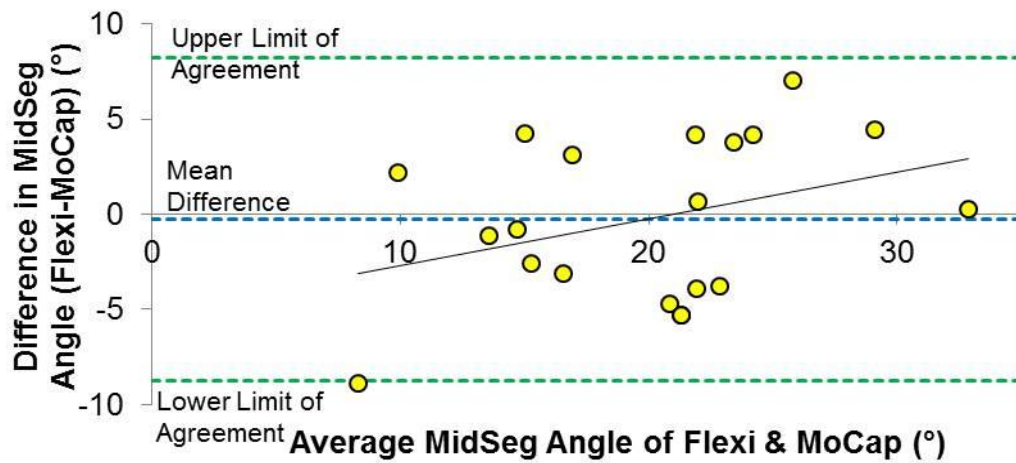


Figure B2. Bland-Altman plot for the MidSeg angle in Upright-Stand.

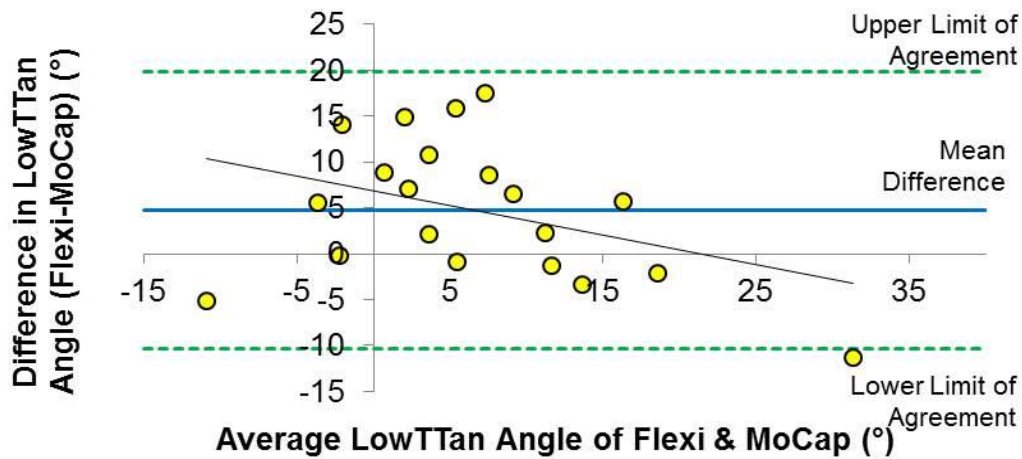


Figure B3. Bland-Altman plot for the LowTTan angle in Upright-Stand.

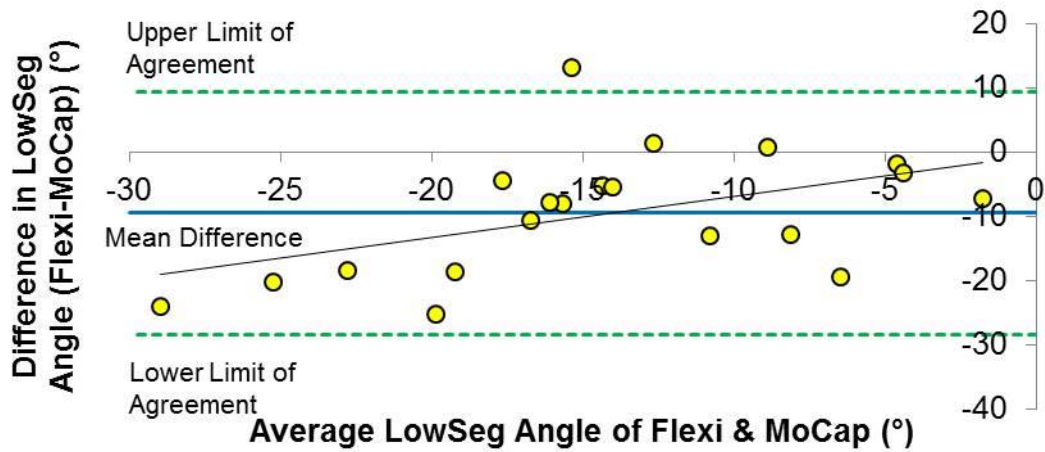


Figure B4. Bland-Altman plot for the LowSeg angle in Upright-Stand.

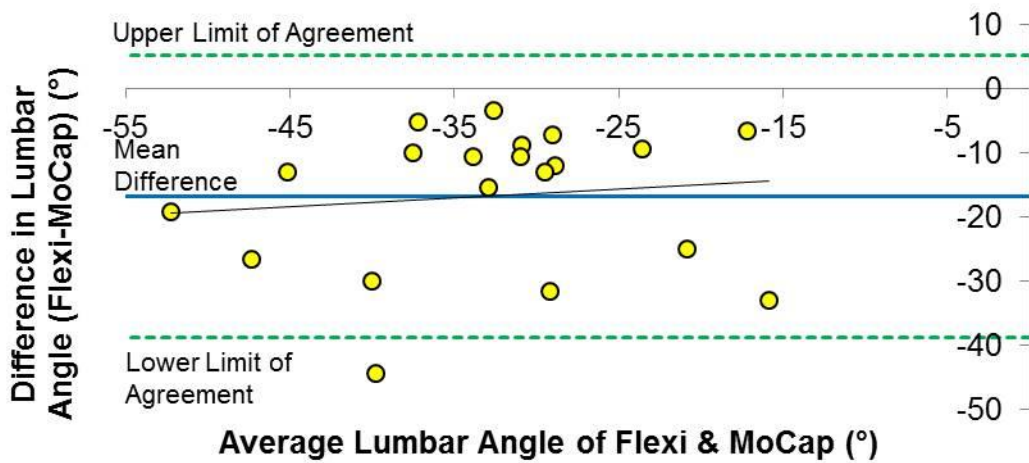


Figure B5. Bland-Altman plot for the Lumbar angle in Upright-Stand.

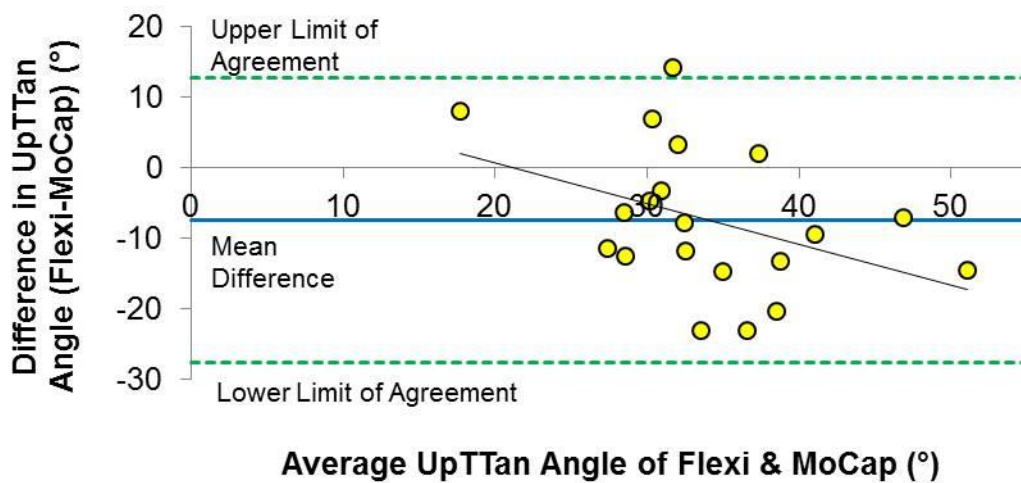


Figure B6. Bland-Altman plot for the UpTTan angle in Flex-Stand.

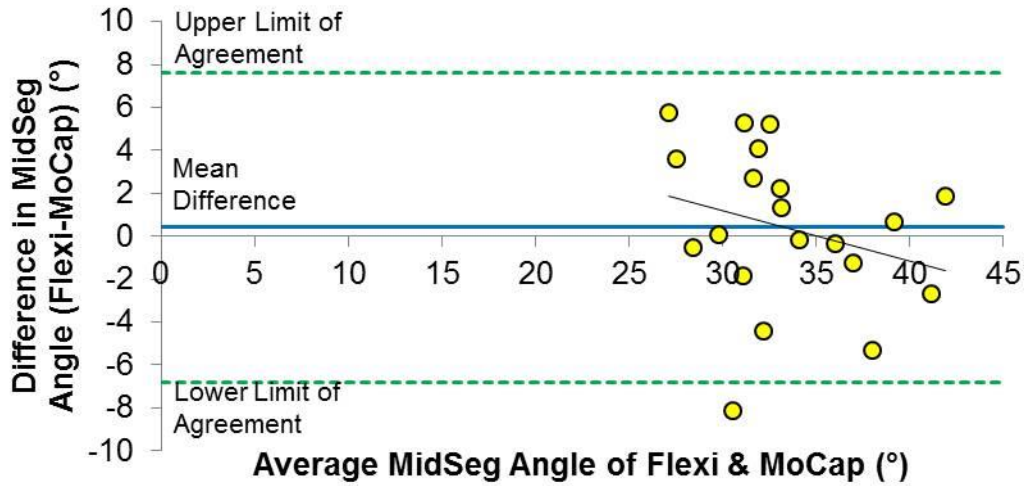


Figure B7. Bland-Altman plot for the MidSeg angle in Flexi-Stand.

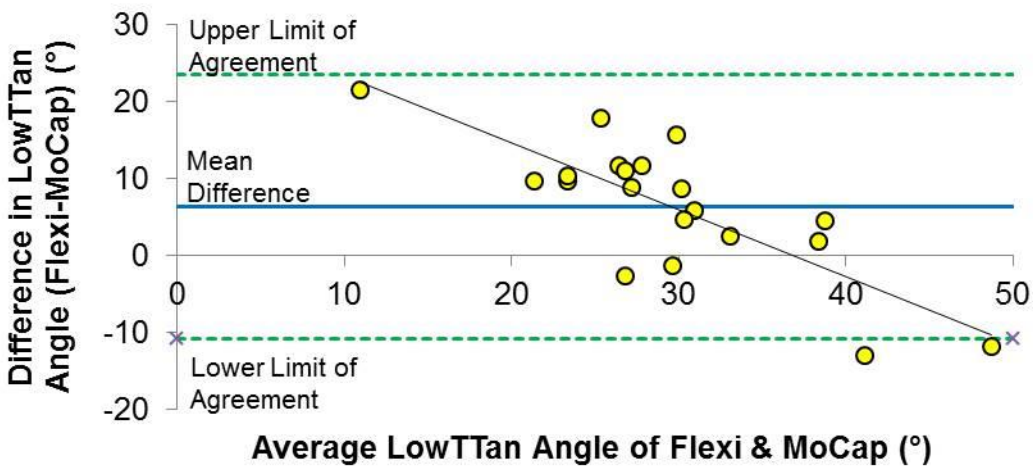


Figure B8. Bland-Altman plot for the LowTTan angle in Flexi-Stand.

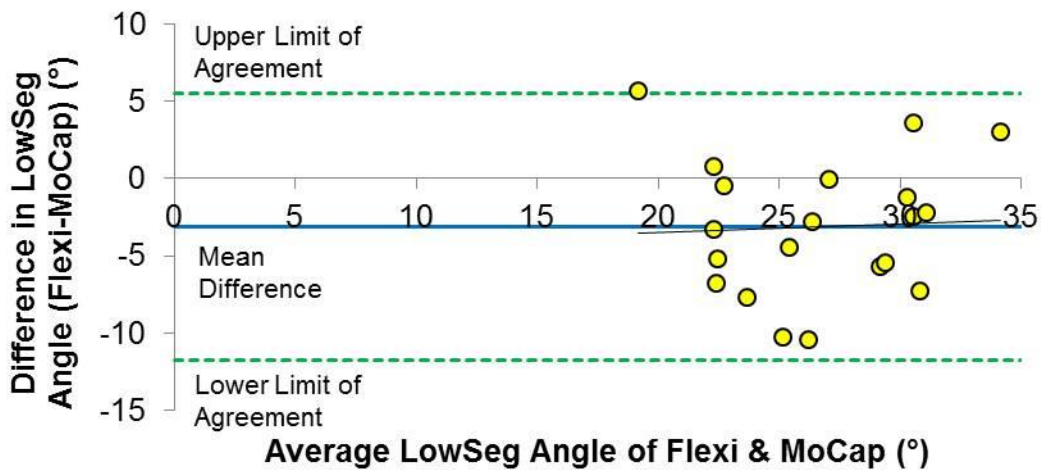


Figure B9. Bland-Altman plot for the LowSeg angle in Flexi-Stand.

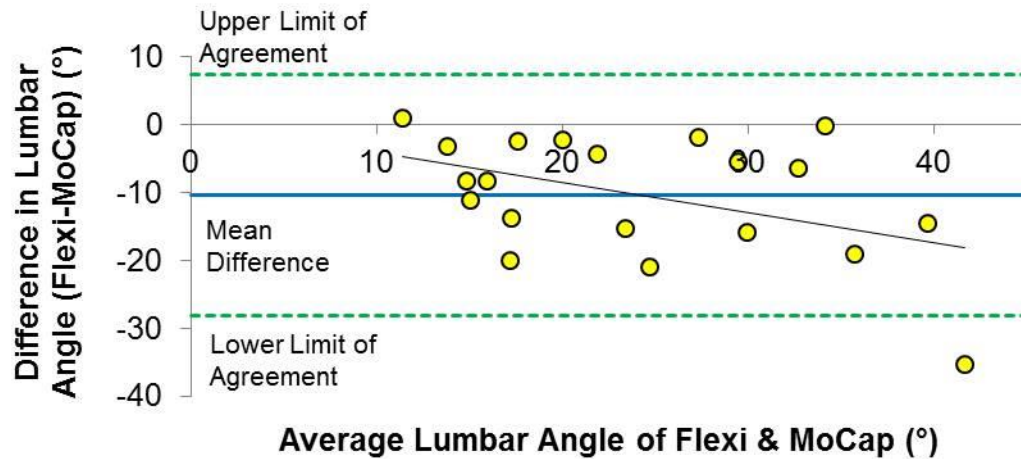


Figure B10. Bland-Altman plot for the Lumbar angle in Flex-Stand.

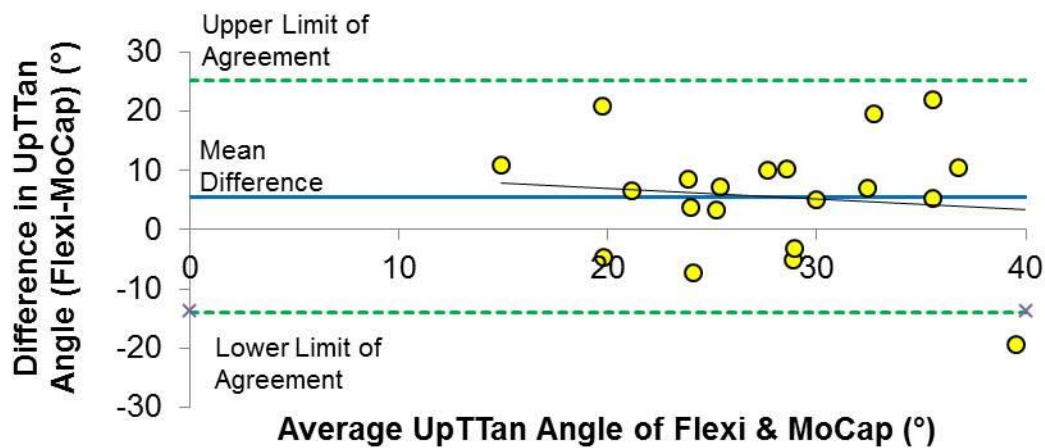


Figure B11. Bland-Altman plot for the UpTTan angle in Slump-Stand.

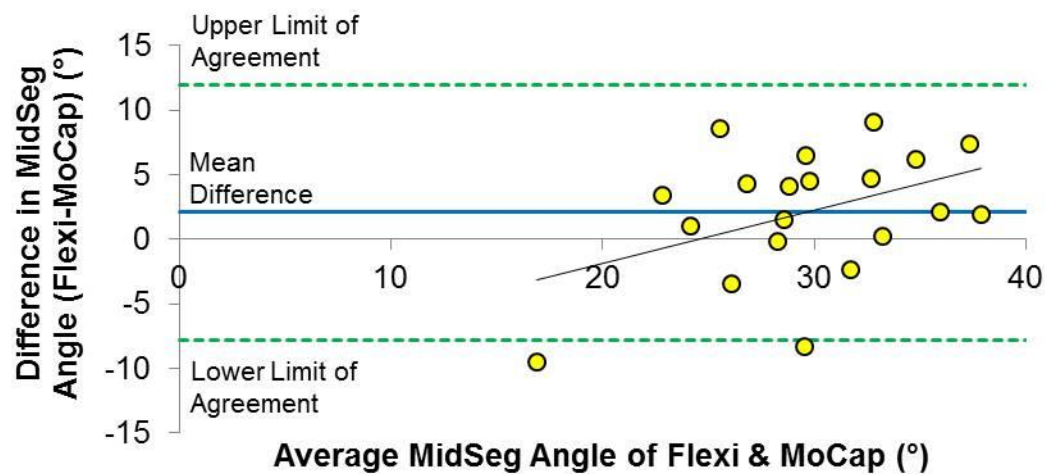


Figure B12. Bland-Altman plot for the MidSeg angle in Slump-Stand.

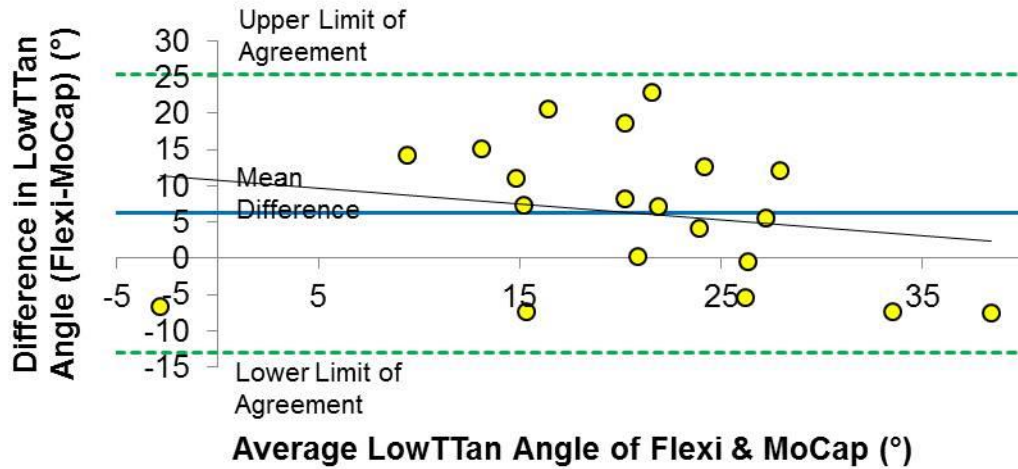


Figure B13. Bland-Altman plot for the LowTTan angle in Slump-Stand.

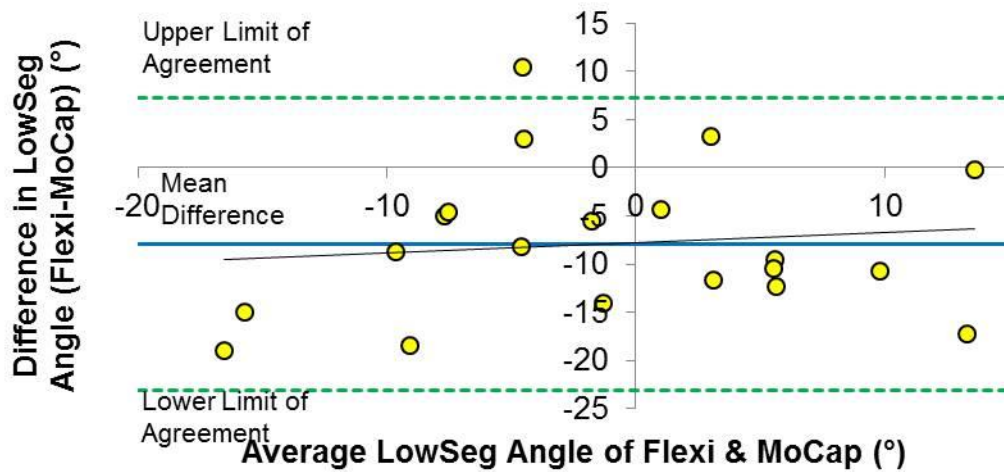


Figure B14. Bland-Altman plot for the LowSeg angle in Slump-Stand.

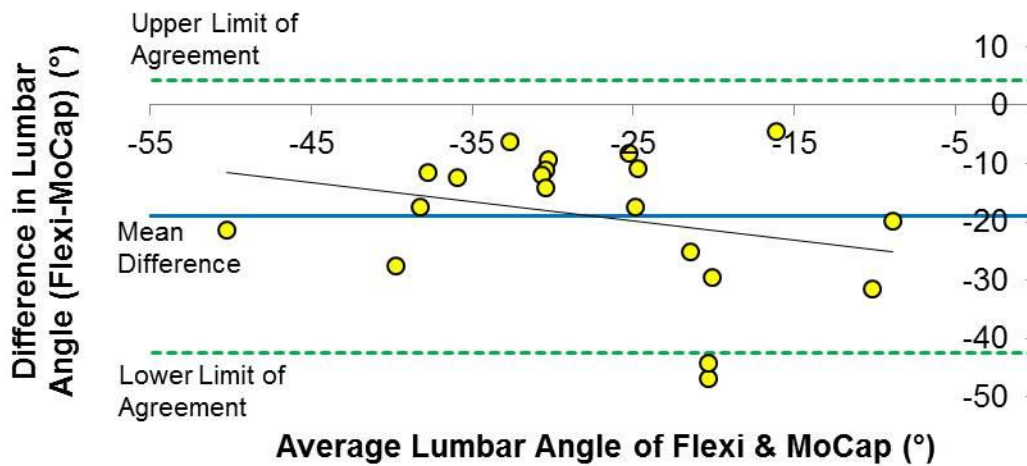


Figure B15. Bland-Altman plot for the Lumbar angle in Slump-Stand.

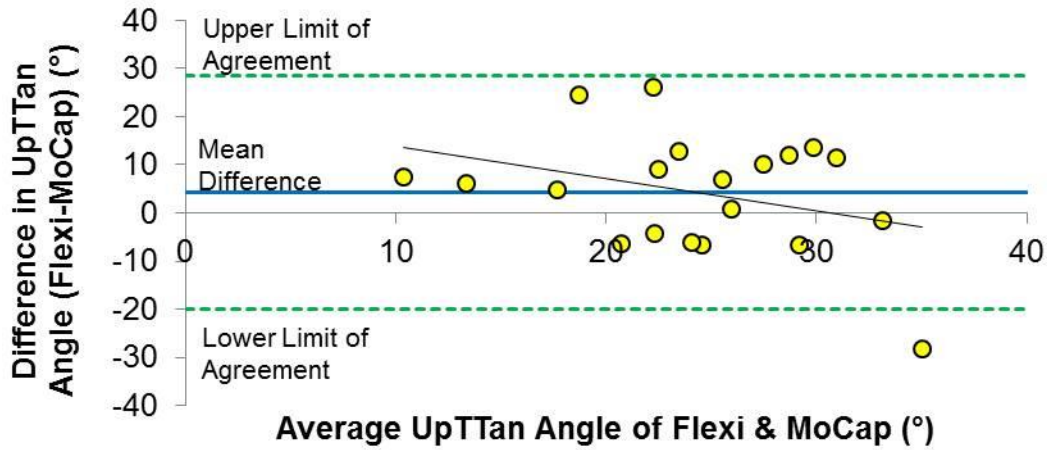


Figure B16. Bland-Altman plot for the UpTTan angle in Upright-Sit.

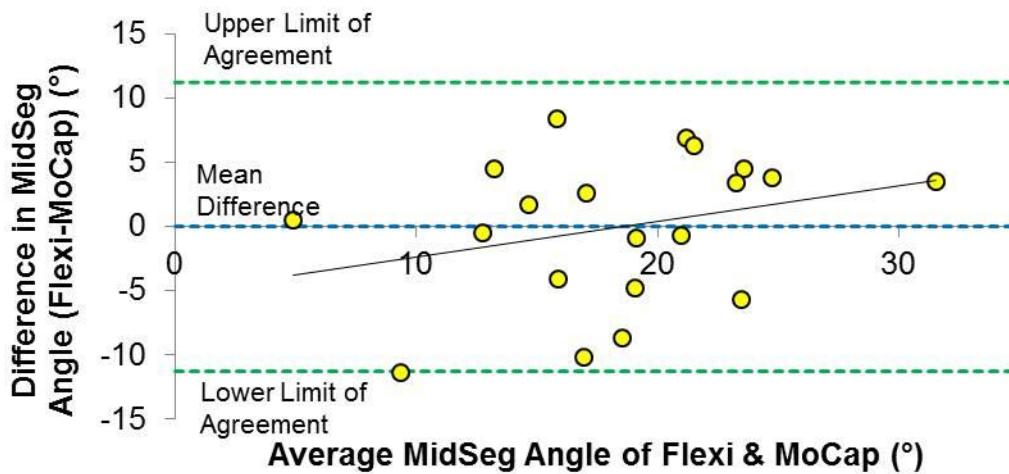


Figure B17. Bland-Altman plot for the MidSeg angle in Upright-Sit.

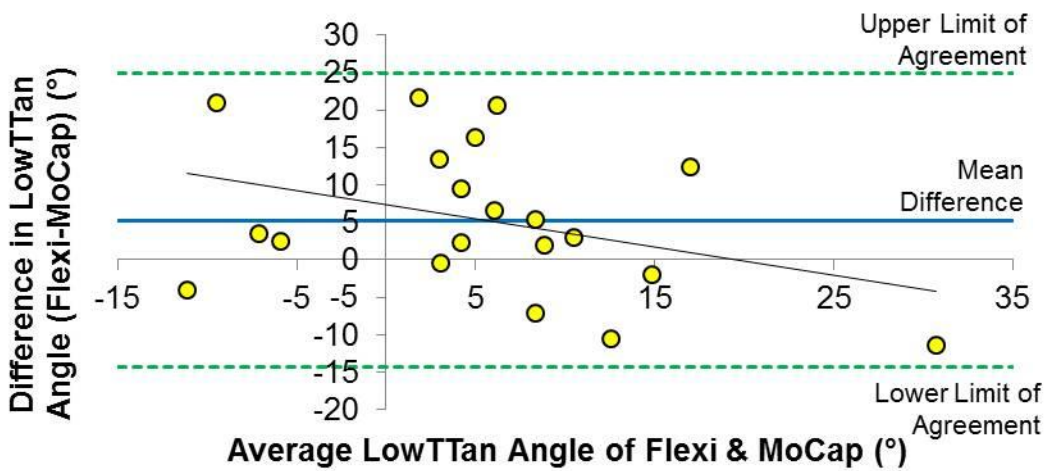


Figure B18. Bland-Altman plot for the LowTTan angle in Upright-Sit.

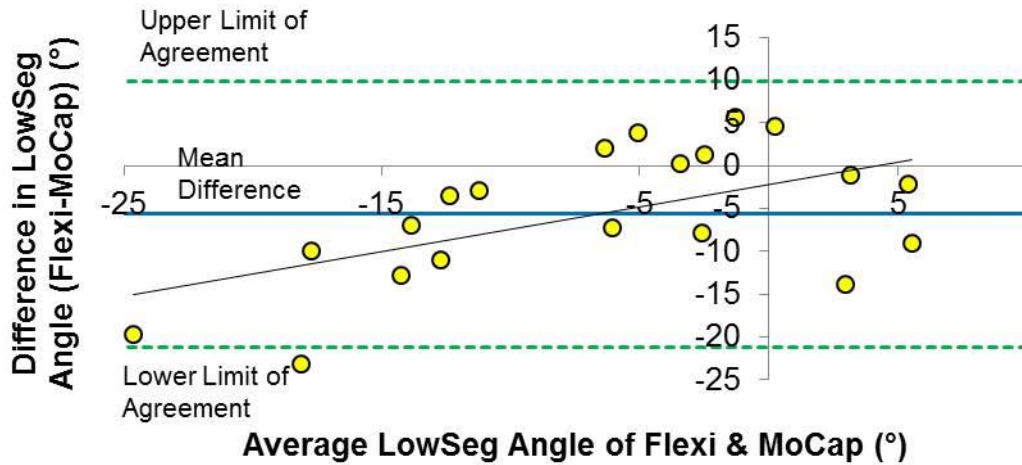


Figure B19. Bland-Altman plot for the LowSeg angle in Upright-Sit.

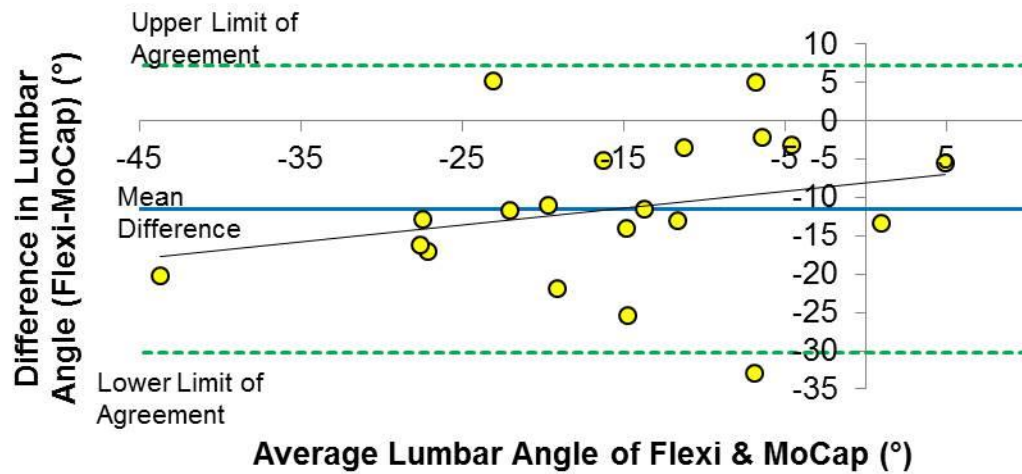


Figure B20. Bland-Altman plot for the Lumbar angle in Upright-Sit.

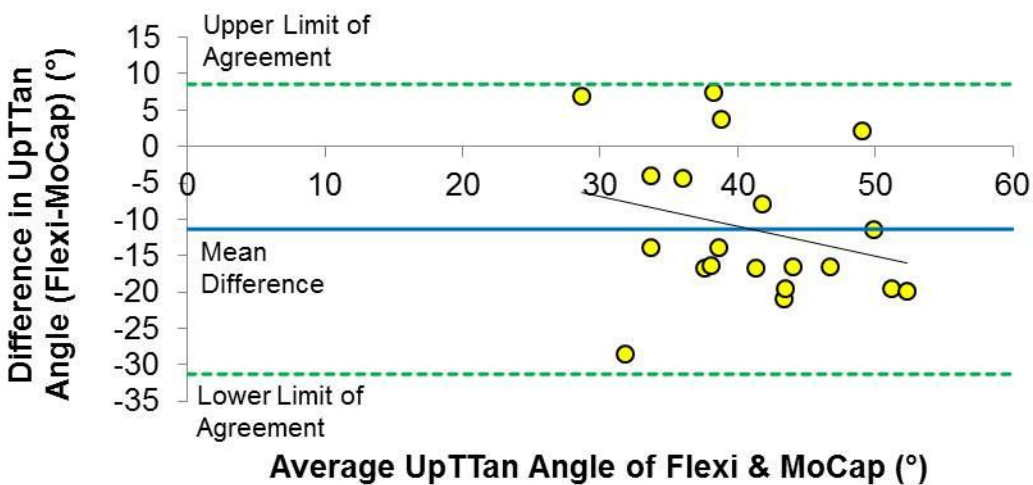


Figure B21. Bland-Altman plot for the UpTTan angle in Flex-Sit.

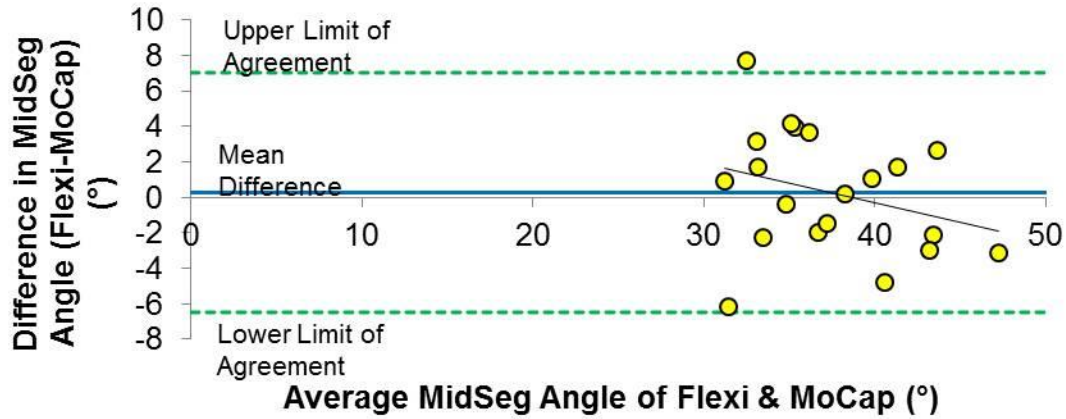


Figure B22. Bland-Altman plot for the MidSeg angle in Flex-Sit.

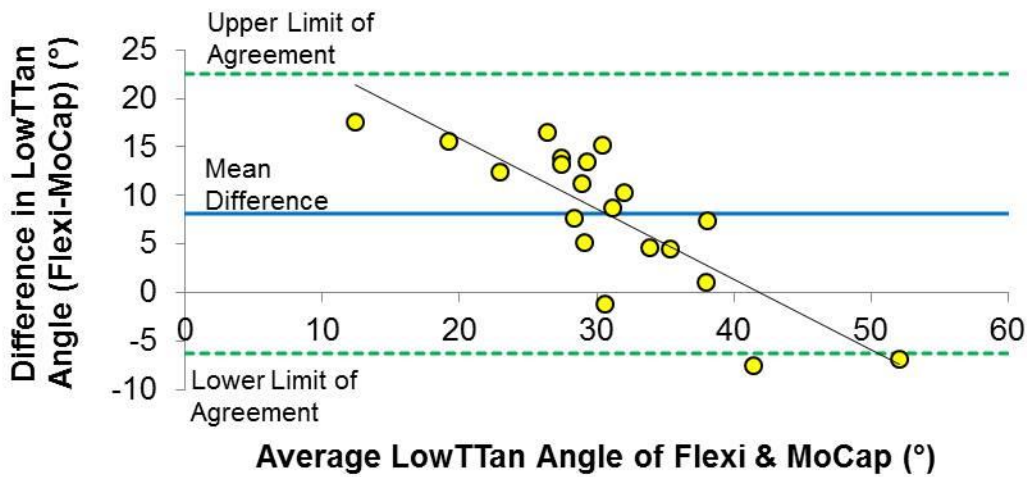


Figure B23. Bland-Altman plot for the LowTTan angle in Flex-Sit.

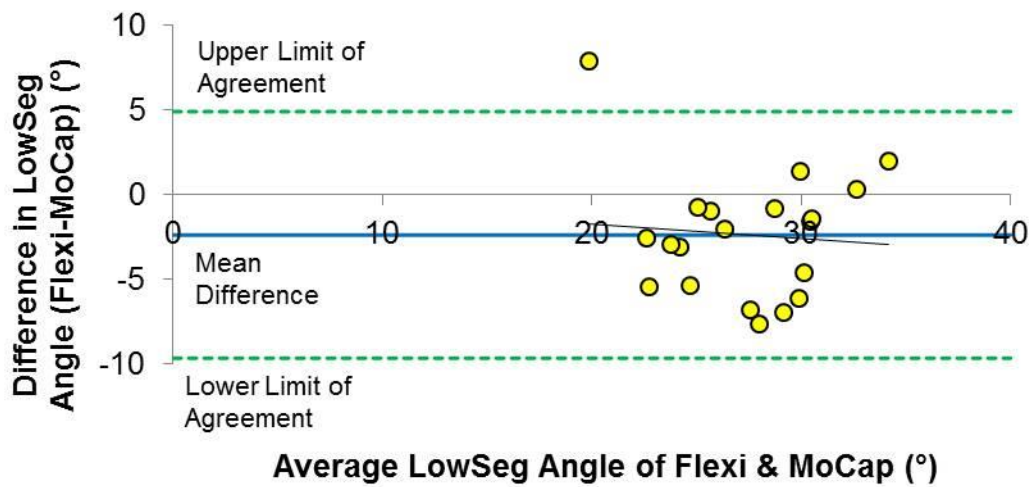


Figure B24. Bland-Altman plot for the LowSeg angle in Flex-Sit.

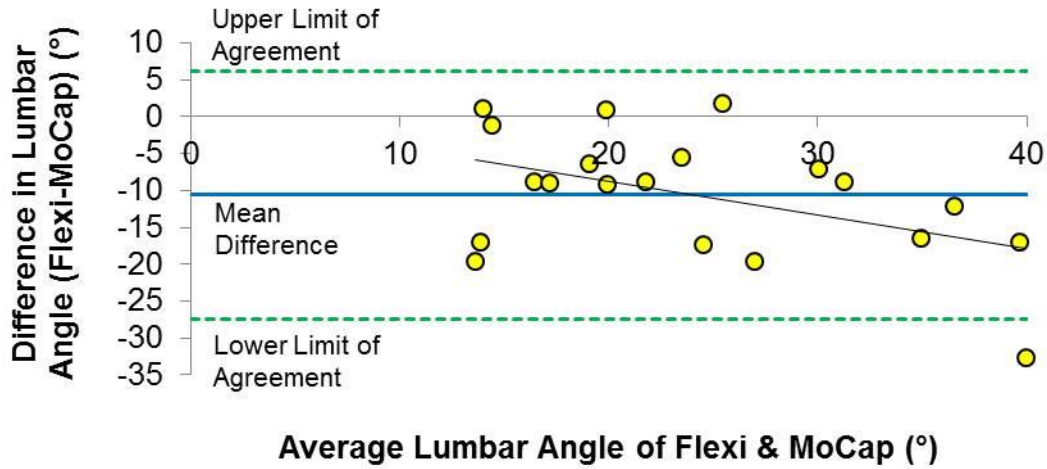


Figure B25. Bland-Altman plot for the Lumbar angle in Flex-Sit.

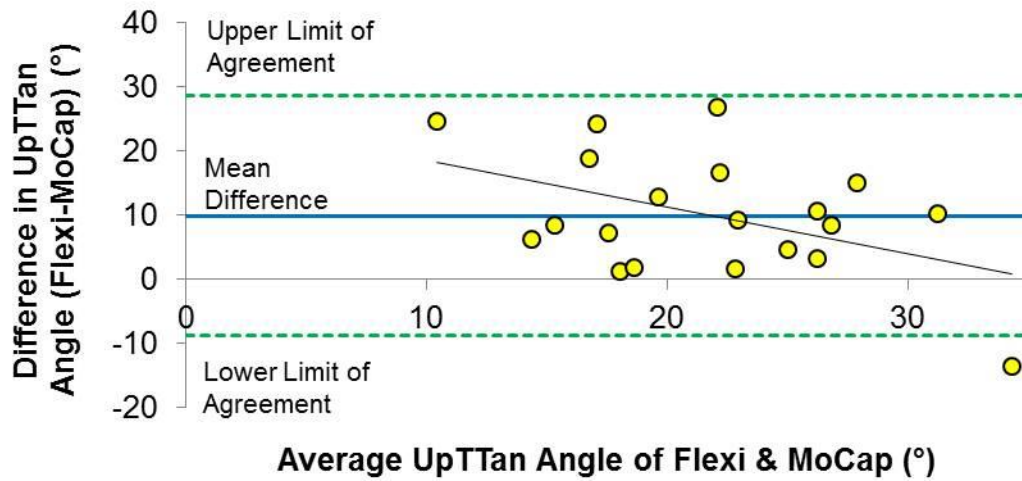


Figure B26. Bland-Altman plot for the UpTTan angle in Slump-Sit.

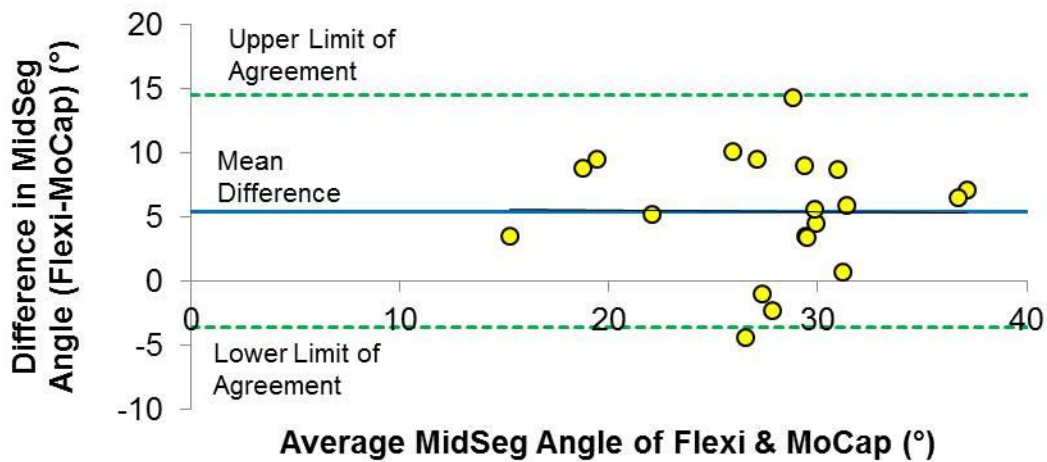


Figure B27. Bland-Altman plot for the MidSeg angle in Slump-Sit.

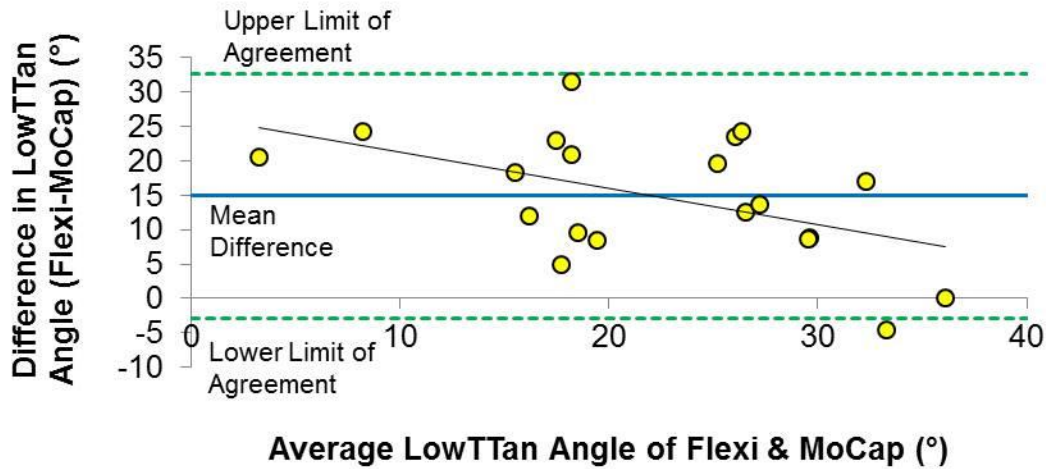


Figure B28. Bland-Altman plot for the LowTTan angle in Slump-Sit.

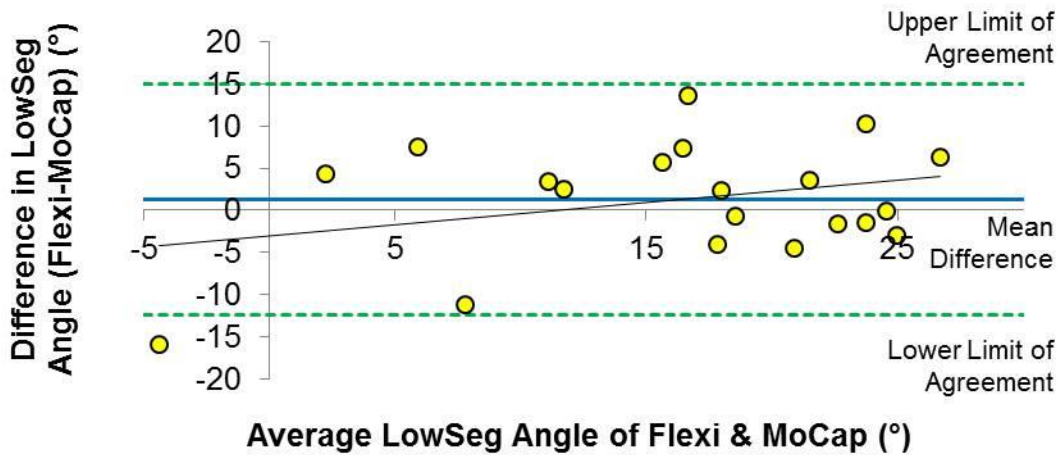


Figure B29. Bland-Altman plot for the LowSeg angle in Slump-Sit.

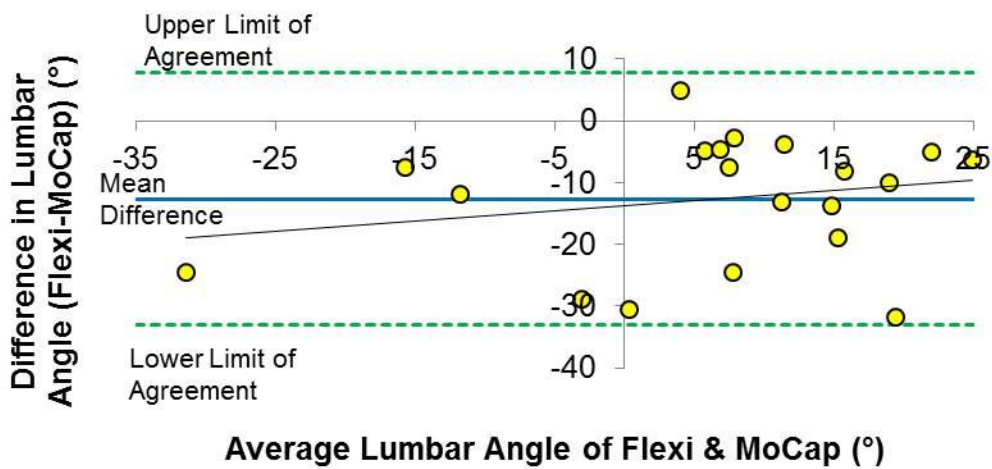


Figure B30. Bland-Altman plot for the Lumbar angle in Slump-Sit.

Table B3. Mean (*SD*) bias analyses from Bland-Altman of the Upright-Stand trial. Proportional bias is based on regression slope significantly different from 0, and systematic bias is based on mean difference being significantly different from 0.

Upright- Stand	Slope of Regression	<i>p</i> -value (sig from 0)	Mean Difference	<i>p</i> -value (sig from 0)	Proportional Bias?	Systematic Bias?
UpTTan	-0.131	0.761	1.61	0.498	No	No
MidSeg	0.244	0.136	-0.26	0.790	No	No
LowTTan	-0.323	0.092	4.76	0.012	No	Yes
LowSeg	0.641	0.033	-9.50	<0.001	Yes	Yes
Lumbar	0.140	0.620	-16.76	<0.001	No	Yes

Table B4. Mean (*SD*) bias analyses from Bland-Altman of the Flex-Stand trial. Proportional bias is based on regression slope significantly different from 0, and systematic bias is based on mean difference being significantly different from 0.

Flex- Stand	Slope of Regression	<i>p</i> -value (sig from 0)	Mean Difference	<i>p</i> -value (sig from 0)	Proportional Bias?	Systematic Bias?
UpTTan	-0.572	0.079	-7.44	0.004	No	Yes
MidSeg	-0.234	0.251	0.41	0.625	No	No
LowTTan	-0.869	<0.001	6.35	0.004	Yes	Yes
LowSeg	0.058	0.824	-3.13	0.005	No	Yes
Lumbar	-0.442	0.048	-10.42	<0.001	Yes	Yes

Table B5. Mean (*SD*) bias analyses from Bland-Altman of the Slump-Stand trial. Proportional bias is based on regression slope significantly different from 0, and systematic bias is based on mean difference being significantly different from 0.

Slump-Stand	Slope of Regression	<i>p</i> -value (sig from 0)	Mean Difference	<i>p</i> -value (sig from 0)	Proportional Bias?	Systematic Bias?
UpTTan	-0.180	0.626	5.57	0.022	No	Yes
MidSeg	0.410	0.064	2.08	0.081	No	No
LowTTan	-0.221	0.395	6.25	0.010	No	Yes
LowSeg	0.107	0.615	-7.91	<0.001	No	Yes
Lumbar	-0.325	0.230	-19.08	<0.001	No	Yes

Table B6. Mean (*SD*) bias analyses from Bland-Altman of the Upright-Sit trial. Proportional bias is based on regression slope significantly different from 0, and systematic bias is based on mean difference being significantly different from 0.

Upright-Sit	Slope of Regression	<i>p</i> -value (sig from 0)	Mean Difference	<i>p</i> -value (sig from 0)	Proportional Bias?	Systematic Bias?
UpTTan	-0.664	0.147	4.26	0.138	No	No
MidSeg	0.275	0.226	-0.04	0.977	No	No
LowTTan	-0.374	0.118	5.23	0.030	No	Yes
LowSeg	0.523	0.010	-5.67	0.005	Yes	Yes
Lumbar	0.218	0.274	-11.51	<0.001	No	Yes

Table B7. Mean (*SD*) bias analyses from Bland-Altman. Of the Flex-Sit trial Proportional bias is based on regression slope significantly different from 0, and systematic bias is based on mean difference being significantly different from 0.

Flex-Sit	Slope of Regression	<i>p</i> -value (sig from 0)	Mean Difference	<i>p</i> -value (sig from 0)	Proportional Bias?	Systematic Bias?
UpTTan	-0.406	0.259	-11.35	<0.001	No	Yes
MidSeg	-0.218	0.212	0.28	0.718	No	No
LowTTan	-0.727	<0.001	8.13	<0.001	Yes	Yes
LowSeg	-0.087	0.717	-2.38	0.01	No	Yes
Lumbar	-0.461	0.036	-10.64	<0.001	Yes	Yes

Table B8. Mean (*SD*) bias analyses from Bland-Altman of the Slump-Sit trial. Proportional bias is based on regression slope significantly different from 0, and systematic bias is based on mean difference being significantly different from 0.

Slump-Sit	Slope of Regression	<i>p</i> -value (sig from 0)	Mean Difference	<i>p</i> -value (sig from 0)	Proportional Bias?	Systematic Bias?
UpTTan	-0.722	0.044	9.88	<0.001	Yes	Yes
MidSeg	-0.013	0.951	5.41	<0.001	No	Yes
LowTTan	-0.529	0.028	14.87	<0.001	Yes	Yes
LowSeg	0.263	0.179	1.22	<0.446	No	No
Lumbar	0.164	0.360	-12.68	<0.001	No	Yes

Appendix C: USI-EMG Additional Results

Table C1. Mean (*SD*) pennation angle and thickness for T4ES, rhomboids, and trapezius for each posture.

	T4ES Angle	T4ES Thickness	Rhomboid Thickness	Trapezius Thickness
Prone	6.4° (1.5)	0.8 cm (0.3)	0.5 cm (0.2)	0.4 cm (0.2)
Upright- Stand	7.6° (1.6)	0.9 cm (0.3)	0.5 cm (0.2)	0.4 cm (0.2)
Upright- Sit	7.4° (2.2)	1.0 cm (0.2)	0.4 cm (0.2)	0.4 cm (0.2)
Flex- Stand	5.5° (1.5)	0.7 cm (0.2)	0.3 cm (0.1)	0.3 cm (0.1)
Flex- Sit	5.2° (1.9)	0.6 cm (0.2)	0.3 cm (0.2)	0.3 cm (0.1)
Slump- Stand	6.8° (1.8)	0.9 cm (0.3)	0.4 cm (0.2)	0.3 cm (0.1)
Slump- Sit	6.3° (2.4)	0.8 cm (0.3)	0.4 cm (0.2)	0.4 cm (0.1)
ThorExt	8.9° (2.4)	1.1 cm (0.4)	0.4 cm (0.3)	0.4 cm (0.2)
LumbExt	8.8° (2.0)	1.1 cm (0.3)	0.5 cm (0.2)	0.4 cm (0.2)
Raise- Stand	8.8° (3.4)	1.1 cm (0.3)	0.7 cm (0.3)	0.7 cm (0.3)
Raise- Sit	8.3° (2.1)	1.1 cm (0.3)	0.7 cm (0.3)	0.7 cm (0.3)
Row- Stand	8.1° (2.5)	0.9 cm (0.3)	0.6 cm (0.3)	0.4 cm (0.2)
Row- Sit	7.5° (2.6)	0.9 cm (0.2)	0.6 cm (0.3)	0.4 cm (0.2)
LatPull- Stand	8.0° (2.7)	1.0 cm (0.3)	0.6 cm (0.4)	0.6 cm (0.3)
LatPull- Sit	8.3° (2.7)	1.0 cm (0.3)	0.6 cm (0.3)	0.6 cm (0.3)